CANADIAN THESES ON MICROFICHE

I.S.B.N.

THESES CANADIENNES SUR MICROFICHE

NOTICE

The quality of this microfiche is heavily dependent upon the quality of the original thesis submitted for microfilming. Every effort has been made to ensure the highest quality of reproduction possible.

If pages are missing, contact the university which granted the degree.

Some pages may have indistinct print especially if the original pages were typed with a poor typewriter ribbon or if the university sent us a poor photocopy.

Previously copyrighted materials (journal articles, published tests, etc.) are not filmed.

Reproduction in full or in part of this film is governed by the Canadian Copyright Act, R.S.C. 1970, c. C-30. Please read the authorization forms which accompany this thesis.

AVIS

La qualité de cette microfiche dépend grandement de la qualité de la thèse soumise au microfilmage. Nous avons tout fait pour assurer une qualité supérieure de reproduction.

S'il manque des pages, veuillez communiquer avec l'université qui a conféré le grade.

La qualité d'impression de certaines pages peut laisser à désirer, surtout si les pages originales ont été dactylographiées à l'aide d'un ruban usé ou si l'université nous a fait parvenir une photocopie de mauvaise qualité.

Les documents qui font déjà l'objet d'un droit d'auteur (articles de revue, examens publiés, etc.) ne sont pas microfilmés.

La reproduction, même partielle, de ce microfilm est soumise à la Loi canadienne sur le droit d'auteur, SRC 1970, c. C-30. Veuillez prendre connaissance des formules d'autorisation qui accompagnent cette thèse.

THIS DISSERTATION HAS BEEN MICROFILMED EXACTLY AS RECEIVED

LA THÈSE A ÉTÉ MICROFILMÉE TELLE QUE NOUS L'AVONS REÇUE

Canadä

0-315-09011-1

56928

PERMISSION TO MICROFILM — AUTORISATION DE MICROFILMER

- Please print or type — Écrire en lettres moulées ou dactylographier

Full Name of Author — Nom complet de l'auteur

ALLAN PATRICK McINTYRE

Date of Birth — Date de naissance	Country of Birth — Lieu de naissance
DEC 25 1952	CANADA

Permanent Address — Résidence fixe

343 RUNDLEVILLE PLACE NE
CALGARY ALBERTA
T1Y 2S3

Title of Thesis — Titre de la thèse

LABORATORY INVESTIGATION OF COAL FLOTATION

University — Université

UNIVERSITY OF ALBERTA

Degree for which thesis was presented — Grade pour lequel cette thèse fut présentée

MSc ENGINEERING (MINERAL)

Year this degree conferred — Année d'obtention de ce grade	Name of Supervisor — Nom du directeur de thèse
1981	L.R. PLITT

Permission is hereby granted to the NATIONAL LIBRARY OF CANADA to microfilm this thesis and to lend or sell copies of the film

The author reserves other publication rights, and neither the thesis nor extensive extracts from it may be printed or otherwise reproduced without the author's written permission.

L'autorisation est, par la présente, accordée à la BIBLIOTHÈQUE NATIONALE DU CANADA de microfilmer cette thèse et de prêter ou de vendre des exemplaires du film.

L'auteur se réserve les autres droits de publication; ni la thèse ni de longs extraits de celle-ci ne doivent être imprimés ou autrement reproduits sans l'autorisation écrite de l'auteur

Date	Signature
JAN. 28 1983	

NL 91 (4 77)

THE UNIVERSITY OF ALBERTA

LABORATORY INVESTIGATION OF COAL FLOTATION

by

Ⓒ A. McIntyre

A THESIS

SUBMITTED TO THE FACULTY OF GRADUATE STUDIES AND RESEARCH

IN PARTIAL FULFILMENT OF THE REQUIREMENTS FOR THE DEGREE

OF MASTER OF SCIENCE

IN

MINERAL ENGINEERING

EDMONTON, ALBERTA

FALL 1981

THE UNIVERSITY OF ALBERTA

RELEASE FORM

NAME OF AUTHOR   A. McIntyre

TITLE OF THESIS   LABORATORY INVESTIGATION OF COAL

FLOTATION

DEGREE FOR WHICH THESIS WAS PRESENTED MASTER OF SCIENCE

YEAR THIS DEGREE GRANTED   October, 1981

Permission is hereby granted to THE UNIVERSITY OF

ALBERTA LIBRARY to reproduce single copies of this

thesis and to lend or sell such copies for private,

scholarly or scientific research purposes only.

The author reserves other publication rights, and

neither the thesis nor extensive extracts from it may

be printed or otherwise reproduced without the author's

written permission.

(SIGNED) ..*Allan McIntyre*....

PERMANENT ADDRESS:

...*1339 Pennsburg Rd SE*...

...*Calgary Alberta*........

....

DATED ...*October 18*.....19 81

THE UNIVERSITY OF ALBERTA

FACULTY OF GRADUATE STUDIES AND RESEARCH

The undersigned certify that they have read, and
recommend to the Faculty of Graduate Studies and Research,
for acceptance, a thesis entitled LABORATORY INVESTIGATION
OF COAL FLOTATION submitted by A. McIntyre in partial
fulfilment of the requirements for the degree of MASTER OF
SCIENCE in MINERAL ENGINEERING.

....
Supervisor

....

...H. A. Hamza...

Date...October 16, 1981...

To Lucia, my wife and inspiration

ABSTRACT

The flotation behaviour of a low volatile bituminous
coal from McIntyre Mines Ltd., Grande Cache, Alberta, was
studied in a laboratory program. Batch tests were performed
in a scaled replicate of the Wemco 120 flotation machine
employed at the McIntyre preparation plant. The optimum
flotation environment was identified with the aid of a
factorial design concerned with the following process
variables: aeration rate, impeller speed, collector and
frother reagent dosages, and particle size distribution.
Values of the three parameters of a kinetic model of
flotation proposed by Kelsall and refined by Lynch were
extracted for each set of test conditions. The model was
executed, using the plant determined nominal residence time,
to estimate yield and concentrate ash level. The model's
predicted performance for nominal plant operating conditions
(factorial design centre point) was in agreement with actual
plant data. By extension, model predictions for optimized
laboratory conditions can be transferred to the plant scale.
This methodology is a powerful screening device for
establishment of pilot plant scale evaluations and is useful
in flowsheet design.

ACKNOWLEDGEMENTS

Table of Contents

List of Tables

List of Figures

List of Plates

xi

A	cross-sectional area of the froth column
A	concentration of air bubbles in the pulp (Eq. 2.9)
a	reaction order with respect to bubble concentration
C	concentration of mineral species in the pulp
c	percentage of combustibles in concentrate
c_m	percent assayed element in the mineral being concentrated
D	impeller diameter
$E(t)$	function defining the distribution of residence times
ES	Schulz separation efficiency index
F	particle floatability
F̲	froth stability factor
F̄	specific flotation rate
$F(K)$	distribution function of first order rate constants
$Fx(S)$	distribution of floatability over particle size
f	percentage of combustibles in feed
FI	Aplan's flotation index
g	gravitational constant
kW	kilowatts
K	nth order reaction rate constant
Ks	rate constant associated with the slow floating fraction of a mineral species
Kf	rate constant associated with the fast floating fraction of a mineral species
M	fraction of floatable material in the feed pulp
m	particle mass
N	impeller speed
N	number of flotation cells in bank (Eq. 2.18)
Np	power number
Nb	number of frother coated bubbles per unit volume of pulp
Nq	air flow number
Nq'	modified air flow number
n	order of the reaction
P	power consumed by the impeller
P	probability of flotation (Eq. 2.18)
Pa	probability of adhesion
Pc	probability of collision
Pe	probability of bubble-particle aggregate stability
Pf	probability that valuable particle survives secondary cleaning
PI	power intensity (kW/m³)
$P(x)$	feed particle size distribution
$Pr(x)$	mass density distribution of floatable particles
Qa	volumetric flowrate of air

Qt	tailings volumetric flowrate
R	recovery of valuable mineral to the concentrate stream
Rx	limited recovery for particle size x
Rf	long range recovery
r	rate of flotation
r	particle radius (Eq. 2.5)
Sx	floatability of a particle of size x
Sx,m	maximum floatability of a particle size x
s	floatable surface area
t	time
Ti	induction time
Tc	contact time
U	valuable mineral fraction remaining in flotation pulp
V	pulp volume (exclusive of air)
W	weight remaining in the pulp after passage through N identical cells
W	weight recovery of concentrate (yield) (Eq. 3.3)
x	particle size

Greek Symbols

ρ_p	pulp density
ρ_s	particle specific gravity
α	fractional yield of floatable material at the cell residence time
θ	nominal residence time for a single flotation cell
$\emptyset$	fraction of feed material which is slow floating

1. INTRODUCTION

Alberta's coal reserves are geographically well distributed. Figure 1.1 illustrates the three major coal regions of Alberta and identifies the coal rank which is particular to each region. The coal regions are contemporaneous, being Cretaceous in age and the coals originate from a common base of non-marine vegetal matter. The heterogenity of coal rank is explained by the degree of geologic metamorphism associated with each region. Mountain coals are carbon enriched because heat and high pressures associated with tectonic activity has driven off moisture, volatile matter, and oxygen from the coal structure. Metamorphic alteration has increased the friability and brittleness of coal. Mining of mountain region coal will generate size consists which are typically 40 percent finer than 28 mesh (600 microns). Flotation is usually the most efficient method of processing these fines. In Alberta preparation plants, flotation is utilized to separate coal from clay material which is interbedded in the coal seams. The objective is to generate a product which conforms to maximum limits of ash content specified by the customer's contract. Flotation practice for Appalachian coals separates coal from pyrite. The objective here is environmental; to limit emissions of SO_2 from coke ovens or thermal power stations.

This project was developed to fulfill four objectives. The initial objective was to study the flotation process in
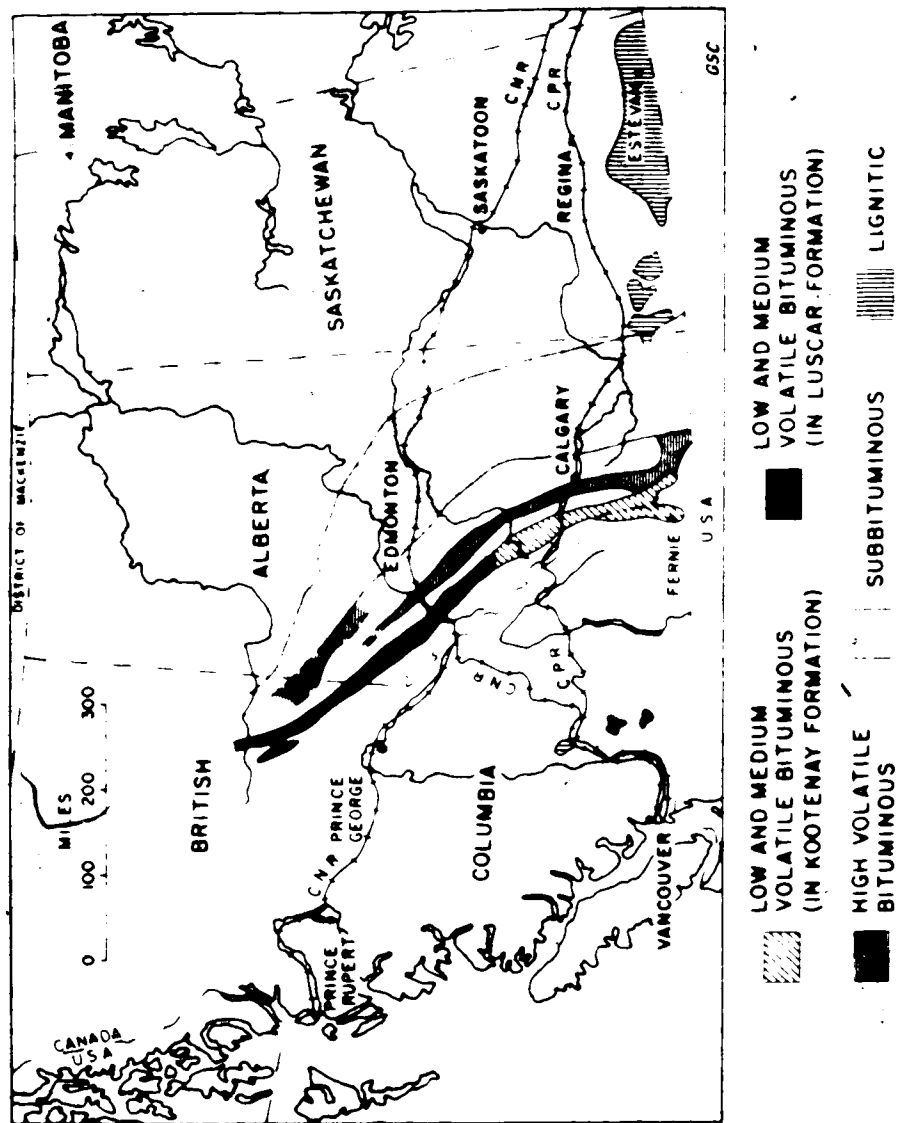
Fig. 1.1   Major Coal Regions of Western Canada

terms of hydrodynamics. The response of mineral particles in an environment developed by the impeller mechanism of a flotation cell is of interest in this approach. The second objective was to develop laboratory scale equipment and procedures which would accurately replicate the plant scale flotation operation. This constitutes an effort to increase the utility of laboratory data and strengthen its role in the design of coal flotation circuits. The third objective involved the application of a mathematical representation (model) to predict yield and quality of coal flotation concentrates. Two models were considered in this section of the work. The final goal was the application of data obtained with the scaled laboratory equipment to the most accurate model in an effort to define optimal flotation conditions and equipment configuration. Economic and technical indices were utilized as terms of reference for the optimization.

The coal selected for study is mined and processed by McIntyre Mines Ltd., Grande Cache, Alberta. This low volatile bituminous coal is primarily exported to Japanese coke makers. It is regarded as one of the world's prime coking coals. This coal was selected because McIntyre operates the only preparation plant in western Canada which practices flotation on the entire spectrum of particles finer than 28 mesh. Other operators restrict flotation practice to a finer size range. The maximum flotation feed particle at both Cardinal River and Fording Mines is 100

mesh (150 microns). This project was executed concurrently with the development of an on-stream ash monitor at the University of Alberta. These projects mesh together as the ash monitor has potential for process control of coal flotation.

2. LITERATURE SURVEY

2.1 Design and Hydrodynamics of Flotation Machines

Flotation machines are classified according to the method by which air enters the cell. Pneumatic machines feature air admission through spargers located on the cell floor. The Callow cell, popular during the period 1900-1920, was an example. A current example of a pneumatic machine is the Heyl and Patterson 'Cyclo-Cell'. By 1930, agitation flotation machines were incorporated in the majority of concentrator flowsheets. Air was entrained into the pulp by means of a vortex generated at the pulp surface. Mineralized bubbles were transferred to a separate quiescent compartment where froth formation proceeded. Agitation machines were replaced by subaeration cells which have maintained dominance to the present day. Air enters a subaeration cell through a standpipe surrounding the impeller shaft. Aeration is promoted either autonomously by suction generated through impeller motion, or extraneously by pressure supplied by turbine blowers. Self-aerating machines can be "supercharged" by supplemental addition of forced air.

The design of subaeration machines has evolved in response to the changing nature of flotation feeds. Utilization of hydrocyclone classifiers has tended to coarsen feeds because of their sensitivity to surging feed flows in which case the cyclone apex outlet can become

5

overloaded, by-passing coarse material to flotation feed.
Flotation cells must be able to suspend coarse particles
(size range: 212-300 microns) and simultaneously promote
flotation of ultrafines (size range: 1-10 microns).
Flotation requirements for the size extremes are different,
prompting the development of cell designs and operating
practices specific to each case [1]. Sulphide mineral
deposits are being developed at steadily decreasing ore
cut-off grades. Concurrently, the size of concentrators is
increasing to realize market demands. Large, rationalized
concentrators respond to requirements of increased flotation
capacity by incorporating machine units of larger volume.
Advantages accompanying economics of scale include
minimization of: capital expenditures, operating, and
maintenance costs.

Two hypotheses exist concerning bubble-particle
attachment in a flotation cell. The gas precipitation
theory, as outlined by Taggart [2] in 1927, holds that
dissolved air precipitates out of solution to form bubbles
at nucleation sites on collector-coated (hydrophobic)
particles. Precipitation is thermodynamically favoured under
conditions of increased temperature and reduced pressure.
Gaudin [3] proposed the direct encounter hypothesis in 1932.
A particle will just touch a bubble if it is moving along a
streamline whose closest approach to the bubble is the
radius of the particle. If the particle moves along a
streamline which is closer to the central plane of the

bubble, definite collision is realized. Three phases are present at the contact point: the gas phase of the bubble, the solid particle, and an intervening water layer which envelops the bubble. To minimize system energy, the particle slides over the hydrated film to its rest position at the bottom of the bubble. The duration of this traverse is the contact time. Contact time increases proportionately with arc length; longer contact times are associated with centrally located streamlines. The collision impact momentum thins the hydrated layer, forming a two phase contact (gas-solid) if rupture occurs. The time required to rupture the hydrated film is labelled the induction time. Induction time is in the order of 0.1 seconds. A bubble-particle aggregate results if contact time exceeds induction time (Figure 2.1). Sutherland [4] stated that induction time is independent of particle size whereas Woodburn et. al. [5] contend that induction time is directly proportional to particle size. A mathematical model of recovery will overestimate the flotation of coarse particles, utilizing Sutherland's principle and underestimate the same with Woodburn's approach.

If the gas precipitation theory predominates, then the flotation rates of all particle sizes should be equal. Morris [6] demonstrated that this is not the case. As well, photographs indicate that single bubbles can carry several hydrophobic mineral particles into the froth in spite of the fact that a bubble nucleation site cannot be distributed
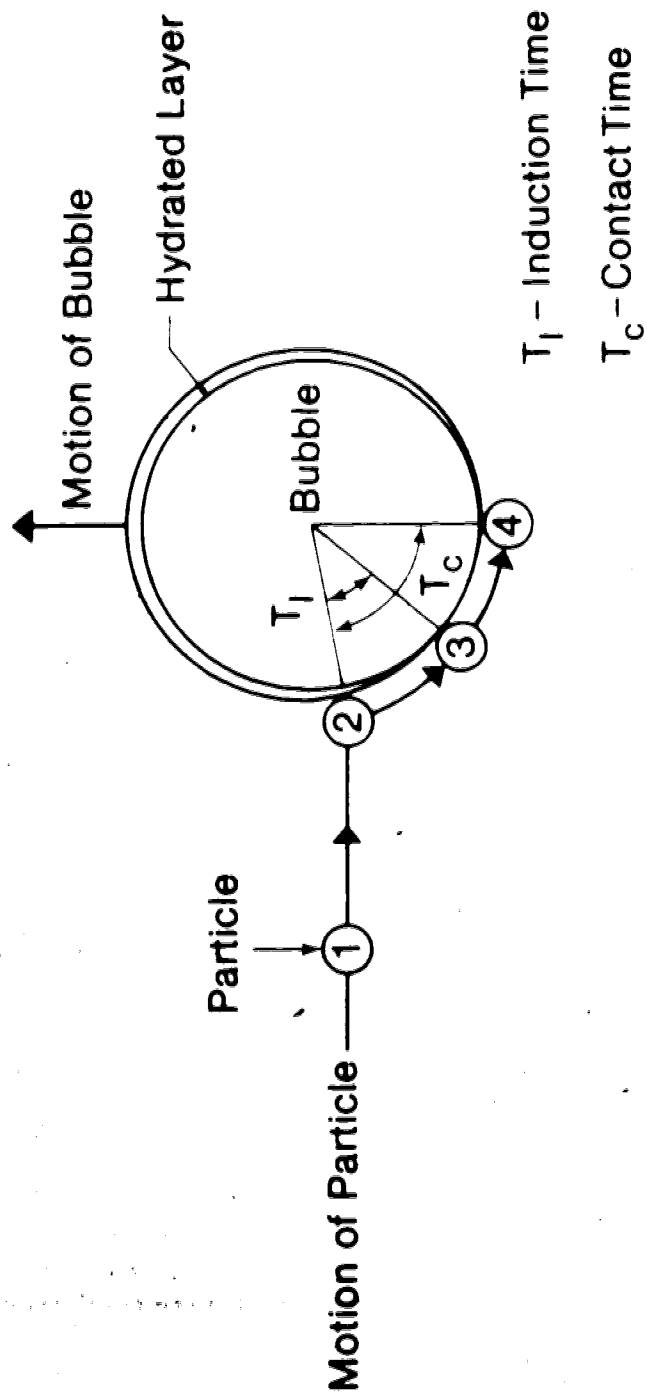
Stage No.	Remarks
1	Particle Moving Along Streamline
2	Particle Impinges on Hydrated Layer
3	Particle-Bubble Aggregate Formation
4	Particle at Low Energy Position

Fig. 2.1 Particle-Bubble Aggregate Formation

between particles. This criticism notwithstanding, it has been suggested that flotation proceeds predominantly via the collision mechanism, with the gas precipitation mechanism acting in a supplemental role.

Figure 2.2 illustrates the principal regions of a flotation cell. The requirements of the impeller can be elucidated from this diagram. The impeller must promote aeration (if the machine is self-aerating) and distribute air uniformly in the two phase mixing region. As well, the impeller acts as a pump, recirculating pulp from remote corners of the tank through the impeller zone. Above all, the impeller must be able to suspend particles in order to provide opportunities for bubble-particle contact and the recovery of valuable mineral particles. The flotation region is a quiescent zone characterized by countercurrent flows of bubble-particle aggregates towards the froth column and gangue particles settling from the froth. Excessive turbulence in this region disrupts bubble-particle aggregates, destabilizes the froth and promotes mechanical entrainment of gangue particles to the concentrate stream. Quiescent conditions are provided by the baffling action of the stator which surrounds the impeller mechanism. The stator prevents vortex swirling around the standpipe by minimizing the tangential velocity component of flow.

An air cavity attaches to the trailing edge of each impeller blade as these are low pressure regions. These cavities reduce the power consumption of the impeller by
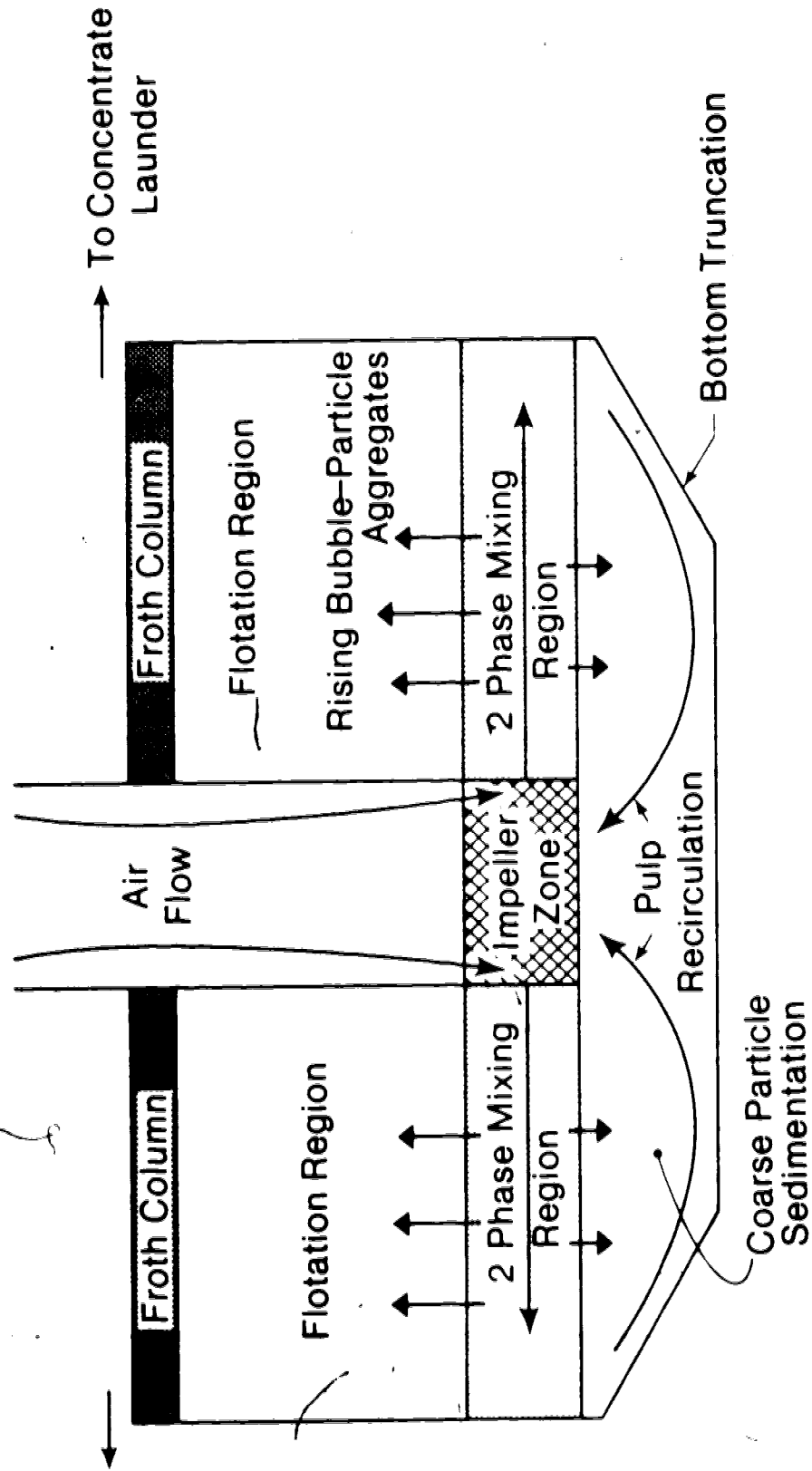
Fig. 2.2 Regions Within A Flotation Cell

Source: Degner and Treweek

hydrodynamic streamlining. The coupling between the impeller (power transmitter) and pulp (power receiver) is detached, causing slippage between these components. Microturbulence in the impeller zone generates bubbles by vortex shedding from the cavity tail. The degree of microturbulence and concentration of frother reagent influences the equilibrium bubble size distribution. Realizing that increased flotation rates are promoted by smaller bubbles, Gaudin [8] contended that any method of reducing bubble size is a positive step to improved recovery of ultrafines. Frother molecules adhere to air bubbles, maintaining bubble shape as small rigid spheres (0.1 to 1.0 mm). In the absence of frother, bubbles, typically 0.5 to 3 mm in diameter, develop elongated tails which reduce hydrodynamic drag and promote high ascent velocities. Considering the longer retention time for smaller bubbles, it follows by extension that the maximum aeration rate of a self-aerating machine is limited by frother concentration. For these machines, aeration rate is a function of impeller speed and submergence. Higher rates are attained with faster rotational speeds. Increased submergence of the impeller mechanism decreases aeration because of increased hydrostatic pressure. Englebrecht and Woodburn [9] claim that optimum recovery is achieved if the hold-up of air is one-half of the cell volume. Typically, the air fraction is lower; Harris [10] suggests an average value of 15 percent of cell volume. High speed photography has dispelled the notion that stator blades serve to

comminute large bubbles. Action to promote reduced bubble
sizes must occur in the impeller zone, specifically through
increased turbulence. Uniformly distributed fine bubbles
reduce the pulp specific gravity and, in turn, the ability
of the pulp to receive power from the impeller. Increased
turbulence adversely affects the stability of coarse
bubble-particle aggregates. Provision for separate treatment
of feed size extremes increases capital costs as more
flotation machines are required. As well, the suspension of
coarse particles could deteriorate in absence of fines since
decreased pulp density increases the terminal settling
velocity of particles according to Stokes' law.

Schubert [11] contends that since the flow regime of
the flotation system is highly turbulent (Reynolds Number:
1 - 7x10'), flotation modelling requires application of
turbulent theory. This is hampered by the lack of
quantitative measurement of turbulence in three phase
systems and the fact that energy dissipation is a function
of position within the machine. Two machines characterized
by equal values of power intensity (power/unit cell volume)
may have dissimilar spatial distributions of enetgy
dissipation (i.e. dissimilar mixing patterns). Schubert
desires incorporation of turbulence into the analytical
model of flotation, however, in the interim he suggests the
application of hydrodynamic criteria to characterize
flotation machine turbulence. This criteria is embodied by
the dimensionless quantities known as the air flow number

and the power number.

The air flow number represents the ratio of linear air velocity to impeller tip speed. In its form given by Equation 2.1, it is useful for comparing flotation machines within the same design family (hence the use of impeller diameter as a characteristic length). Harris advocates usage of the modified air flow number (Equation 2.2).

$$Nq \equiv \frac{Qa}{ND^3} \equiv \left(\frac{1}{ND}\right) \cdot \left(\frac{Qa}{D^2}\right)$$

<div align="center">inverse impeller tip speed   linear air velocity</div>

(2.1)

where:

Nq is the air flow number,

Qa is the volumetric flowrate of air,

N is impeller speed.

D is impeller diameter

$$Nq' \equiv \frac{Qa}{AND} \equiv \left(\frac{1}{ND}\right)\left(\frac{Qa}{A}\right)$$

(2.2)

where:

Nq' is the modified air flow number,

A is the cross-sectional area of the froth column

Arbiter et. al. [12] have shown the influence of the flow number on the particle suspension capabilities of the flotation machine. For narrow size fractions, stable particle suspensions are possible for flow numbers less than a critical value. At the critical value, which Koch, (as

quoted by Schubert) labled as the 1-s suspension criterion, particles sediment as the air saturated pulp loses ability to accept power. This phenomenon is illustrated by plotting the power ratio (power consumed under aerated conditions compared to power consumed without aeration) versus the flow number. Figure 2.3 illustrates the relationship between power ratio and flow number. Coarsest particles sand out at low flow numbers, with progressive sedimentation of finer particles as the flow number increases. Curve 3 of Figure 2.3 show the continuous progression of suspension failures which occurs over a broad size spectrum. To reduce suspension failure, Arbiter suggested that aeration be throttled for commercial self-aerating cells. Aeration (and the flow number) is more precisely controlled, however, in forced aeration machines. Recovery of wide size spectrum flotation feeds is maximum at medium flow numbers. If flow number increases, suspension failure of coarse particles combined with turbulence induced froth instability reduces recovery. If flow number decreases, insufficient bubbles and turbulence induced bubble-particle aggregate disruption also decreases recovery.

The power number, which is the ratio of Newtonian drag stress to inertial stress, is a complex function of the Reynolds number, the Froude number, and geometrical aspects of the impeller-stator assembly. For highly turbulent regimes, the dependence on Reynolds number can be ignored. In the absence of vortex swirl, the Froude number can be

Curve	Size Fraction
1	35 × 42 Mesh
2	65 × 80 Mesh
3	Unclassified

Material: Hematite

Source: Arbiter et. al.
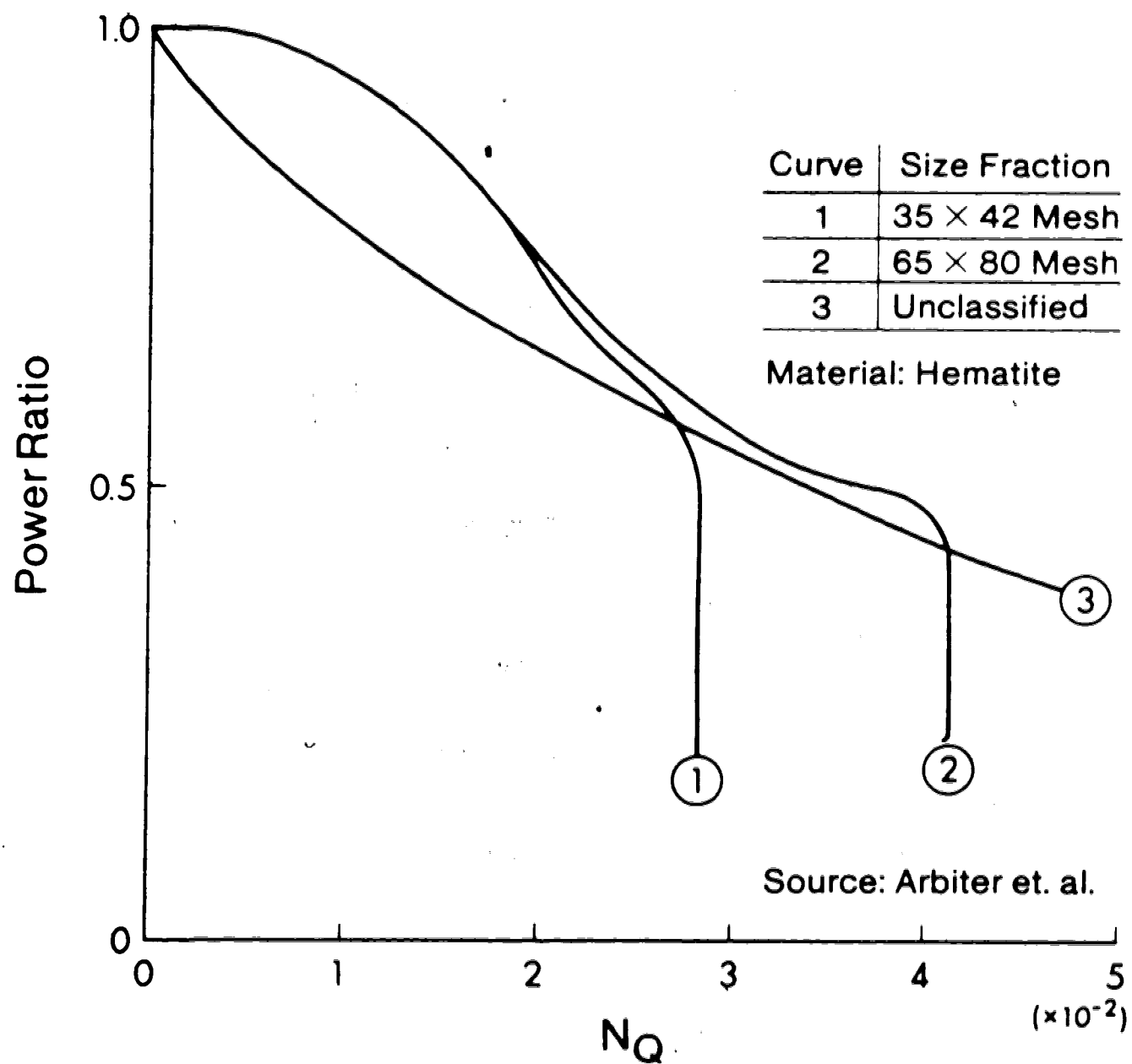
Fig. 2.3 Power Ratio vs. Flow Number

similarly dropped. The Froude number, being the ratio of inertial stress to gravitational stress, is a key parameter in boat hull design. Thus, the power number simply reflects the interaction between impeller and stator. Algebraically, the power number is given by:

$$Np = \frac{Pg}{\rho_p N^3 D^5}$$

(2.3)

where:

Np is the power number,

P is the power consumed by the impeller,

g is the gravitational constant,

ρ_p is pulp density

For rotating machinery the power number reflects the flow straightening characteristics of the stator. Impeller rotation imparts a large tangential velocity component to pulp flow. This undesirably leads to vortex swirl and pulp stratification. The stator transforms the tangential flow component into the radial flow component plus heat of friction. Aerated pulp travels radially to the extremities of the cell. Because of lower momentum, bubbles do not travel as far as particles or fluid components. Instead, they rise through the two phase mixing region interacting with potentially floatable particles. At the cell walls, the impinging radial flow component is transformed to the longitudinal component (plus heat); particles drop to the cell floor where they are pumped radially inward to the

impeller. Truncation of the cell bottom promotes transformation of longitudinal flow to radial inward flow. A false floor may be utilized to partition the radial flow directions. The spitzkasten, which is a form of truncation included in earlier deep cell designs, has lost popularity due to large floor area requirements.

The volumetric circulation capacity of a flotation machine is determined by impeller design and operating speed. Subaeration machine impellers of the turbine type are categorized into three design groups. Low profile turbine impellers are favoured by machines of deep submergence such as those manufactured by the Denver Equipment Co. [10] These machines are lightly baffled with a stator (Np = 2.0) positioned as a hood over the impeller. Additional tank corner baffles are required to prevent vortex swirl. To improve pulp recirculation to the impeller zone, Denver machines are fitted with a tapered inverted cone surrounding the impeller. Harris used residence time distribution tests to identify this "D-R ring" assembly as a perfect mixer. The Wemco [14] type flotation cell features a deep bladed star shaped impeller in conjunction with a disperser ring stator (Np = 5.0). The impeller is extruded from a flexible plastic which causes the bottom half to be twisted to a more streamlined shape under influence of torsional stress. Outokumpu [15] has designed a third type of impeller which facilitates bubble generation from deep regions of the impeller. Pulp is pumped within sections of ten inverted V

shapes arranged in circular fashion, apexes pointed inward. Air is distributed outwards between these sections. In order to offset increasing hydrodynamic forces at greater depth, the impeller profile is shaped as a paraboloid of revolution, apex down.

The impeller brings together the air and pulp phases along opposite longitudinal flow paths. Pulp is ejected from the leading edged of turbine blades while air bubbles are shed from trailing edges. Both travel concurrently towards the stator. The power consumption of the impeller is related to the net increase in the tangential velocity component imparted at the impeller tip. Pulp streams emerging from the impeller zone must have sufficient initial velocities which, after stator conversion to the radial component, transport coarsest particles to and from the most distant points in the cell. Sedimentation occurs at points where critical radial velocities (which are proportional to particle size) are not maintained. The impeller extends the two phase mixing region to the cell walls. In order to accomplish this, power transmission to the pulp must be assured by proper balancing of impeller speed and aeration.

Larger flotation cells require higher power inputs and stators of higher power number. Manufacturers downplay high power requirements through utilization of the power intensity quantity. Power requirements are more accurately expressed if power intensity applies only to the two phase mixing region. The quiescent flotation region should be

discarded in power estimations. For calculation purposes, the two phase mixing region refers to the volume swept out from the aeration section of the impeller to the cell walls. The aeration section represents the top half, and two-thirds for the Wemco and Outokumpu impellers, respectively.

Hydraulic performance maps illustrate the relationship between power intensity and flow number under conditions of variable impeller speed and aeration rate. Figure 2.4 is an example of a hydraulic performance map. Schubert determined that recovery is influenced by hydrodynamics. Recovery of coarse particles is maximized by operation at high flow numbers and with power inputs which are marginally above the 1-s suspension criterion. These conditions necessitate the generation of desirably larger air bubbles in the impeller zone and minimize turbulence in the two phase mixing region. Ultrafines should be recovered at increased power inputs and reduced flow numbers. Increased microturbulence of the impeller region reduces bubble size and increased collision momentum raises the probability of bubble-particle aggregate formation.

The proper machine for flotation of sulphide ores features low aeration rates since the majority of the flotation feed reports to the tailings stream. The number of bubble-particle collisions required is proportional to the feed grade. The froth surface area to cell volume ratio should be low to facilitate development of a stable froth phase. Rougher section froths should be only 6 to 8 inches

Region	Appropriate Flotation Conditions For:
1	Coarse Particles >100 Microns
2	Intermediate Particles 10 - 100 Microns
3	Ultrafines < 10 Microns
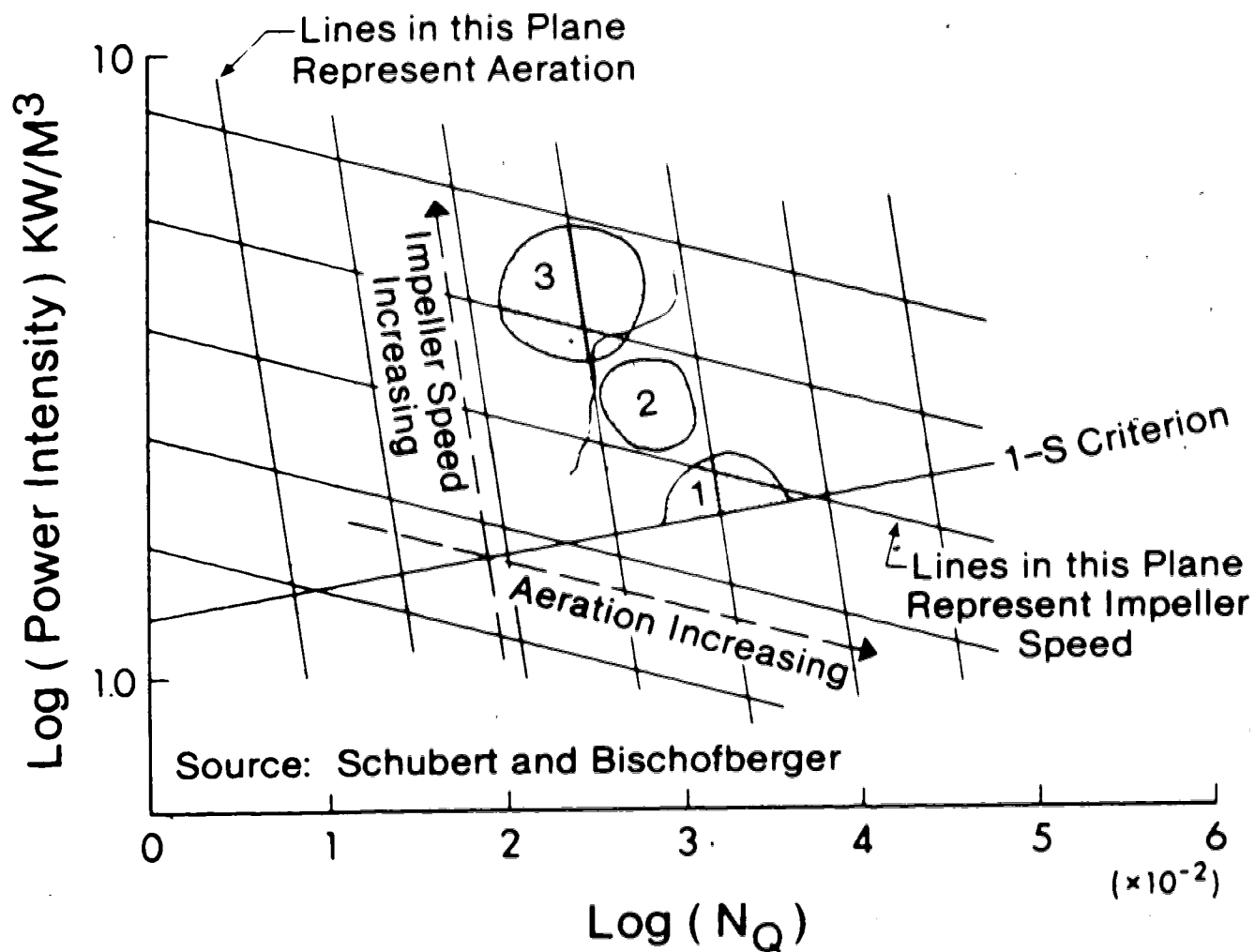
Fig. 2.4 Hydraulic Performance Map

thick in order to maximize recovery. Thicker froths (12 to
16 inches) at the cleaner section are required to accomplish
concentrate grade objectives. Aeration requirements are
greater at this section, hence, the froth area to cell
volume ratio increases. Processing of high grade flotation
feeds such as coal, potash, and phosphate, implies that the
majority of feed reports to the concentrate stream. It is
desirable to maintain high aeration rates and high ratios of
froth area and concentrate launder lengths to cell volume.
High values of the latter ratio facilitates froth removal,
preventing the step from becoming rate determining for the
flotation process. The Dutch State Mines presented the
Kleinbentink coal flotation cell in 1958 [16]. It was an
inverted circular conical section which featured scraping of
the entire froth surface by radial paddles with discharge
into the circumferential concentrate launder. For reasons
unknown, universal application of this design was not
realized.

Laboratory scale flotation machines must be designed in
an attempt to duplicate the flotation environment and
metallurgical response experienced at the plant scale.
Duplication at reduced scale requires control of: impeller
speed, aeration rate, pulp level, and concentrate removal
rate. Scaling is complicated by the lack of unified
criteria. Machines have evolved within the framework of
manufacturers' design families such as: Denver, Wemco, and
Agitair. The lack of domination by a particular design

suggests that all are achieving specified performance objectives. It appears that machine selection is a function of salesmanship and subjective preference of design engineers associated with concentrator construction. Another aspect which complicates scaled development of laboratory equipment is the fact that a universally standard flotation test procedure is not available. Each metallurgical laboratory performs tests which simulate rougher and cleaner flotation stages, locked cycle tests, and flotation rate tests with its own habitual methodology.

Kinematic similarity between machine sizes of the same family, is one criterion for scaling. This implies constant geometric scaling along with the principle that corresponding locations between machines have velocities in constant ratio. The indicator of kinematic similarity is constancy of Froude number which leads to the concept that impeller peripheral speed is proportional to the square root of impeller diameter. Outokumpu is the only manufacturer which designs machines with this principle.

The criteria for similar particle dispersion in machines of different sizes within the same family is constancy of: geometric scaling, power number, and power intensity. This implies that impeller peripheral speed is proportional to the cube root of impeller diameter. Of all designs, the Wemco machine is closest in fulfilling this criteria. Harris suggests that air flow numbers for machines of different size within the same design family differ by a

constant of proportionality.

Flotation machine design should be concerned about providing opportunities for bubble-particle collisions, necessary hydrodynamic conditions, and adequate material transport paths. If machine scaling incorporates these consideration, attainment of metallurgical performance objectives will be assured. Emphasis would then shift to aspects of regulatory control features, longevity and reliability of component parts, and the elimination of unnecessary features, in efforts to reduce flotation machine capital and maintenance costs.

2.2 Fundamentals of Coal Flotation

Flotation is currently practiced with low and medium volatile bituminous coals. The principal reason for limited application is economics. The value of the product must support the significant capital and operating expenditures associated with coal flotation. Low and medium volatile bituminous coals are presently sold to coke makers at approximately $65 per ton, over twice the price of high volatile bituminous and sub-bituminous thermal coals. Flotation costs cannot be recovered for thermal coals. The secondary reason for exclusivity is the variation of floatability according to coal rank. Floatability is classically quantified by the bubble-particle contact angle. Higher contact angles are indicative of high floatability. The relationship between contact angle and coal rank, as established by carbon content, is given in Figure 2.5. Research is required to apply flotation to high volatile bituminous coals. This research will be stimulated by the desirability of providing coke oven feeds which are blends of different coal ranks. In essence, high volatile bituminous coals will serve to extend the static life index of the world's coking coals.

The surface components theory of coal flotation was postulated by Sun [18] in 1954. Basically, flotation feed particles are binary mixtures of floatable coal and non-floatable gangue. Floatability of a particle is established intrinsically by the dominant component as

Fig. 2.5   Floatability According to Coal Rank

The figure shows a plot of Bubble–Particle Contact Angle, Degrees (y-axis, 10 to 70) versus Carbon Content of Coal, % (DMMF) (x-axis, 80 to 96). The regions marked along the top are: High Volatile Bituminous, Medium, Low Volatile Bituminous, and Anthracite.

Source: Aplan

Note: Coal Ranked According to Aplan, Table 3, Not ASTM
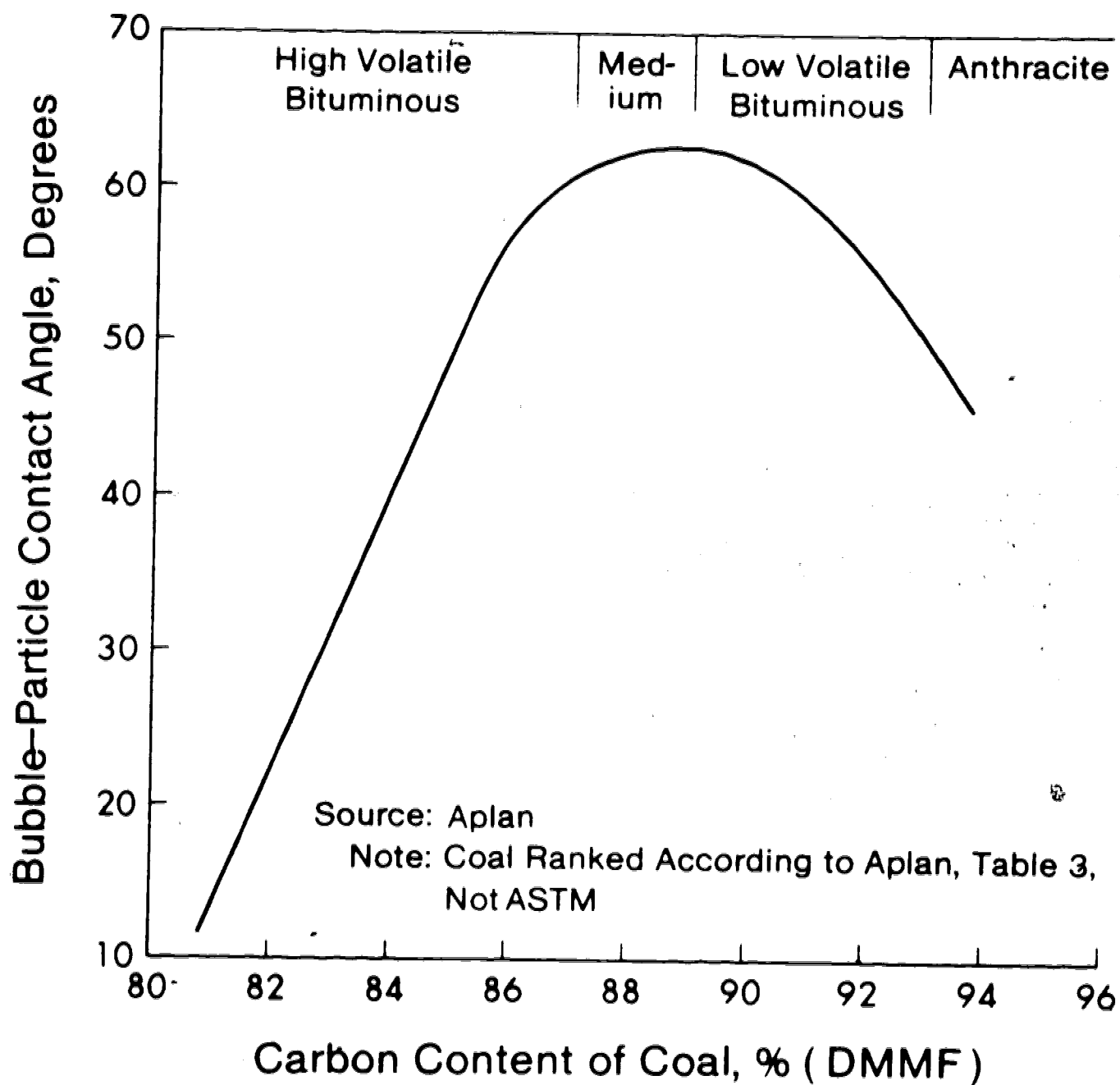
expressed in terms of surface area. A particle, dominated in terms of volume composition by the non-floatable component may respond as a floatable particle if the non-floatable gangue is concentrated at the centre and is surrounded by a shell of floatable coal. Miller et al [19] included particle specific gravity in their generalized explanation of coal flotation. Particle floatability is considered to be proportional to the floatable coal component of surface area and inversely proportional to particle mass. This relationship is given in Equation 2.4. Equation 2.5 expresses this relationship in terms of particle radius.

$$F \propto \frac{f(s)}{g(m)}$$

(2.4)

where:

F is particle floatability,

f(s) is a function of floatable surface area,

g(m) is a function of particle mass

$$F \propto \frac{4\pi r^2}{\rho_s (4/3\pi r^3)} \longrightarrow \frac{3}{\rho_s r}$$

(2.5)

where:

r is particle radius,

ρ_s is particle specific gravity

For particles of constant specific gravity, the surface area to mass ratio increases with decreasing particle size. This

implies that selectivity of the flotation process improves
for coarser sizes (+100 mesh). Miller concluded that
flotation should be restricted to coarser particles such as
14x100 mesh and that finer particles should be handled by
hydrocyclones. Surface area effects do not influence the
hydrocyclone classification mechanism. Cyclones rely on the
responses of particles of varying mass subjected to
centrifugal forces. Cyclones are efficient separators for
coarse feeds, however, operating inefficiency is high for
particles finer than 100 mesh.

Table 2.1 outlines the distribution of floatability
over coal maceral groups. Western Canadian coals are
composed of approximately 70-80 percent vitrinite and 20-30
percent inertinite. Vitrinite is a reactive maceral group,
melting with evolution of volatiles upon application of
heat. Inertinite remains intact during the carbonization
process. Vitrinites are distinguished according to the
reflectance of light from an oil immersed polished surface
during petrographic examination. Vitrinites of low
reflectance are high in oxygen content, hence lower in rank
and floatability. As much variation in floatability exists
within the vitrinite group as exists over the spectrum of
maceral groups. Exinite enhances fluidity during
carbonization and is a desirable coke oven feed constituent.
Appalachian coals contain 5-20 percent exinite, however,
Australian coals of Permian age are less than 1 percent
exinite and up to 85 percent inertinite. Maceral composition

Table 2.1 Floatability As a Function of Maceral Groups

	MACERAL GROUP	COMMENTS
D		
E		
C		
R	VITRINITE	Composed of cellular woody tissue of trees buried in peat swamps
E		
A		
S		
I		
N		
G		
F	EXINITE	Remains of algal bodies, spores, and leafy cuticular tissue
L		
O		
A		
T		
A		
B		
I		
L		
I		
T	INERTINITE	Originates from 'humic mud', fossil fungi remains. Most commonly, carbonized wood; evidence of pre-historic forest fires
Y		

is a function of plant species and depositional history of
the particular coal. In view of this, blending to obtain
desirable coke oven feeds has become an exact science (see
Pearson [20] - Figures 16, 17).

2.2.1 Flotation Reagents

In the majority of cases, coal flotation is
accomplished with only two classes of reagents - collector
and frother. The role of the collector is to gently "nudge"
the coal into a more floatable state by slightly increasing
the bubble-particle contact angle. The collector, which is a
non-polar hydrocarbon molecule such as kerosene or diesel
oil fulfills its objective by smearing particle surfaces. In
metallic mineral flotation, collector adsorption occurs
either by formation of a metal-collector molecule complex at
the valuable mineral surface or by electrostatic attraction.
Typically, the hydrocarbon collector dosage ranges between 1
and 3 liters per tonne of flotation feed.

The frother reduces surface tension at the interface
between the flotation region and froth column (Figure 2.2).
This permits establishment of a foam which evolves into a
froth phase as mineralized bubbles are pushed upwards from
the foam. Frother molecules are heteropolar, the polar end
(OH group) is orientated downwards into the flotation region
because of hydrogen bonding with water molecules. The froth
column sits on the non-polar hydrocarbon ends presented at
the interface. The original frothers were pine oil and

cresylic acid, especially the latter because it is a cheap coke oven by-product readily consumed by an intergrated coal preparation plant. Both are, however, "impure" frothers because molecules tend to adsorb onto coal surfaces. The price advantage of these frothers was lost because adsorbed molecules must be replaced to maintain stable froths. Short chain aliphatic alcohols such as methyl isobutyl carbinol (methyl amyl alcohol) and the "Dowfroths" are current popular frothers. The increased cost of these "pure" frothers is recovered by lower dosage requirements. Frothers are typically applied at one-tenth of the hydrocarbon collector dosage (0.1 - 0.2 liters per tonne of flotation feed). Aplan [21] suggests that emulsification of frother in the fuel oil reduces total reagent consumption. This is challenged by Goncharova et al [22] who maintain that maximum flotation activity of coal is attained when the interaction between non-polar collector molecules and heteropolar frother molecules is minimized. Water soluble frother molecules may accumulate on emulsified drops of collector in the pulp. Collector molecule smearing is precluded by the presence of OH groups extending from frother coated collector drops. To maximize yield, frother addition is made just prior to aeration, with allowance for collector addition at an upstream point such as a distribution box (e.g. McIntyre Mines) or a conditioning tank.

The role of the frother reagent can be fulfilled by solutions of inorganic metal salts. Iskra and Laskowski [23] have performed laboratory investigations with 0.2 N NaCl solutions in lieu of frother reagent, Several Russian coal preparation plants utilize sea water in the flotation process. Presence of the metal cations raises the specific gravity of the flotation pulp, promoting suspension and lower settling velocities of coarse coal particles. In essence, a hybrid process of froth flotation and static bath heavy media separation is created. Deterioration of the froth phase may occur if cation concentration is not regulated. For example, excessive zinc sulphate, added to depress sphalerate in galena flotation, will cause thin, fragile froths of low mobility.

Depressant reagents are utilized in special circumstances of coal flotation. If reverse flotation is practiced to selectively concentrate pyrite and reject valuable coal to the non-floating stream, additions of starch, or tannic acid, or potassium permangenate serve to depress the coal. Starch and tannic acid form micelles which adsorb onto coal surfaces, blocking bubble attachment sites. Permanganate oxidizes the coal surfaces to reduce floatability. Optimum flotation yield has been established in the pH range 6-8. This obviates the requirement for pH modifying reagents excepting circumstances of extremely poor process water quality.

2.2.2 Flotation of Oxidized Coal

Oxidation of coal proceeds by two mechanisms. Primary oxidation occurs in-situ as oxygenated groundwater percolating through the coal seam reacts with the contacted coal molecular structure. Secondary oxidation is atmospheric, occurring on coal surfaces exposed during mining and processing. Oxidation products are water soluble humic acids; oxalic acids have been identified as the major oxidation product of Carboniferous age Appalachian coals and ketonic acids are the dominant oxidation product of Cretaceous western Canadian coals [24]. Oxidized coals are identified by Free Swelling Index (FSI) of zero and low flotation yield.

Two approaches have been attempted in the flotation of oxidized coal. Removal of the oxidation product by attrition scrubbing and chemical leaching was attempted in early work. Ultrasonic wave energy has even been applied to destroy the oxidized product layers. Sun [25] has concluded that "once original surfaces of coals are appreciably deteriorated by oxidation, they cannot be restored through washing with water or alkaline solutions". A recent approach takes advantage of special characteristics accompanying oxidized surfaces. Wen [26] and McIntyre [27] have noted that the surface charge of coal particles in water, determined by electrophoresis, becomes increasingly negative with increasing severity of oxidation. A cationic fatty acid collector (lauryl amine) improved flotation yield of

artificially oxidized coal in both investigations. The
cation of the collector molecule was electrostatically fixed
to negatively charged oxidized coal surfaces. An air bubble
rising through the two phase mixing region would "see" the
hydrocarbon ends of the collector molecule rather than the
hydrophilic oxidation products, thus increasing the
probability of bubble mineralization.

2.2.3 Coal Flotation Practice

Western Canadian operators practice coal flotation in a
single stage of rougher cells. A simplified flowsheet of the
flotation section at McIntyre Mines is illustrated in Figure
2.6. The ash content of flotation concentrates is low enough
to eliminate the necessity of cleaner flotation stages. This
is not the case in South Africa [28] as middling particles
reporting to rougher flotation concentrates must be removed
at a subsequent cleaner flotation stage. Figure 2.7
illustrates a flowsheet which is being considered for the
Durban Navigation Collieries. This sensible flowsheet is in
reality an application of Aplan's [29] "grab and run" scheme
which in turn is similar to a flowsheet proposed by Steiner
[30] for complex sulphides. Fast floating, high grade coal
particles quickly recovered in the first few rougher cells
are routed directly to the dewatering section. Coarse
middling particles are recovered at latter rougher cells and
report to cleaner flotation. The majority of operating
expenses and efforts are concentrated on the feed type

Deslime Screen
Under Flow
(−28 Mesh)

Water

Diesel Collector

Distributor
Box

Frother

4 Parallel Flotation Banks

| Cell 1 | Cell 2 | Cell 3 | Cell 4 |

Tailings
to Thickner

Total Solids Flowrate : 120 TPH
Pulp Consistency : 9%
Ash Content : 18%

Clean Coal Concentrate
to Disc Filters

Approx. Solids Flowrate: 90 TPH
Ash Content: 9%
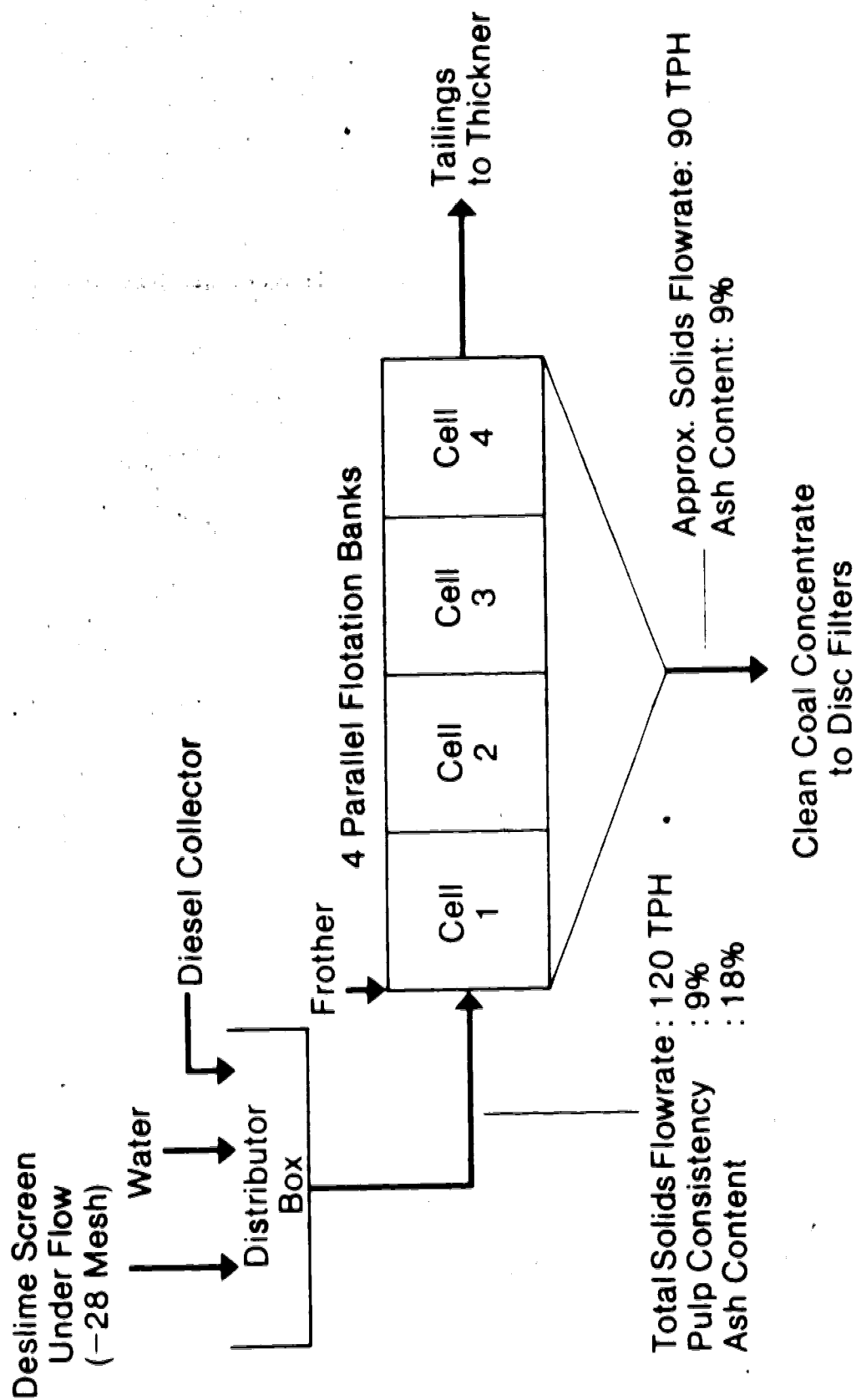
Fig. 2.6   Flotation Section at McIntyre Mines

35

Fig. 2.7   Flotation Scheme Proposed for Durban Navigational Collieries
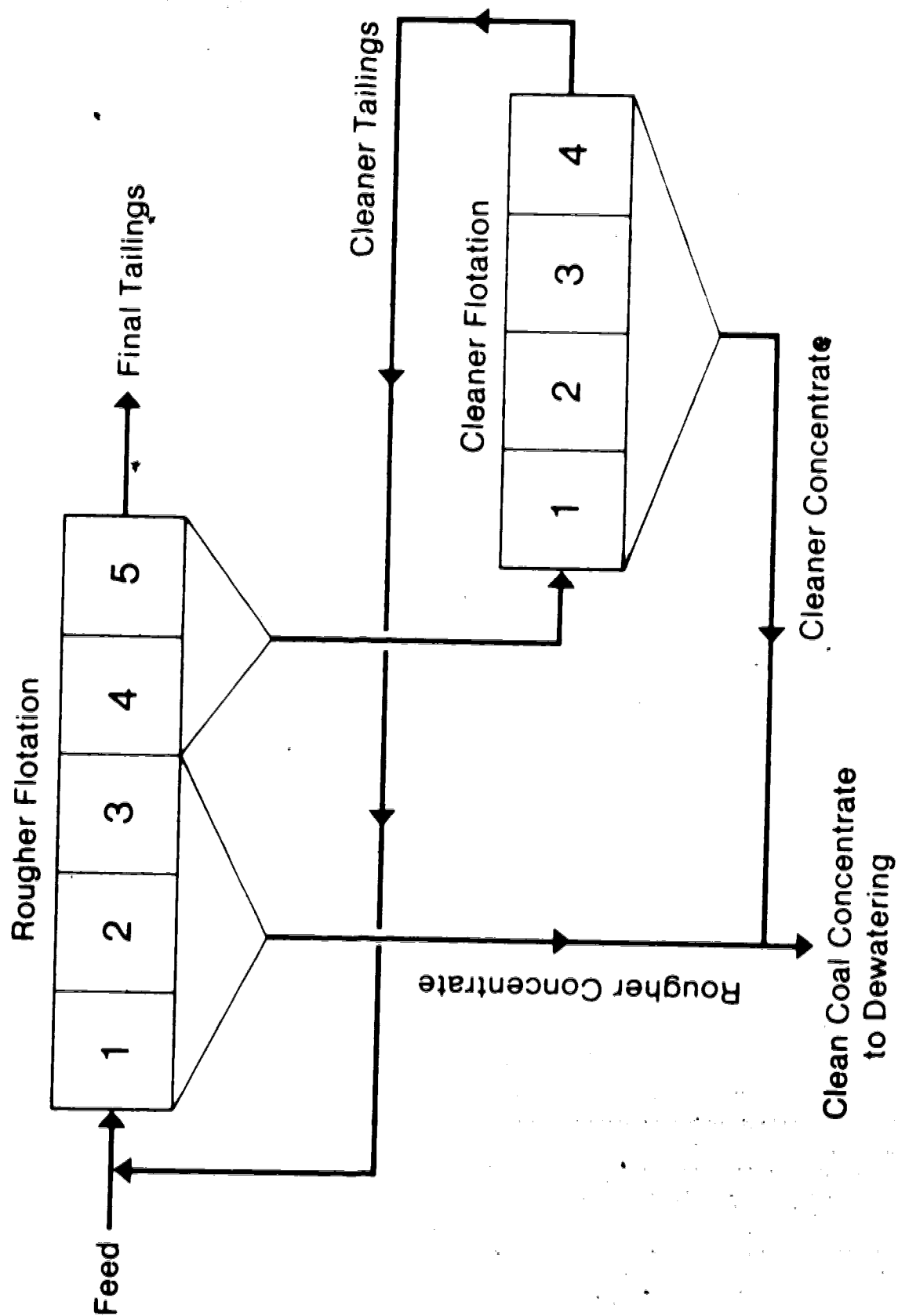
Source: Botha

requiring most attention - the middlings particles.

Aplan proposed the "grab and run" scheme to separate pyrite from Appalachian coals. He made provisions for the conventional cleaning stage as shown in Figure 2.7, but he also suggested the option of reverse flotation at the cleaner stage. Coal would be depressed with dextrine starch and xanthates used to collect pyrite. Aplan emphasized that the rougher cells are to be operated with gentle conditions: low impeller speed to prevent destabilization of coal bubble-particle aggregates, and low aeration rates to . prevent suspension failure of coarse particles (Figure 2.3). (Note the differences between Aplan's and Schubert's flotation environment for coarse particles.) In this scheme, flotation classifies particles according to size. Coarse high grade particles are scalped in the rougher stage while the cleaner operates on the fines.

Firth et al [31] studied the effect of particle size on poorly floating Australian coals. Particles coarser than 250 microns responded to flotation only when isolated from finer particles. Poor floatability in the wide feed size spectrum is attributed to the fact that fine particles adsorb a disproportionately greater amount of collector (because of high surface area) at a disproportionately higher rate. Coarse particles are virtually starved for collector. Two methods were proposed to remedy this situation. Firstly, the flotation feed should be subjected to split conditioning [1]. Coarse and fine particles are conditioned separately to

ensure equitable distribution of collector. After
conditioning, the sizes are reunited and presented as
flotation feed in a common stream. The second proposal is
addition of collector by incremental stages. The initial
increment is applied at the conditioner; subsequent addition
points would be identified at latter rougher cells.
Interaction beween collector and frother must be minimized
in application of the staged addition strategy.

2.3 Mathematical Representation of Flotation

Researchers have formulated mathematical representation of the flotation process for over 35 years. These representations, also known as models, have been utilized mainly in the description of the recovery of valuable minerals as flotation concentrate products. Application of flotation models generates benefits which are both academic and economic in nature. Fundamental understanding of the flotation process is enhanced by models. Coincidently, models provide a scientific basis for the optimization of design and operation of flotation circuits. King [32], however, has observed that the majority of mineral concentrators, operating at profit, were designed utilizing the traditional methods of bench scale preliminary testing followed by pilot plant evaluation. In his estimation, flotation models should be restricted to the assessment of pilot plant data and the development of strategies for the computer control of flotation plants.

In 1970 Steiner [30] presented a flotation circuit developed according to a kinetic model. This circuit, or hybrids of it, has been successfully incorporated in concentrators treating complex sulphide ores in Sweden, Finland, West Germany, and Australia. Flotation models possess vast potential for applications at all levels of concern including the laboratory, pilot plant, and the operating plant.

According to Woodburn [33], the basic requirement of a flotation model is precision rather than elegance. A model is developed in two stages. Initially it is formulated as a mathematical expression (or set of expressions). Then it is executed with the aid of a digital computer. The application of the computer can promote the misconception that the model form is trivial. The model, however, should not be a cumbersome form with many parameters. It should be expressed in a manner which takes advantage of the economy available through reduced computing time.

In a structural sense, models can be classified into the following categories:

a. Analytical Models The mathematical statements involved are rooted in fundamental scientific laws. In his model, Sutherland [4] described the hydrodynamics aspects of flotation of a single particle in the context of the bubble encounter hypothesis. He extended his model to deal with a flotation feed by incorporating distributions of particle and bubble sizes, and induction times.

b. Heuristic Models Plausible equations are proposed to describe flotation. These models can be customized to accommodate special conditions such as the reporting of fine gangue particles to the concentrate by a mechanical extrainment mechanism rather than bubble attachment. Heuristic models typically use kinetic rate expressions to describe

the recovery of valuable mineral.

Significant contributions to the development of heuristic models have been made by: Bushell [34], Jowett [35], Woodburn [5], Lynch [36], and Kelsall [45].

Application of an analytical model to a flotation plant entails the on-stream estimation of parameters such as: particle and bubble diameters, shape factors, and forces disrupting bubble-particle aggregates. The equipment required to measure these variables is either unavailable or prohibitively expensive. Thus, analytical models have restricted utility. Heuristic models use observations like fractional recovery rates of concentrate, and tailings flowrates to generate a "lumped" parameter such as a flotation rate constant. Model predictions are made in terms of these inferred parameters. Heuristic models offer facility of application which has established their role as the preferred model type. The development of heuristic flotation models is outlined in the balance of this section.

2.3.1 Initial Developments of Heuristic Flotation Models

In 1942 Schuhmamn [37] suggested that recovery and grade provide an incomplete picture of flotation behaviour. He insisted that quantitative measurement of the rate of flotation would facilitate accurate understanding of flotation mechanisms. Experimentally measured rates of flotation would be used in the derivation of a new quantity which he called the specific flotation rate. Algebraically,

the new quantity was written as:

$$\bar{F} = \frac{r}{CV}$$

(2.6)

where:

$\bar{F}$ is the specific flotation rate,

r is the rate of flotation (experimentally measured),

C is the concentration of valuable mineral in the pulp,

V is pulp volume (exclusive of air)

Schuhmann related the specific flotation rate to the kinetics of particle bubble attachment by the encounter hypothesis. Analysis of the encounter theory requires consideration of a probability of collision (Pc) and a probability of adhesion (Pa). Pc is a function of aeration rate, agitation, and hydrodynamic behaviour of the particles. Pa is a function of hydrophobicity of the particle surface, and the hydraulic and inertial forces tending to disrupt the two phase aggregate. Morris [38] suggested that Pa is directly proportional to particle size.. The specific flotation rate can be equivalently expressed as:

$$\bar{F} = Pa \cdot Pc \cdot F$$

(2.7)

where: F is the froth stability factor, $0 \leq F \leq 1$

Schuhmann intended the froth stability factor to represent the detachment of particles from bubbles in the froth phase. Detachment of gangue particles (and subsequent re-entry into the pulp) is a desirable mechanism called secondary cleaning. Excessive detachment of valuable particles, however, is indicative of improper froth characteristics.

In his experimental work, Schuhmann used continuous testing methods to verify that the flotation machine acts as a perfect mixer if the rate of concentrate product removal is considered negligible. This allowed the tailing sample of a continuous flotation test to be representative of the pulp body.

Schuhmann defined the "coefficient of mineralization" as the ratio of the concentration of valuable species in the froth product to the concentration of the same in the pulp. He considered this to be a measure of the kinetics of bubble levitation and froth drainage. It also described the floatability of a species relative to the rate of water recovery to the concentrate. Grade is generally a function of froth height and the coefficient of mineralization quantitatively describes the degree of secondary cleaning provided by a particular froth. High values of the coefficient, indicative of good separation between values and gangue, are associated with thick froths.

Brown and Smith's 1954 study [39] proposed that flotation proceeds in two stages. Initially, the surfaces of valuable feed particles (coal in this case) are prepared in

order to increase the probability of adhesion. Subsequently, hydrophobic valuable particles are separated from gangue and carried into the concentrate stream. They suggest that this separation occurs in both the pulp and froth.

They contend that the initial flotation stage is essentially analogous to a chemical process although a chemical reaction is not implied. This can be described by the general rate equation:

$$- \frac{dC}{dt} = KC^n$$

(2.8)

where:

C is the concentration of mineral species in the pulp,

n is the order of the reaction,

K is the nth order reaction rate constant

According to Brown and Smith, applicability of the model is restricted to the bubble attachment mechanism in the pulp phase. The rate of flotation, dC/dt, is equal to the rate of recovery if the rate of mass transfer of mineralized froth to the concentrate stream is large enough to minimize the amount of material which drains back from the froth to the pulp. This implies that the froth stability factor is equal to 1, hence, the froth phase was effectively ignored in the model. The reduced separation efficiency of fine clay particles (less than 10 microns) was reflected by high coefficients of mineralization. This implied that the

recovery of this species is proportional to the recovery of water, discounting the applicability of the bubble encounter mechanism to this species.

Morris [38] showed that flotation rates were maximum at an intermediate size of about 60 microns, and decreased monotonically at both size extremities. Likely, the probability of bubble-particle collision is low for small particles. To maintain high values of Pc for the fines fraction, bubble diameters must be reduced. This is accomplished by either increasing the frother reagent concentration, or increasing the turbulence in the impeller region. Gaudin et al [8] noted that flotation rate is independent of particle size below a value of 5 microns. This observation confirms Brown and Smith's statements concerning recovery of clay fines in coal flotation.

2.3.2 Refinements of the Kinetic Model

Jowett and Safvi [35] rationalized the applicability of chemical kinetics to flotation by noting the analogy between atomic and molecular collisions and bubble-particle collision. They considered that the rate of flotation is a function of the concentration of air bubbles as well as floatable particles. Their kinetic expression is given in Equation 2.9.

$$- \frac{dC}{dt} = KC^n A^a$$

(2.9)

where:

A is the concentration of air bubbles in the pulp,

a is the reaction order with respect to bubble concentration

Under conditions of constant aeration, A is also constant and this model reduces to the form of equation 2.8. With this reduction, the rate constant is modified (lumped!) to reflect simultaneous influences of both aeration and floatable particle concentration. Jowett [35], Brown and Smith [39], and Bushell [34] contend that flotation is a first order rate process such that in the model, n assumes a value of 1. Arbiter [40] suggested that improved accuracy is realized if n is equal to 2 (second order reaction). de Bruyn and Modi [41] suggest that the order is split, being first order for particles finer than 65 microns and of order 3.2 for coarser particles.

With n equal to 1, the integrated form of the kinectic model given in Equation 2.8 is expressed as:

batch flotation: $C = C_{\bullet} \exp(-Kt)$

(2.10)

where: $C_{\bullet}$ is the concentration of valuable mineral in the pulp at $t=0$

continuous flotation: $C = C_o/(1+K\theta)$

(2.11)

where: existence of a single perfect mixer is

assumed,

θ is the nominal residence time for a single

flotation cell

Jowett and Safvi selected bituminous coal as a
preferred experimental material because only a frothing
agent was required due to the inherent hydrophobicity of
their samples. Also, coal's low specific gravity minimized
the possibility of sanding and stratification. Salt was
selected as a frothing agent because of its low adsorption
capacity on coal surfaces. This promoted true equilibrium
conditions which they claim were absent from Brown and
Smith's experiments due to continual adsorption of the
cresylic acid frother on coal surfaces.

If the residence time in a flotation cell is infinite,
all of the floatable feed material will report to the
concentrate. At realistic flotation periods, a small
fraction of floatable material remains in the tailings
stream. Attainment of 100 percent recovery from batch tests
which use the concentrates of previous tests as feed
material, is not possible. Morris attributed this to the
fact that floatable material is recovered with the proviso
that it is present in quantities which assure the
maintenance of minimum values of Pc and Pa. Pulp density is
an important factor of flotation recovery. Jowett restricted

the applicability of the kinetic model to describe only the recovery of the floatable component of the feed material. For continuous flotation proceeding with first order kinetics, the modified model is given by Equation 2.12

$$R = K \left[\frac{M(1 - \alpha)}{Qt} \right]$$

(2.12)

where:

M is the fraction of floatable material in the feed pulp,

α is the fractional yield of floatable material at the cell residence time,

Qt is the tailings volumetric flowrate

M is quantified as the maximum recovery of a batch test conducted under conditons simulating the continuous operation.

Bushell [34] contended that since collector reagents adsorb to some extent on all particle species the success of flotation is a matter of selectivity. In kinetic terms, selectivity implies the establishment of differential rates of flotation amongst the species present in the feed. The non-floatable fraction of a species consists of heterogeneous mixtures of values and gangue (locked particles), and liberated values which are insufficiently collector activated. Figure 2.8 illustrates the recovery of the floatable component from a batch test. The model which describes this situation is:
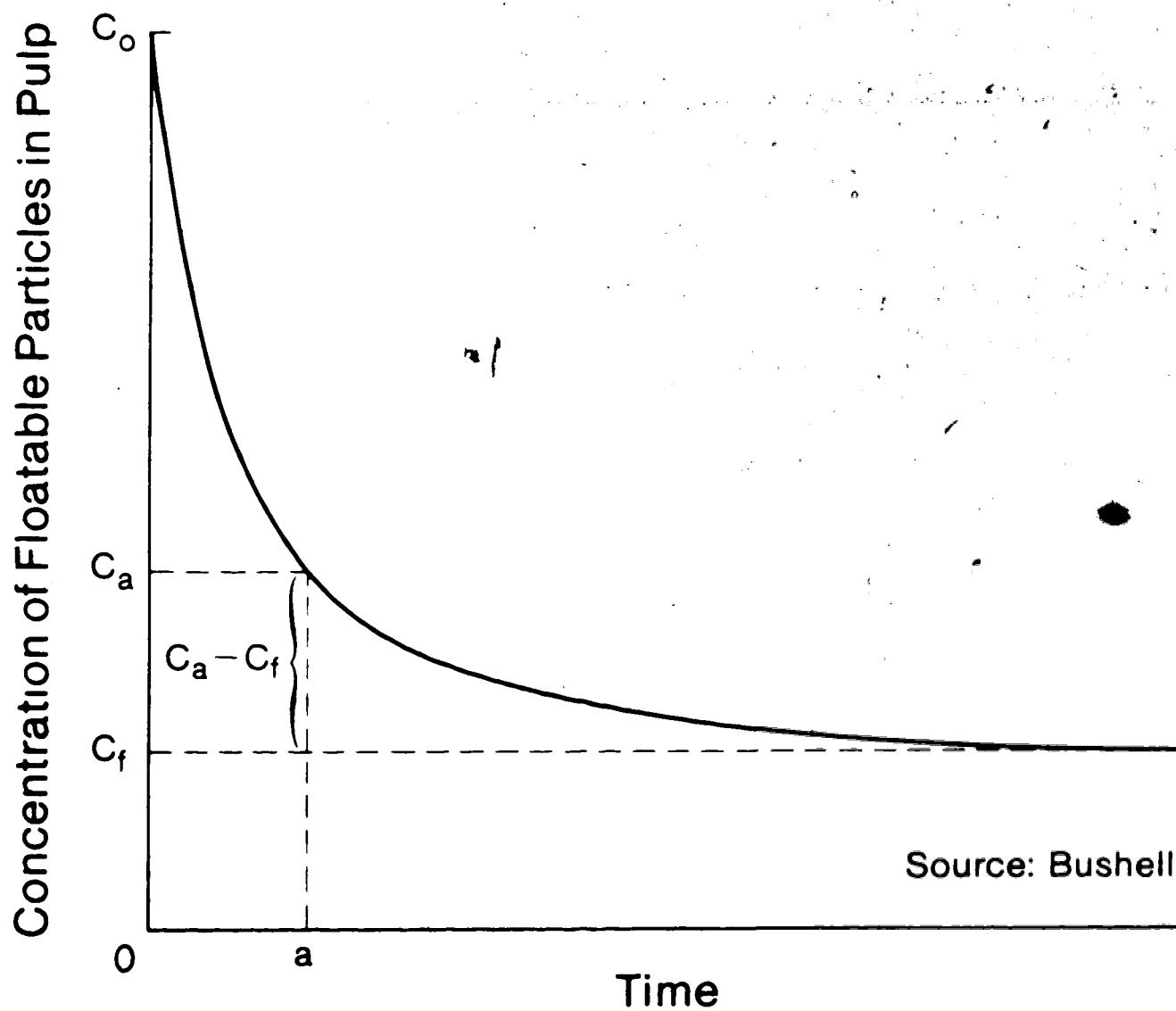
Fig. 2.8 Concentration of Floatable Particles in the Pulp as a Function of Time

$$Ca - Cf = (C_0 - Cf)[exp(-Kt)]$$

(2.13)

Recalling Schuhmann's consideration of the froth phase, Bushell formulated a differential equation to describe mass transfer across the froth. This is expressed by Equation 2.14.

$$- \frac{dC}{dt} = - \frac{dB}{dt} + \frac{dP}{dt}$$

(2.14)

where:

$\frac{dB}{dt}$ is the rate at which bubble-particle aggregates enter the froth,

$\frac{dP}{dt}$ is the rate at which particles drain from froth to pulp

Tomlinson and Fleming [42] examined three flotation regimes. Flotation occurring under "free" conditions implies that no deficiencies of available collecting sites on bubble surfaces exist at any·time. Bubbles entering the base of the froth are sparsely coated which implies high levels of Pa. Free flotation is a first order process, favoured at conditions of low pulp density. Inhibited flotation represents the opposite extremity. It is characterized by a saturation of particles at the bubble surface - no collecting sites are available. Inhibited flotation is independent of the concentration of floatable particles and , as such is a zero order process. The inhibited regime is promoted by high pulp densities, deep flotation cells, and

coarse flotation feeds. Transitional flotation occurs between these extremes. The flotation rate is a compound function of floatable particle concentration and air bubble concentration. The order of the reaction is between zero and one. Flotation proceeds by the inhibited regime at the early stages of a batch test. With increasing time (or position along a continuous bank of cells), the regime evolves through the transitional stage and eventually, free flotation is realized. Using this approach, Tomlinson and Fleming declared the overall flotation reaction to be of indeterminate order.

Imaizumi and Inoue [43] suggested that the overall flotation process is a composite of the following independent mechanisms:

1. Encounter of particles and bubbles in the pulp phase,

2. Attachment of particles to the bottom of the froth column as promoted by agitation in the pulp phase,

3. Selective precipitation of gas dissolved in water onto particles in the pulp phase,

4. Mechanical entrainment of particles into the froth column by water.

Valuable mineral particles are recovered predominately by the first mechanism whereas gangue particles are placed in the concentrate via the fourth mechanism. Assuming there is no interaction between the four mechanisms, the number of particles floated per unit time is given by the sum of the particles floated according to each regime. This in turn is

proportional to the number of particles in the system, hence, the flotation process ideally conforms to the first order rate equation.

There exist two contributors to deviation from first order behaviour. One source is due to the interaction between the four courses of flotation. A more important source is the distributed nature of rate constants with respect to physical characteristics such as particle size and specific gravity. In essence, the flotation feed is considered to be an assemblage of distinct classes of homogeneous flotation behaviour. The first order rate equation with distributed rate constants is expressed as:

$$C = C_o \int_0^\infty F(K) \exp(-Kt) dK$$

(2.15)

where: $F(K)$ is the distribution function of first order rate constants

A graphical procedure is used to determine the distribution function $F(K)$, as a line spectrum with discrete values of K. The ambiguous nature of K is realized since the model describes overall recovery without specifying which of the above mechanism(s) is preferred. The lumped parameter K is a function of both the flotation machine conditions and the degree of floatability displayed by the particles. Quantitative comparison of the floatabilities of two species is provided by the ratio of K values for the species. This ratio is a separation index measuring the efficiency of the

flotation operation. Aplan [29] uses this ratio concept in the derivation of his flotation index which is applied to coal-pyrite separations. Aplan's index is illustrated in Equation 2.16.

$$FI = \sqrt{(y_1 - 50) \cdot (Kc/Kp)}$$

(2.16)

where:

FI is Aplan's flotation index,

y_1 is yield after 1 minute in a batch test,

Kc is the first order rate constant for coal,

Kp is the first order rate constant for pyrite

Imaizumi and Inoue confirmed Morris' observation of the distribution of flotation rates over particle size. This relationship is illustrated in Figure 2.9. The flotation efficiency of fines is controlled by van der Waal's and electrostatic forces. By Jowett's [44] revision, reduced flotation rates of fine particles is a result of decreased momentum of particle particle collisions. Flotation efficiency of intermediate particles is controlled by the duration of bubble-particle contact relative to induction time. In the coarse range, contact angles, and the influences of hydrodynamics and turbulence are the controlling variables. Figure 2.9 also shows the influence of collector concentration on flotation rates. Adjustments of collector dosage has greatest impact on the coarse particles, diminished influence on fines, and minimal
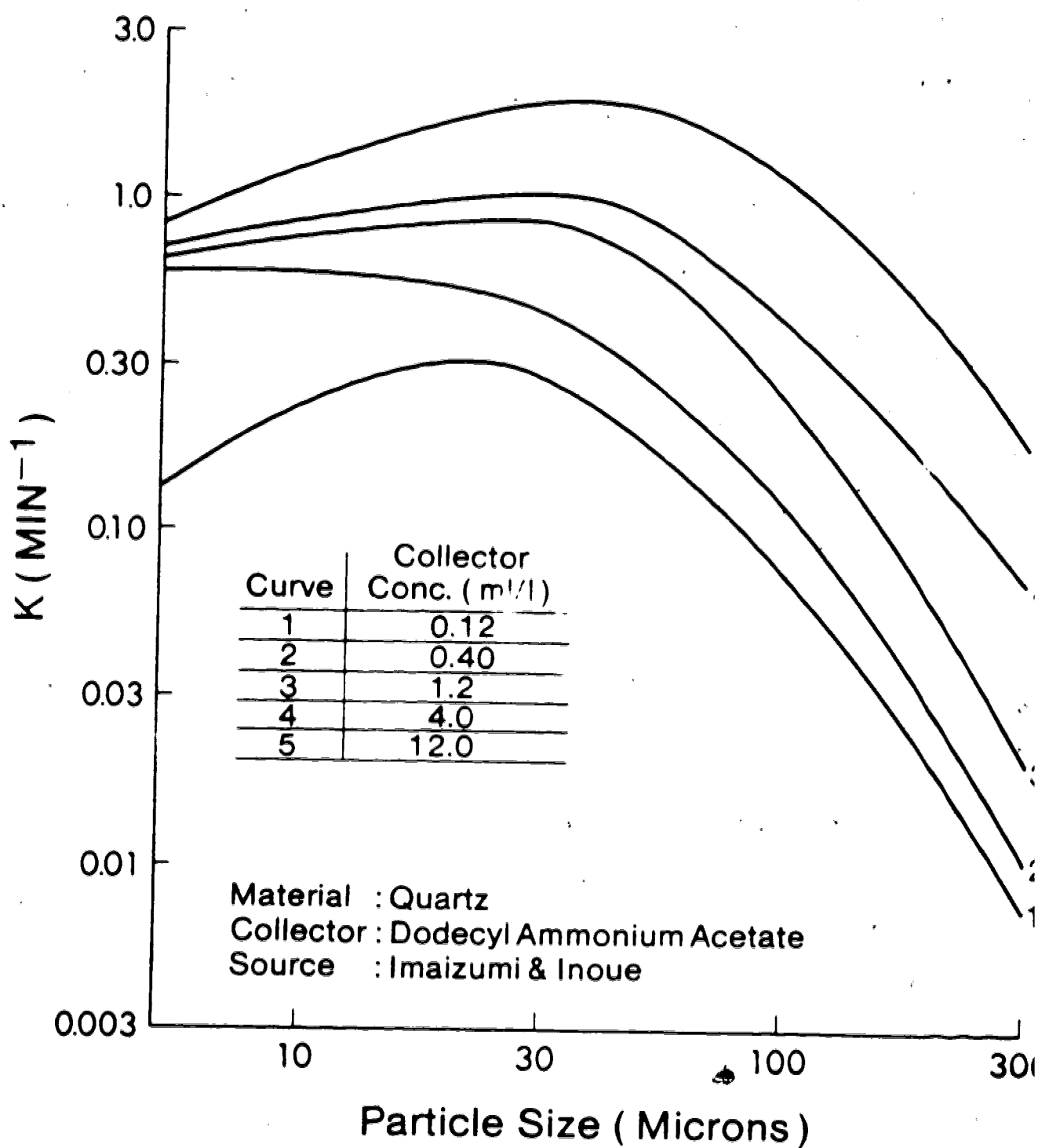
Fig. 2.9   Flotation Rate as a Function of Particle Size

effects on the intermediate size. This relationship was also noted by Steiner.

Kelsall [45] considered flotation feeds as binary mixtures of valuable and gangue species. The valuable fraction has a relatively high level of flotation probability, while a low flotation probability is assigned to the complement (gangue). Paralleling Imaizumi and Inoue, the score was defined as the ratio between high and low probabilities. Focusing on the valuable species of the flotation feed, liberated particles are associated with a high probability whereas locked valuable-gangue composites constitute the low probability fraction. The degree of liberation should be in the order of 90 percent implying that the majority of the values will display the high level of probability. The overall probability displayed by the valuable fraction is a weighted average of the probabilities represented by the liberated and locked particles.

The probability values are lumped products of contributions stemming from flotation cell hydrodynamics and the interaction between the mineral species and the flotation envirnment. In their work, Tomlinson and Fleming expanded this idea into the form expressed in Equation 2.17.

$$P = Pa \cdot Pc \cdot Pe \cdot Pf$$

(2.17)

where:

P is the probability of flotation,

Pe is the probability that the bubble-particle

aggregate is stable in the pulp,

Pf is the probability that the particle survives

secondary cleaning action and reports to the

launder

Schuhmann's original Pa has been factored into a probability

Pe, representing the stability of the bubble-particle

aggregate, and Pa which indicates the relationship between

contact and induction time.

Algebraically, Kelsall's probability model is expressed

as:

$$W = W_{\bullet}(1 - P)^N$$

(2.18)

where:

$W_{\bullet}$ is the weight of valuable species in the feed,

W is the weight remaining in the pulp after passage

through N identical cells,

P is the probability of flotation in any cell

Rearranging Equation 2.18;

$$W/W_{\bullet} = (1 - P)^N$$

(2.19)

The right side of Equation 2.19 can be expressed using the

binomial theorem expansion:

$$(1 - P)^N = 1 - \left\{ \begin{matrix} N \\ 1 \end{matrix} \right\} P + \left\{ \begin{matrix} N \\ 2 \end{matrix} \right\} P^2 - \left\{ \begin{matrix} N \\ 3 \end{matrix} \right\} P^3 \cdots$$

$$(2.20)$$

If N is large, and because P is less than 1, the binomial coefficients are approximated as:

$$\left\{ \begin{matrix} N \\ 1 \end{matrix} \right\} \simeq N, \quad \left\{ \begin{matrix} N \\ 2 \end{matrix} \right\} \simeq \frac{N^2}{2!}, \quad \left\{ \begin{matrix} N \\ 3 \end{matrix} \right\} \simeq \frac{N^3}{3!}, \cdots$$

Therefore:

$$(1 - P)^N \cong \left[1 - NP + \frac{(NP)^2}{2!} - \frac{(NP)^3}{3!} \cdots \right]$$

$$(2.21)$$

which is the Maclaurin series expansion for $\exp(-NP)$. Under the conditions which Equation 2.11 was derived, W/W_o is equivalent to C/C_o. Thus, $\exp(-NP)$ is equivalent to $\exp(-Kt)$. This illustrates the common ground between first order kinetic and probablistic flotation models. Jowett et al [46] emphasized that kinetic models must be applied with consideration of the flow regime associated with the flotation process. In batch flotation, an equal residence time exists for all particles in the reactor (flotation cell). This is analogous to the plug flow regime and the first order recovery of a species is given by Equation 2.22.

$$Rp = 1 - [\exp(-Kt)]$$

$$(2.22)$$

where: Rp is the recovery at time t with conditions of piston flow

With continuous flotation, the residence time distribution

is generally more complex, consisting of some combination
of: piston flow, perfect mixing, and stagnant volume. The
perfect mixer recovery model, as shown in Equation 2.23
applies in this case.

$$Rm = 1 - \frac{1}{(1 + K\theta)^N}$$

(2.23)

where:

Rm is the recovery with conditions of perfect mixing

2.3.3 The Three Parameter Model

Lynch et al [47] studied the primary and secondary
cleaning sub-processes. They applied a kinetic model to
describe recovery over the pulp and froth phases and
suggested manipulation of the froth phase as a method of
controlling the flotation circuit. They considered that the
most important variables affecting flotation should be
characterized and related to circuit performance.
Independent variables acting on the flotation process (as
opposed to being reflections of the process) are categorized
as either manipulated or disturbance types. The former
essentially determines the flotation environment through
adjustments of reagent concentrations, pulp level, and
aeration rates. In Woodburn's terminology these are process
variables. Examples of the latter include: head grades,
degree of oxidation, and fineness of natural grain size.
These are inherent properties which Woodburn calls State

variables.

Lynch considered that a first order kinetic model for continuous flotation of a heterogeneous feed should acknowledge the distribution of rate constants with respect to particle size and residence time within the flotation cell. In algebraic terms the model is:

$$C = C_0 \int_0^\infty \int_0^\infty \exp(-Kt)E(t)F(K)dtdk$$

$$(2.24)$$

where: $E(t)$ is the function defining the
distribution of residence time

A form of the function $E(t)$ has been suggested by Imaizumi and Inoue. It is described by Equation 2.25.

$$E(t) = \frac{1}{(N-1)!\theta^N} \cdot (t^{N-1})\left[\exp(-t/\theta)\right]$$

$$(2.25)$$

With Imaizumi and Inoue as a precedent, Lynch et al discretized the rate constant distribution to simplify the model. Leaning on Kelsall's flotation probability theory, mineral species of the feed were segregated into two components. The fast floating component was characterized by a high rate constant, Kf, relative to that of the slow floating component Ks. The proportion of the slow floating material, $\emptyset$, constitutes the third parameter of the model. For continuous flotation, the first order model is:

$$C = C_o \ [\emptyset exp(-Kst) + (1-\emptyset)exp(-Kft)]E(t)dt$$

$$(2.26)$$

where:

Ks is the rate constant associated with the slow

floating fraction of a mineral species,

Kf is the rate constant associated with the fast

floating fraction of a mineral species,

$\emptyset$ is the fraction of feed material which is slow

floating

Values of the three parameters are estimated from batch test

data. Figure 2.10 describes the relationship between these

parameters.

The model, expressing recovery from a continuous bank

of flotation cells (operating as perfect mixers) is given by

Equation 2.27.

$$Rm = 1 - \left[\frac{\phi}{(1 + Ks\theta)^N} + \frac{1 - \phi}{(1 + Kf\theta)^N} \right]$$

$$(2.27)$$

If flotation proceeds with the piston flow regime (batch

condition) then:

$$Rp = 1 - \{\emptyset[exp(-Kst)] + (1-\emptyset)[exp(-Kft)]\}$$

$$(2.28)$$

A component is defined as all material which responds

in the same way to a particular mass transfer driving force.

Three components are isolated within sulphide ore flotation

feeds. These are: valuable sulphide particles, gangue
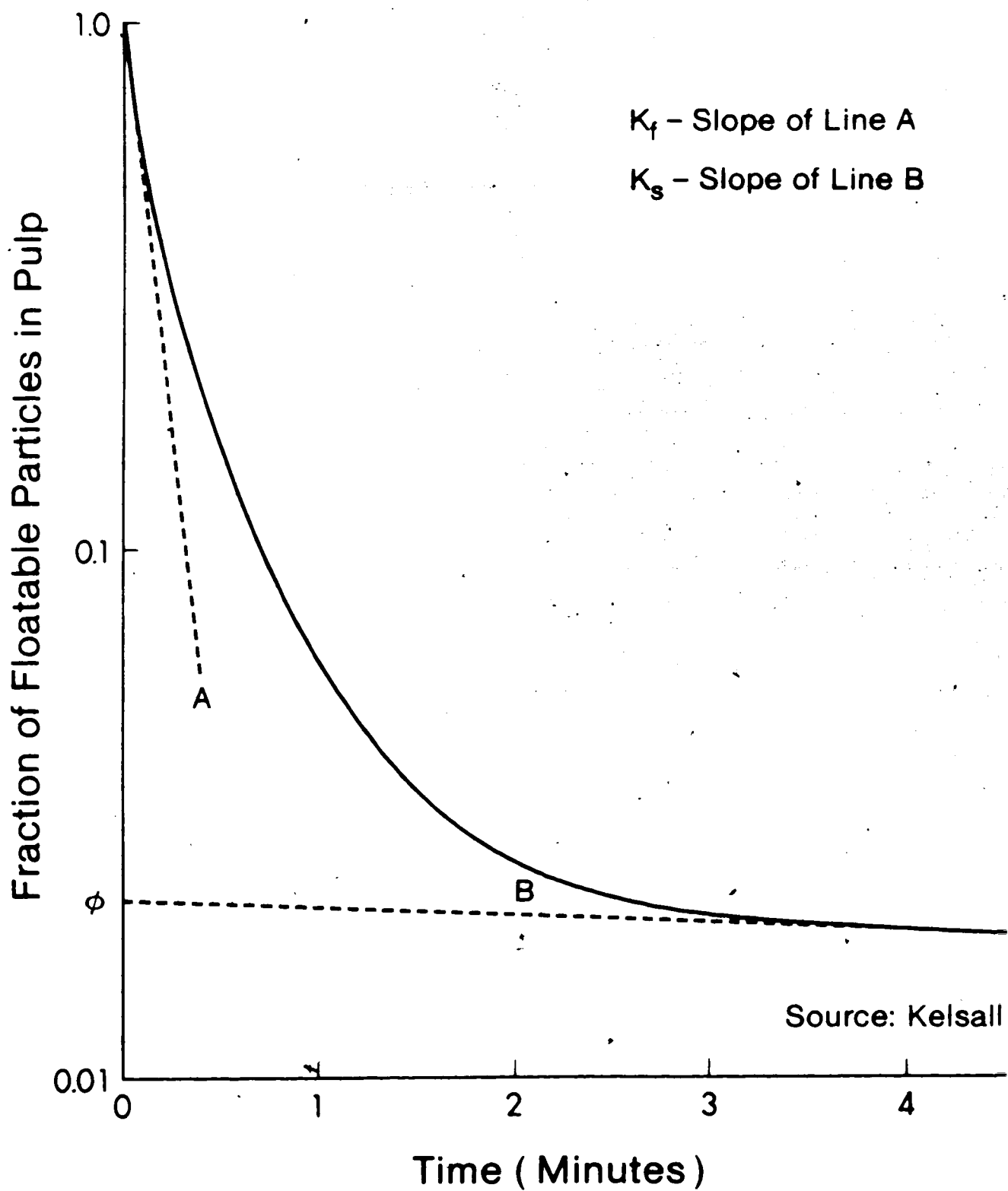
Fig. 2.10 Derivation of Parameters K_f, K_s, ϕ (Batch Test Data)

sulphide particles, and non-sulphide gangue particles. In a concentrator treating a complex ore by differential flotation, an economic mineral like galena is a valuable sulphide within its own flotation circuit but is a gangue sulphide in the sphalerite flotation section. Valuable and gangue sulphide components are recovered predominantly by bubble attachment; the latter being recovered at a slower rate. The mechanism for recovery of liberated non-sulphide gangue particles is mechanical entrainment with water. To account for this, empirical linear models are developed describing gangue recovery as a function of water recovery.

The fast floating fraction Kf of the valuable sulphide component consists of intermediate size liberated particles. The slow floating group Ks includes locked intermediates together with the fine and coarse extremities of the liberated values. With respect to the gangue sulphide component, Imaizumi and Inoue, as well as Englebrecht and Woodburn [9] commented on the dual nature of pyrite recovery. During the initial stages of flotation, pyrite recovery is independent of water recovery to the concentrate. In time, however, the recovery rate diminishes and is controlled by the water recovery.

The influence of manipulated variables on the parameter has been studied. Steiner observed that increased collector concentration promotes coarse liberated values into the fast floating fraction ($\emptyset$ is reduced). Recovery increases but only to a certain level as shown in Figure 2.11. Ideally,
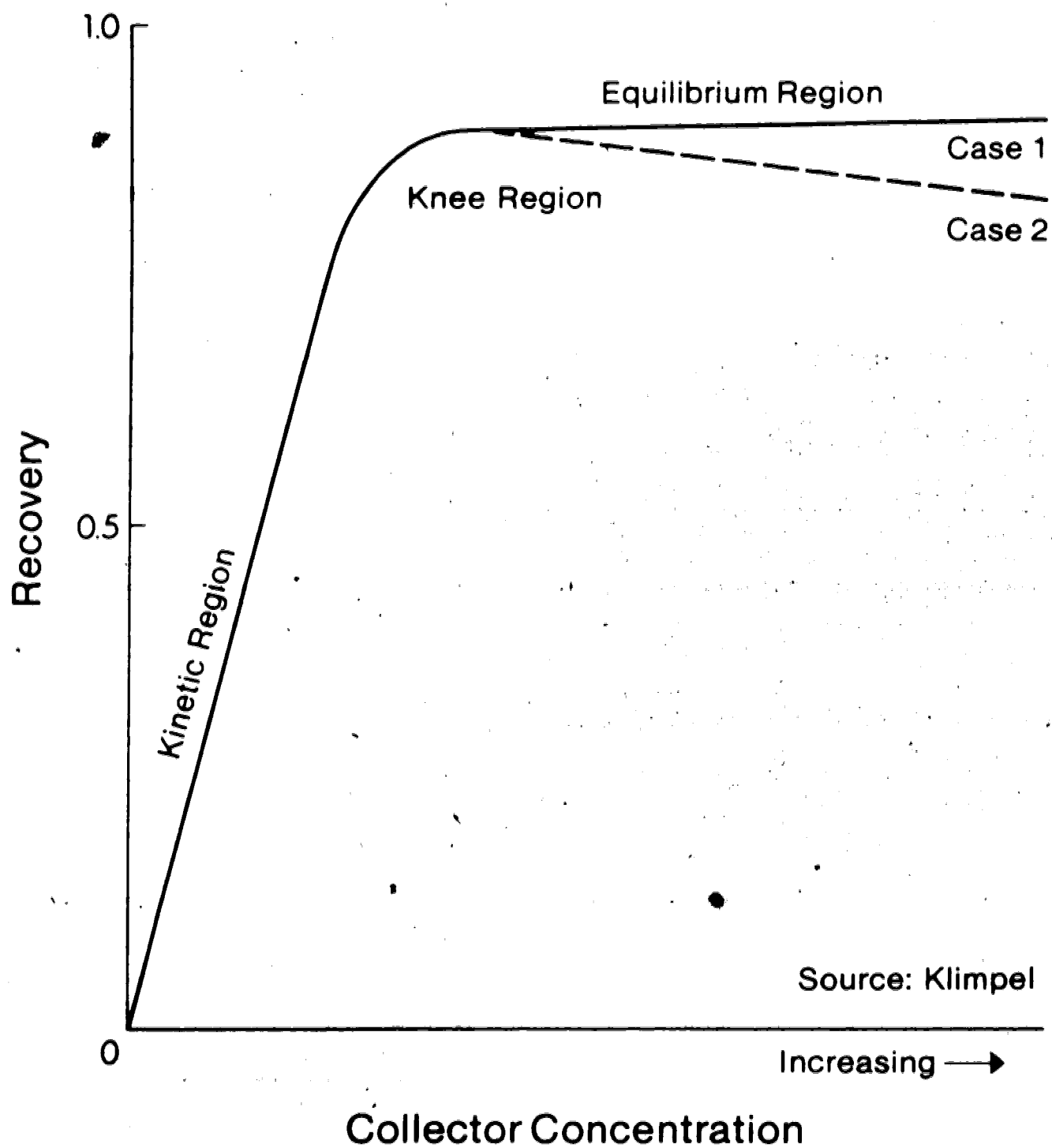
Fig. 2.11   Relationship Between Recovery and Collector
Concentration

collector dosage will maintain the flotation operation in the "knee" region of this curve. Low economic efficiency is associated with the equilibrium region. Case 2 of Figure 2.11 illustrates the difficulty of operating with a strategy that maximizes grade at constant recovery. It is difficult to determine proper collector dosage adjustments which are necessitated by excursions of recovery from set point. Aeration controls recovery in a linear fashion. Aeration predominately influences Kf[50,61], however, this lumped parameter reflects the influence of other variables as well. The recovery of water is controlled by froth height and aeration. Flint [48] contends that recovery of water and concentrate is a function of froth residence time which in turn is linear with respect to froth thickness. The latter is easily controlled through regulation of pulp level with respect to the concentrate overflow lip. Changes in fractional volume of air in the pulp, and position of the tailings overflow weir will promote changes in pulp level. A thin film of water envelops each bubble entering the froth. If aeration is decreased, fewer bubbles enter the froth, hence, water recovery is reduced. Reduced water recovery is reflected by increased values of and concentrate grade.

The three parameter model was incorporated with the flotation control strategy developed at Mount Isa Mines [49]. The first four rougher flotation cells are used to characterize the response of the feed to the flotation environment. Characterization is performed with on-stream

assaying and flow measurement performed with high frequency. The model is executed and adjustments of collector dosage and aeration are made to maintain constant recovery from the roughers. These manipulated variables are simultaneously adjusted at the cleaner circuit in a feed-forward manner. It is essential to realize that characterization of the fast floating fraction of the valuable sulphide is performed. The model is accurate for rougher flotation, however, if it is applied directly to scavenger and cleaner stages, erroneous predictions may occur because the characterization would not be representative of the particles in the pulp at these latter stages. These particles are representative of the slow floating fraction of the valuable sulphide.

Lynch et al [50] applied the three parameter model (Equations 2.27, 2.28) to describe flotation of bituminous coals. Coal flotation feeds are assumed to consist of: a combustible coponent, an incombustible component, and water. The latter represents water added to the feed solids, not the moisture content of the coal. Inherent ash and locked particles renders hypothetical the distinction between incombustible and combustible fractions. Particles of the latter contain randomly distributed fragments of the former, which are inseparable at the preparation phase of coal processing. In terms of the model, the distinction between these two components is subtle. It is considered that the incombustible fraction is recovered by the same mechanism as the combustible fraction but at a slower rate (lower values

of Kf). The model is applied to both components to estimate respective recoveries. Then the results are combined (the feed is reconstituted) to obtain an estimate of concentrate grade.

No correlation was observed between the lumped parameters and specific manipulated variables. At constant levels of Kf and Ks, however, it was shown that collector concentration affects $\emptyset$ in the manner reported by Steiner. Optimum flotation control is realized by maintaining collector dosage in the knee region of Figure 2.11.

An "overloaded" froth condition develops when an excessive rate of transfer of solids from pulp to froth freezes the froth layer, reducing its mobility. Englebrecht and Woodburn state that water recovery to the concentrate is a function of froth mobility which in turn depends on numerous factors. If there is a large number of colloidally dispersed solids, the froth is pinned, reducing the transverse motion towards the concentrate overflow lip. Particle and bubble size distributions and the chemical environment through its effect on bubble armouring also determine froth mobility. An overloaded froth is undersirable since froth residence time increases, translating to decreased recovery. If it occurs, froth overloading is displayed in the first few cells of a bank. Recovery is not easily regained at cells downstream because of short bank retention time (length). Also, the secondary cleaning action of downstream cells is reduced and the

designed performance of the flotation equipment not realized.

Lynch proposed the control of coal flotation according to the flowsheet given in Figure 2.12. This scheme is currently being plant tested. The first two cells of the bank characterize the response of the feed to the flotation environment. Recovery from this section is maximized by prevention of froth overloading. Collector addition is low and water recovery, stimulated by frother addition, is high. The balance between collector and frother additions is adjusted to minimize feed induced excursions from a recovery set point. The second section of the bank is dedicated to the maintenance of the customer's ash specification. The bulk of the collector addition is made here. Froth overloading is not likely as the majority of the fast floating fraction is recovered in the first section. Interaction between collector and froth reduces water recovery and entrained incombustibles. In addition $\emptyset$ is reduced by the collector addition and coarse combustible particles are promoted to the fast floating fraction. This situation is undesirable if the promoted particles represent a middlings species. Promotion of these locked coarse particles jeopardizes attainment of the contracted concentrate grade. To be effective, coal flotation control strategies must be customized to suit the nature of individual feeds.
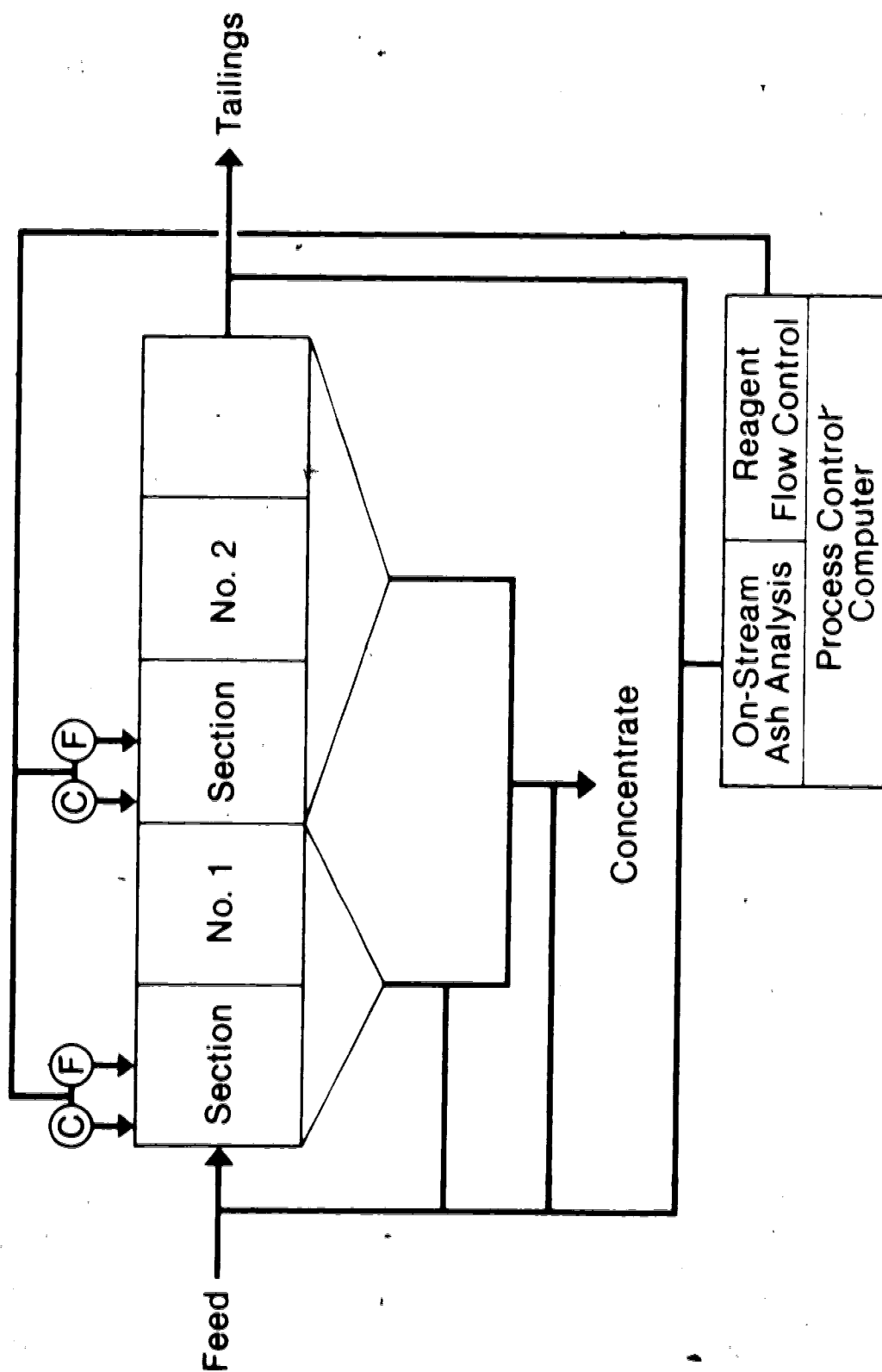
Fig. 2.12   Control of Coal Flotation

Source: Lynch

C – Collector
F – Frother

2.3.4 The Two Parameter Model

Harris [51] perceives the evolution of kinetic models towards the ideal expression in which parameters are uniquely related to independent process variables. The two parameter model presented by Klimpel et al [52] retains the lumped parameter form, yet, is an evolutionary advance. Improved computing efficiency is realizable as the valuable species is represented by a single rate constant. The slow floating rate constant Ks is essentially a curve fitting parameter which maintains the accuracy of the model prediction. In this context, its physical meaning is reduced and Ø becomes the primary descriptor of the slow floating fraction. Klimpel shows that accuracy is available with a single rate constant. Retention of an additional rate constant constitutes "excess baggage" in the computational routine.

In the batch form of the model, the concentration of floatable particles in the pulp is a function of size, floatability, and time:

$$C = f(x,Sx,t)$$

(2.29)

where:

x is particle size,

Sx is floatability of a given size

Floatability is the product of probabilities of collision and adhesion $(Sx=Pa\,Pc)$. A floatable particle is

sufficiently hydrophobic to have a high value of Sx, irrespective of species; valuable and gangue particles are floatable. Recovery by water entrainment is not elaborated by the model. The first order batch model is given in Equation 2.30.

$$z(x,Sx,t) = \frac{C(x,Sx,t)}{C(x,Sx,0)} = \exp(-Nb \cdot Sx \cdot t)$$

(2.30)

where Nb is the number of frother coated bubbles per unit volume of pulp

Given the upper limit of recovery of floatable particles within discrete size ranges of a feed, the long range batch cell recovery, Rf is described as:

$$Rf = \int_{x_0}^{x_m} Rx \cdot P(x)dx$$

(2.31)

where:

Rf is ultimate recovery of the valuable component,

Rx is the ultimate recovery for particle size x (valuable component),

$P(x)$ is the feed particle size distribution (valuable component),

$x_.,x_m$ are smallest and largest particle sizes

The mass density distribution of floatable particles, $Pr(x)$ is given by:

$$Pr(x) = \frac{Rx}{Rf} \cdot P(x)$$

(2.32)

The distribution of floatabilities over size x is represented by $Fx(S)$. The recovery of valuable species over time is the product of the total fraction of the species present at time zero and the fraction of floatable material already removed from the cell. The former quantity is represented by the expression $Fx(s)RfPr(x)dxds$ and the fraction remaining unfloated at time t is $z(x,Sx,t)$. Therefore, the fraction of valuable mineral particles yet to be recovered is written as:

$$U = \int_{x_0}^{x_m} \int_0^{Sx,m} z(x,Sx,t) \, Fx(S)RfPr(x)dSdx$$

(2.33)

where Sx,m is the maximum floatability of a

particle, size x

Recovery is subsequently described by Equation 2.34, and the recovery for a monodisperse feed (single size range within the feed) is given in Equation 2.35.

$$R = Rf(1 - U/Rf)$$

(2.34)

$$R = Rf[1 - \int_0^{Sm} z(S,t)F(S)dS]$$

(2.35)

Woodburn suggested that $F(S)$ can be represented by a truncated gamma function. If, however, a rectangular distribution $(F(S)=1/Sm)$ is considered, then Equation 2.35

is reduced to:

$$R = Rf \left\{ 1 - \frac{1}{Sm \cdot Nb \cdot t} \left[1 - \exp(-Sm \cdot Nb \cdot t) \right] \right\}$$

(2.36)

Recalling Jowett's incorporation of air bubble concentration
(Equation 2.9), the first order rate constant can be
expressed:

$$K = Sm \cdot Nb$$

(2.37)

The final form of the two parameter batch flotation model is
given by Equation 2.38.

$$R = Rf\{1 - [1-\exp(-Kt)] / Kt\}$$

(2.38)

Klimpel tested this model from experiments with
Pennsylvanian bituminous coal. He observed that the total
mass removal of valuable coal plus incombusible gangue is a
first order process. This differs from Jowett's concept that
recovery of only the valuable is first order. The latter
principle applies to sulphide mineral flotation, where the
majority of the feed reports to the tailings stream.
Applying Jowett's concept to coal, Klimpel concluded that
something more complex than first order form would be
required. This is due to the majority of coal flotation
feeds reporting to the concentrate.

Klimpel [53] isolated frother concentration as a manipulated variable having great influence on recovery. The relationship between Rf and frother concentration resembles that illustrated in Figure 2.11. Operation at the knee of the curve is preferred to the equilibrium region. If the operating point is in the "kinetic" region (below the plateau), increased frother dosage contributes to increased recovery and economic performance.

If adjustment of one manipulated variable such as collector dosage or, aeration level promotes significant change in the value of K while Rf remains constant, then this adjustment predominately influences the mass removal rate. If the flotation circuit is underdesigned such that cell capacity is too small to accommodate the volumetric throughput, adjustments which increase K are desirable. Improvements in Rf reflect positive adjustment of the chemical environment. Improved recovery is attainable providing that the froth removal process is not rate controlling. Under circumstances of froth overloading, it is sensible to apply methods to increase K rather than Rf in efforts to restore high recovery levels.

3. EXPERIMENTAL

3.1 Apparatus

3.1.1 Cell Design

It is a tenet of metallurgical design engineers that the continuous mode pilot plant facility acts as the bridge between laboratory evaluation of a flotation flowsheet and the full scale plant. A pilot plant installation represents a considerable capital expenditure and requires co-ordination of a highly skilled laboratory staff. King [32] states that "a kinetic model to described the behaviour of single cells should be capable of providing a quantitative description of an entire flotation plant; otherwise, it would not be of much use as a tool for plant design and operation'." He performs batch flotation tests in cells which are geometrically scaled models of those constituting the flotation circuit under investigation. A similar approach was used in this study.

The flotation cell utilized by McIntyre Mines is the Wemco model 120. The identification scheme is based on cell length, the model 120 being 120 inches long. The width and height to the concentrate overflow lip are 7ft-6in and 4ft-5in respectively. Capacity, excluding the standpipe-impeller assembly, is 300 ft³. Including this assembly, cell volume reduces to 255 ft³. At McIntyre Mines,

sixteen cells are arranged in four parallel, identical rougher banks (see Figure 2.6).

The Wemco laboratory flotation machine is equipped with a bowl type cell of glass construction. Vortex swirl, indicative of the predominance of the tangential flow component, accompanies the operation of this machine. When a square cell common to the Denver type laboratory machines is substituted, the vortex is eliminated. This underscores the role of cell corners as baffles. The Wemco information brochure [55] details the high intensity cyclonic action which the disperser (stator) impacts during conversion of the tangential component of flow emerging from impeller blade tips. This was evidenced by the etching of the pattern of disperser apertures on the interior surface of the glass bowl. Construction of the scaled cell evolved around the impeller/disperser mechanism of the Wemco laboratory machine. It was hoped that constancy of power number between the two scales would be inherent with this procedure.

Dimensions of the scaled cell were derived from the impeller diameter of the laboratory machine. The fundamental scaling principle is maintenance of constant aspect ratio between the two scales. Aspect ratio exists between a "characteristic" length of the cell and the impeller diameter. The obvious characteristic length is the model identifying dimension. In some calculations, other dimensions may be labelled "characteristic".

3.1.1.1 Cell Length

<u>Scaling principle:</u> constancy of aspect ratio

<u>Model 120</u>   <u>Scale Model</u>

Characteristic length: 120 in
Impeller diameter: 22 in   Impeller diameter: 2 in
Aspect ratio = L/D = 120/22   Cell length = 2(5.45)
                = 5.45   = <u>10.9 in</u>

3.1.1.2 Cell Width

<u>Scaling principle:</u> geometric correspondence between
                    points

$$A = K(A) \cdot L^2$$

where: A is the froth area,
       L is the characteristic length,
       K(A) is the proportionality constant for A

<u>Model 120</u>   <u>Scale Model</u>

Froth area: 75 ft^2
Characteristic length: 10 ft

$$\begin{aligned}
&A = K(A) \cdot L^2 \\
K(A) &= A/L^2 \quad\quad = 0.75(10.9\text{in}/12\text{in}/\text{ft})^2 \\
&= 75 \text{ ft}^2/(10\text{ft})^2 \quad\quad = \underline{8.19 \text{ in}} \\
&= 0.75
\end{aligned}$$

3.1.1.3 Cell Height

<u>Scaling principle:</u> constancy of aspect ratio

<u>Model 120</u>   <u>Scale Model</u>

Cell height: 53 in
Aspect ratio = H/D   Cell height = 2(2.41)
             = 53/22   = <u>4.82 in</u>
             = 2.41

3.1.1.4 Cell Volume

<u>Scaling principle:</u> geometric correspondence between points

$$V = K(V) \cdot L^3$$

where: V is the cell volume,
L is the characteristic length,
K(V) is the proportionality constant for V

<u>Model 120</u>   <u>Scale Model</u>

Cell volume: 300 ft^3
Characteristic length: 10 ft   Cell volume = 0.3(10.9/12)^3

$$K(V) = V/L^3 \qquad\qquad\qquad = \underline{0.25\ ft^3}$$
$$= 300ft^3/(10ft)^3 = 0.3$$

To facilitate construction, calculated dimensions were rounded to the closest integral value. The construction dimensions are given in Table 3.1. An illustration of the scaled cell is given in Figure 3.1 and Plate 1 shows the position of the cell within the equipment assemblage. Material of construction was 3/8 inch thick acrylic plastic.

Clean coal discharges into launders along the widths of each Model 120 cell. Two way discharge minimizes the residence time of floated particles in the froth structure which in turn maximizes yield. This feature is not readily duplicated in the scale model. As the best alternative, an inclined deflector or crowding board was installed at the rear wall. The crowding board was a trademark of machines manufactured approximately 40 years ago by the Minerals Separation Company [2]. It was also incorporated in the Leeds "Auto-Float" laboratory cell developed in 1972 [56].

Table 3.1 Construction Dimensions of a Scaled Flotation Cell

	Calculated Dimension	Construction Dimension
Length	10.90 in	11 in
Width	8.19 in	8 in
Height	4.82 in	5 in
Volume	0.25 ft^3	0.25 ft^3

Fig. 3.1 Laboratory Scale Wemco 120 Flotation Cell

6 Equispaced
Drain Holes

Scraper Blade

Froth Paddle
7¾ Long × 1½ Wide

Froth Paddle
Drive Shaft Supports

Drain

Level Detector Access

Make Up H₂O In

O/F Level

Units Inches
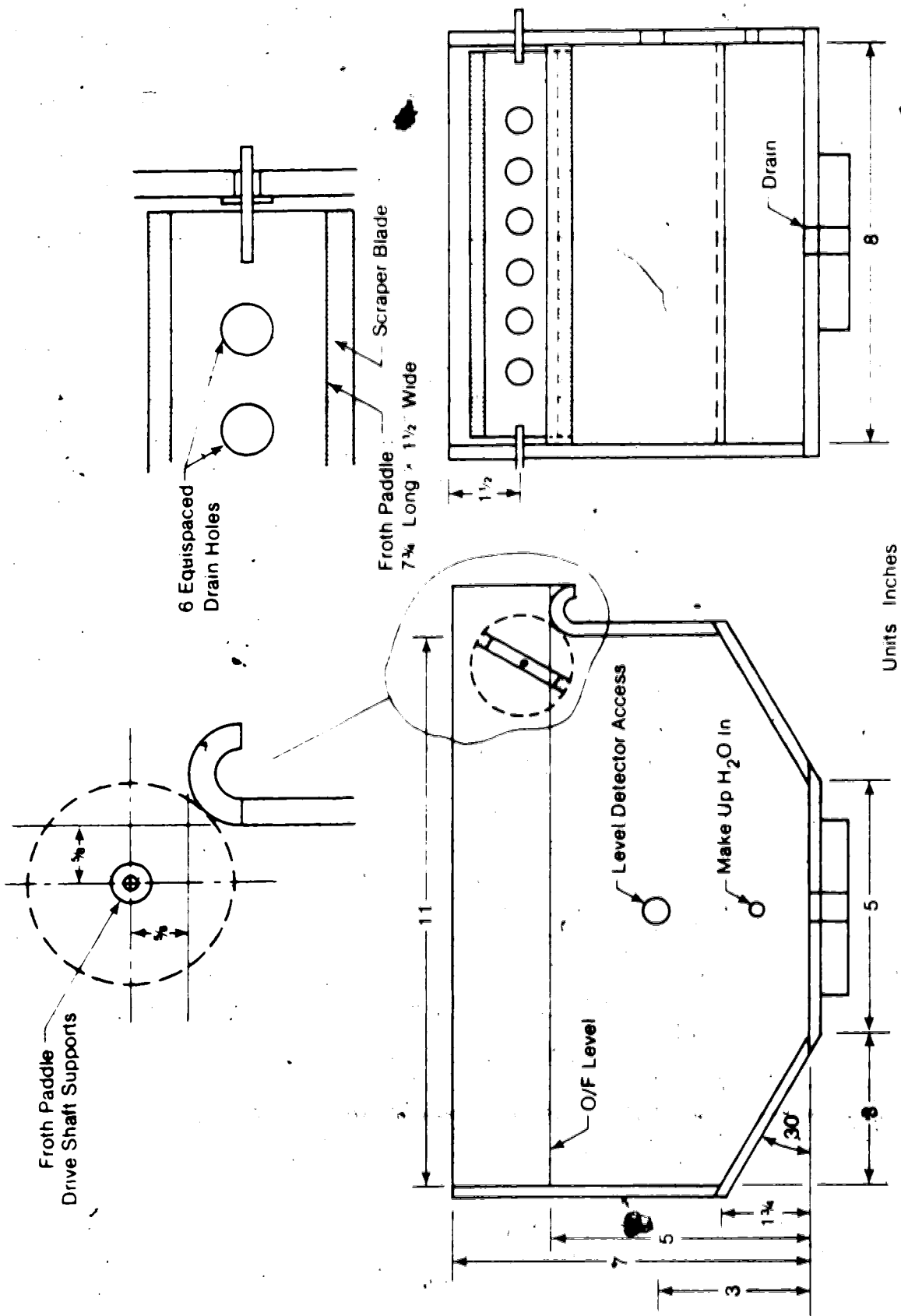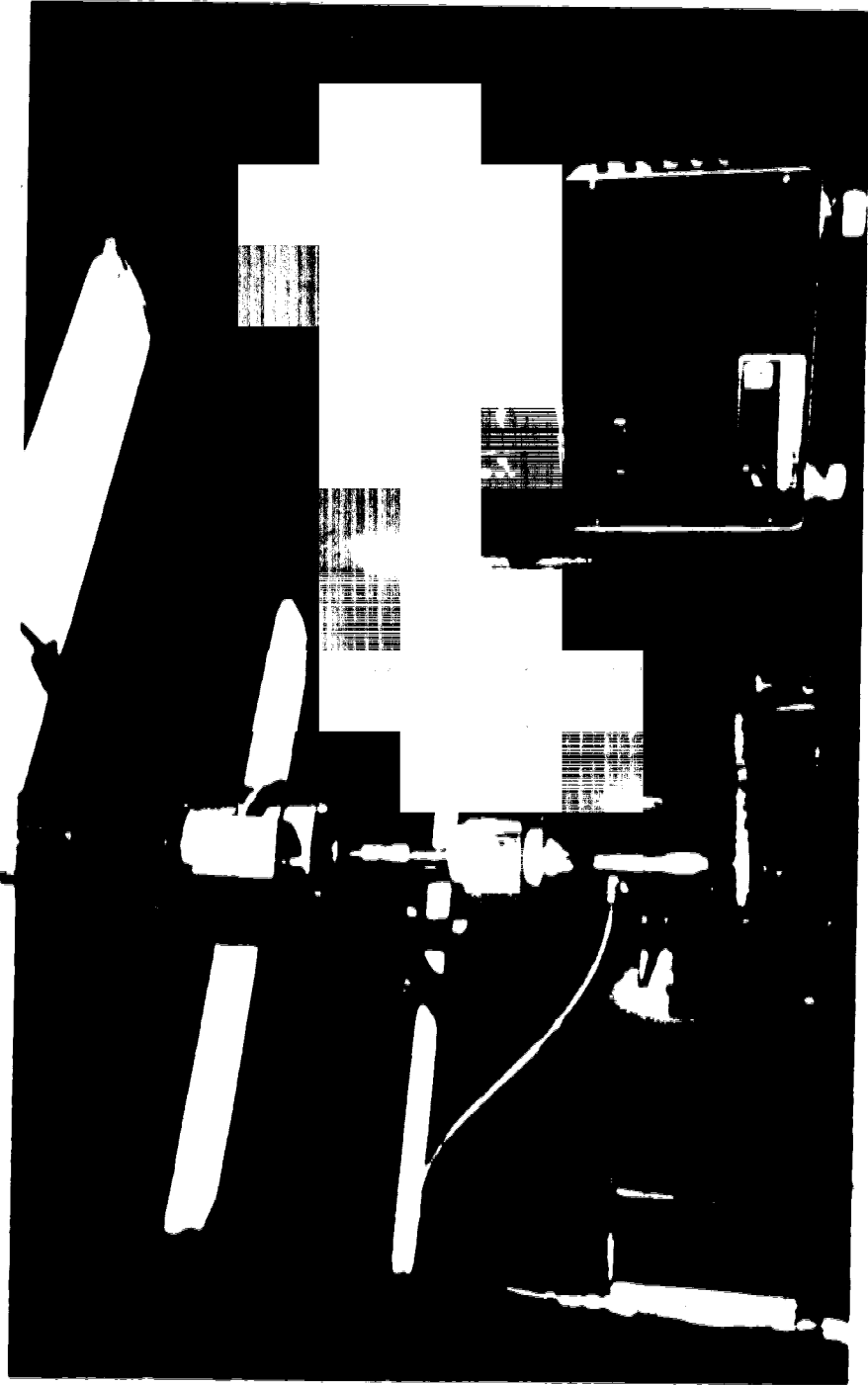
Plate 1. Laboratory Scale Flotation Machine

Particle-bubble aggregates impinging on the crowding board are deflected across the froth layer towards the concentrate overflow lip. At the lip, a two blade paddle scraper rotating at 50 rpm ensures regular discharge of clean coal into collection pans. Froth scraper blades were fabricated from self adhesive weatherstrip material. The automatic froth paddle also eliminates subjective bias associated with manual froth removal.

3.1.2 Measuring and Regulating Devices

3.1.2.1 Impeller Speed and Power

The impeller of a standard laboratory machine is usually driven by a 1/4 horsepower alternating current motor mounted parallel to the impeller shaft, at the rear of the machine frame. Power is transmitted by a drive belt turning through spring loaded split sheaves mounted on the motor and impeller shafts. Speed adjustment is available by varying the pressure on the drive sheave.

The flotation machine utilized in this study was driven by a 1/8 horsepower direct current motor mounted above the impeller. Selection of this motor was based on two reasons. Adjustment to the desired impeller speed is more easily accomplished through a potentiometer located in a master control panel. Secondly, estimation of power consumed by the impeller was facilitated. Consumed power was derived from a torque measurement taken with a spring scale fixed between

the machine frame and a rigid beam extending from the bearing mounted motor. The moment arm was 18.5 inches in length. The torque measuring assembly is shown in Plate 2. This method overestimates power consumed by the impeller because friction losses experienced by the impeller shaft bearing and the transmission coupling are not discounted. A more precise power measurement is obtained if the motor is fixed and the cell, equipped with torque measuring assembly, pivoted on bearings. Procedural considerations, however, require the cell to be a fixed, rigid structure.

Impeller speed was measured by two methods. A dial tachometer mounted on the motor shaft indicated approximate impeller speeds. Precise measurements were obtained with a portable stroboscope. The tachometer consistently overestimated "true" speed by 70 rpm. In performance of a test, the stroboscope frequency was set to the desired impeller speed and the motor potentiometer adjusted to "freeze" the rotating transmission coupling. To prevent excursions from the set speed, the motor was controlled by a thyristor feedback control circuit.

The impeller speed simulating plant conditions was determined to be 1100 rpm. The scaling calculations are as follows:
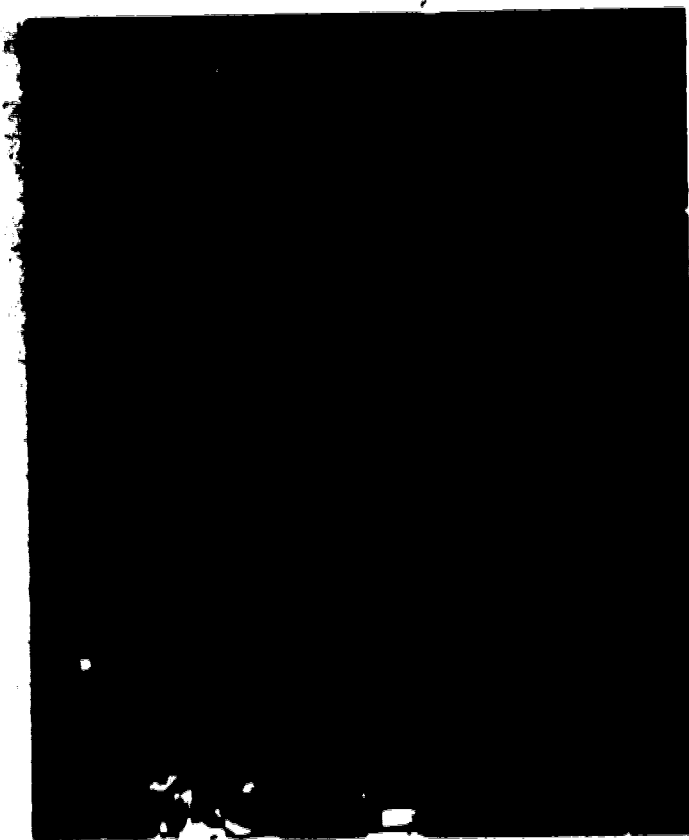
Plate 2. Torque Measuring Assembly

<u>Scaling principle</u>: similarity of particle dispersion

$$S = K(S) \cdot D^{\cdot \cdot \cdot}$$

where: S is impeller tip speed,
D is impeller diameter,
K(S) is the proportionality constant for S

<u>Model 120</u>	<u>Scale Model</u>
Impeller diameter: 22 in	Impeller diameter: 2 in
Impeller speed: 220 rpm = 21.1 ft/sec	$S = 17.3(2in/12in/ft)^{\cdot \cdot \cdot}$ = 9.57 ft/sec
$K(S) = S/D^{\cdot \cdot \cdot}$ = 17.3	$N = 9.57/3.14/(2/12)$ = <u>1100 rpm</u>

3.1.2.2 Aeration Rate

Air was introduced to the impeller region under pressure through a nipple in the upper region of the standpipe. Aeration rate was controlled by a regulator attached to a rotameter gauge. Accuracy of this gauge was determined by coupling it in series with a high quality gauge for which a calibration chart was provided. The flotation machine rotameter consistently underestimated "true" aeration rates. The least squares regression correlation between true and gauge value aeration rates is given by Equation 3.1.

True aeration rate = 1.555·(gauge value)+0.359

(3.1)

Regular inspections of tubing, fittings and the oil seal surrounding the impeller shaft were performed to detect the

presence of pressure leaks.

The scaled aeration rate simulating plant conditions was determined to be 5 litres per minute. The calculations are detailed below.

Scaling principle: linearity of Nq' with machine size

$$Nq' = K(Nq') \cdot D$$

where: K(Nq') is the proportionality constant for Nq'

Model 120	Scale Model

Air flow: 240 ft³/min
Froth area: 66 ft²

Froth area: 88 in²

$$Nq' = 240/(66 \cdot 220 \cdot 22/12)$$
$$= 9.02 \times 10^{-3}$$

$$Nq' = 4.92 \times 10^{-3}(2/12)$$

$$K(Nq') = Nq'/D$$
$$= 9.02 \times 10^{-3}/(22/12)$$
$$= 4.92 \times 10^{-3}$$

$$= 1.64 \times 10^{-3}$$

Air flow = 0.18 ft³/min
$$= 5 \text{ l/min}$$

3.1.2.3 Pulp Level

In the course of a batch test, the pulp level drops as concentrate is removed from the cell. The rate of drop is high for coal flotation as significant volumes of water are entrained in the copious froth moving over the concentrate lip. Changing pulp level adversely affects test procedure in two ways. Dispersed flotation reagents are transported out of the cell with concentrate water. This implies that the chemical environment of a batch test is not constant. As well, dropping pulp level renders the froth removal paddle ineffective. To alleviate these problems, a regulated supply

of replenishment water maintains constant pulp level during a test. An on/off controller detects the movement of an air-water interface in a manometer tube (connected to a diaphragm mounted on the tank wall) through changes in capacitance. At low level, a solenoid valve opens and replenishment water (plus frother) flows by gravity from an external source. The accompanying rise of water in the manometer triggers the circuity to shut the valve when the sensor level is passed. The diaphragm, manometer sensing device, and replenishment water inlet are detailed in Plate 3. This simple control system is extremely well behaved.

3.2 Experimental Materials

The coal consumed in the experimental program was obtained during a visit to McIntyre Mines in May 1979. Samples were retrieved from the plant feed stockpile at a location close to the rotary breaker building. Samples were stored in pails with tight fitting lids to prevent oxidation.

McIntyre extracts coal from both underground and open pit developments. Equipment used in the underground operation generates a particle size distribution which is finer than open pit material. From the preparation plant engineer's viewpoint, the feed stockpile has been poorly developed. Run of mine material from the different sources has been stacked in a fashion lying between the extremities
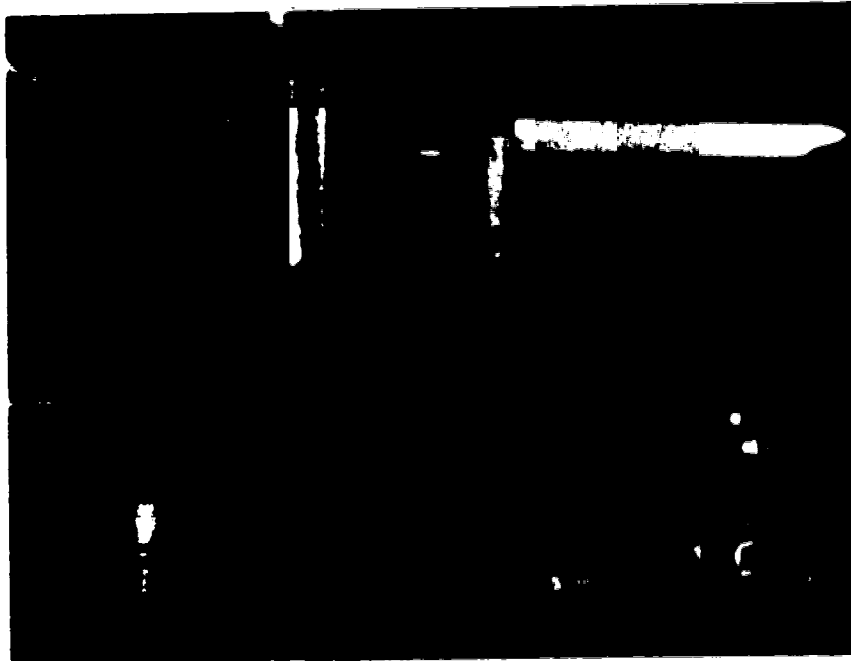
Plate 3. Pulp Level Control Device

of blending to produce consistency of plant feed and segregation to schedule "quasi-batch" plant operation at parameters tailored to a particular feed supply. The plant engineer constantly adjusts operating parameters without benefit of a feed supply forecast.

A particle size distribution of flotation feed was obtained by Flintoff [57] in August 1979. This distribution is given in Table 3.2. The Gaudin Schuhmann function was fit to the data using linear regression. The result is given in Equation 3.2.

$$y = (d/771)^{\cdots}$$

(3.2)

where:

y is the cumulative percent passing a given particle size,

d is the size modulus (100 percent passing size)

The most important feature concerning this flotation feed size distribution is the presence of particles coarser than 28 mesh. The plant flowsheet specifies that these particles are to be processed by the heavy media separation equipment, however, screening ineffeciency, created by aperture enlargement through wear, misplaces oversize particles in flotation feed. This feature was accounted for in the laboratory as some test feed samples were prepared according to the distribution given in Table 3.2.

Initially, the sample was split at 20 mesh with a high capacity vibratory screen. Oversize material was stage

Table 3.2 Particle Size Distribution of Flotation Feed

MESH	MICRONS	CUMULATIVE WT % PASSING
+28	+600	90.6
28x48	600x300	69.2
48x100	300x150	47.9
100x200	150x74	34.5
200x270	74x53	30.3
-270	-53	27.1

reduced by jaw and gyratory crushing; these products were screened to ensure a maximum particle size of 20 mesh. Stage crushing was utilized to prevent the possibility of generation of excess fines (particles 10 to 100 microns). Next, the sample was segregated into the size ranges indicated Table 3.2. This was a batch procedure; 150 gram lots of sample were dry sieved for 20 minutes with a Ro-Tap apparatus. Sieves were ultrasonically cleaned to prevent aperture blinding. Bulk quantities of each size range were established. Because of limited material handling in the laboratory, as compared to plant conditions, the two finest ranges were sparsely populated. Coarser particles were subjected to disc pulverizing in order to distribute particles into these ranges. Prior to each flotation test, specified amounts of each range were riffled from the bulk supplies and blended to generate a controlled feed size distribution. Thus, the size distribution typical of plant conditons (Table 3.2) was reproducable together with other distributions designed to monitor the influence of particle size on flotation. Control of ash content of flotation feed is not practicable because of the complex distribution of ash forming minerals into liberated and inherent components.

The selection of reagents was based on consistency with plant operation. Diesel oil was utilized as the collector reagent and Dowfroth 1012 was selected as the frother. The latter is a polypropylene glycol methyl ether having the basic molecular structure: $CH_3-(O-C_3H_6)-OH$. Klimpel [52]

recently reported superior performance of a frother molecule which substitutes a hydroxyl for the methyl group. This frother is marketed as Dowfroth 400. It was not included in this investigation, however, future evaluation could prove beneficial.

The addition rates for reagents to each cell bank at McIntyre are set at 800 cc/min. for diesel collector and 60 cc/min. for Dowfroth 1012. Adjustments required to maintain reagent flowrates at these levels are performed manually. The flotation operator lacks the authority to modify reagent addition parameters. Considering the average throughput of coal to be 30 tons/hr/cell bank average reagent dosages are 1.6 cc diesel collector and 0.12 cc Dowfroth 1012 per kg of coal feed. These dosages were maintained in the laboratory. Diesel collector addition to the flotation pulp was made at full strength with a microlitre syringe. Dowfroth 1012, being water soluble, was diluted to a 1% stock solution and additions performed with a 10cc syringe.

3.3 Method

Flotation tests were performed in the batch format according to the procedural flowsheet illustrated in Figure 3.2. A pulp having solids consistency of 9.1 weight percent was prepared in the cell by addition of 5 litres of distilled water to 500 grams of prepared coal. With the impeller rotating at 500 rpm, clusters of hydrophobic

```
┌─────────────────────────────────┐
│   Preparation of 500g Flotation │
│ Feed According to Pre-Determined│
│          Size Consist           │
└─────────────────────────────────┘
                 │
                 ▼
┌─────────────────────────────────┐
│  Add Feed & 5 Litres H₂O to Cell│
└─────────────────────────────────┘
                 │
                 ▼
┌─────────────────────────────────┐
│         Add Collector,          │
│      Condition 4 Minutes,       │
│    Regulate Impeller Speed      │
└─────────────────────────────────┘
                 │
                 ▼
        ┌──────────────────┐
        │   Add Frother    │
        └──────────────────┘
                 │
                 ▼
┌─────────────────────────────────┐
│            Aerate,              │
│    Regulate Impeller Speed      │
│         Measure Torque          │
└─────────────────────────────────┘
                 │
                 ▼
```

Froth Collection	
Increment No.	Cum. Time (sec)
1	15
2	30
3	60
4	120
5	180
6	240
Tailings	∞

```
┌─────────────────────────────────┐
│      Filter, Dry, Weigh         │
│        Test Products            │
└─────────────────────────────────┘
                 │
                 ▼
┌─────────────────────────────────┐
│        Sieve Analysis           │
└─────────────────────────────────┘
                 │
                 ▼
┌─────────────────────────────────┐
│        Ash Analysis of          │
│      Sized Concentrates         │
└─────────────────────────────────┘
                 │
                 ▼
┌─────────────────────────────────┐
│    Parameter Estimation,        │
│          Modelling              │
└─────────────────────────────────┘
                 │
                 ▼
┌─────────────────────────────────┐
│        Evaluation of            │
│          Results                │
└─────────────────────────────────┘
```

Fig. 3.2   Flowsheet of Laboratory Procedure

particles were broken to promote uniform dispersion. Pulp pH
was measured; adjustments to pH 7 were to be made only if pH
was outside the neutral range (6-8). The diesel collector
was added and a conditioning period of 4 minutes elapsed,
during which concentrate collecting trays were arranged and
impeller speed adjusted to the desired level. At the end of
the conditioning period frother solution was added and air
admitted to the impeller zone at a controlled rate. The
froth layer was established for 5 seconds prior to
collection. Concentrate was collected in six successive
intervals as outlined in Figure 3.2. The duration of each
interval, increased as collection proceeded to allow for the
exponential decay of the rate of mass transfer from pulp to
froth. This phenomenon is a feature of batch testing. Cell
walls, standpipe, and crowding board were rinsed with a jet
of water to prevent froth adherence at these locations.
Plates 4 and 5 show the flotation cell in operation. The
concentrate increments and tailings products were filtered,
dried, and dry sieved to determine the influence of particle
size on flotation rate. The weight of each size fraction was
recorded and ash content determined by oxidizing
approximately one gram of material at 750°C for one hour.
Associated with the ash analysis procedure is the evolution
of waters of hydration of the ash forming minerals such as
kaolinite ($Al_2O_3 \cdot 2SiO_2 \cdot 2H_2O$). To determine the weight of
mineral matter initially present, the ash content is
multiplied by the mineral matter/ash ratio. A ratio of 1.1
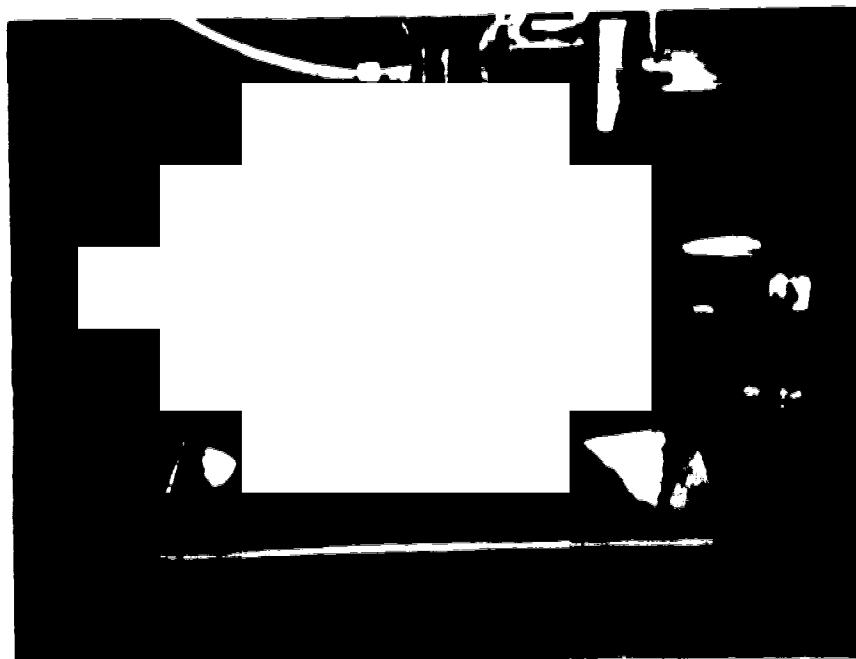
Plate 4.   Operation of Laboratory Scale
Wemco 120 Flotation Cell

Plate 5.   Froth Discharge From Laboratory
Flotation Cell

is an average value for the numerous ash forming minerals
such as illite, kaolinite, and montmorillinite.

Test data was arranged in a form describing the
"disappearance kinetics" of feed material (coal plus ash).
This relates the mass fraction of feed material remaining in
the cell as a function of time. This data was input to a
FORTRAN version of the Nelder-Mead Simplex search routine
[58] to compute the best valves of model parameters. This is
an off-line optimization procedure similar to the Simplex
Self Directing Evolutionary Operation method (SSDEVOP) which
is useful for plant optimization [59]. The coded program is
included in Appendix III. The three parameter model given by
Equation 2.27 was selected for use because its precision has
been established in numerous applications ranging from
sphalerite to coal. Model parameters were computed for each
size range and the composite flotation feed. This procedure
was duplicated for the ash component of the feed.

A residence time distribution (RTD) was determined for
a flotation bank at McIntyre Mines by the tracer impulse
method [57]. Comparison of the experimental and theoretical
RTD profiles indicated that the flow regime consisted of a
plug flow component (17%) plus 4 perfect mixers in series
(83%). The nominal residence time for the cell bank was 4.82
minutes. This includes the plug flow component. Thus, the
single cell average residence time was: 4.82/4 = 1.21
minutes. The parameter sets obtained for each test condition
and the single cell average residence time were fed to a

FORTRAN version of the flotation model. Data output consisted of yield and ash content of the concentrate product calculated for each cell along the bank and the overall, cumulative product. Results were also presented according to size fraction. The FORTRAN version of the flotation model is given in Appendix IV.

The experimental program was executed according to a 2^{5-2} fractional factorial design. This technique, described by Mular and Bull [59], permits the investigation of several factors simultaneously. Factors and interactions between factors which significantly affect (in a statistical context) the measured test response are revealed by this technique. This method has been successfully utilized by: Agar [60], Malhotra et. al.[61], and Somasundaran and Prickett [62]. Five factors were selected for investigation. These were: collector dosage, frother dosage, aeration rate, impeller speed, and fraction of flotation feed finer than 200 mesh. Centre point levels were established for these factors to simulate plant oprating conditions. High and low levels, equidistant from the centre points were determined. The design matrices of coded and uncoded levels are given in Table 3.3 and 3.4 respectively. Three centre point runs are included in the experimental design. The runs were performed in random order to eliminate bias. The design is "saturated" or, of Resolution III. This implies that main effects are not confounded with each other in order to prevent ambiguity. Significant two factor interactions can be

determined, however, higher order interactions are not resolvable.

The test response selected for use was the separation efficiency, *Es*, described by Schulz [63]. This is a single efficiency figure which permits the simplest and most precise means of comparing the efficiency of a separation process at different operating conditions. The separation process is considered to be ideal. Incorrect placement of particles stems from feed material which by-passes the separator and randomly contaminates the sorted products. The separation efficiency represents the proportion of feed material which is subjected to perfect separaton in any concentration process. At the extremes, *Es* is 0 for a sampling operation and 100 for ideal separation with the associated condition of perfect liberation. The inherent ash component of coal precludes complete liberation and the attainment of high values of *Es* (greater than 40). The algebraic form of *Es* is given by Equation 3.3.

$$Es = W \cdot \frac{c_m(c - f)}{f(c_m - f)} \tag{3.3}$$

where:

W is the weight recovery of concentrate (yield),

Table 3.3 Experimental Design Matrix: Coded Levels

		FACTORS				
RUN	TEST NO.	DIESEL X_1	AIR X_2	RPM X_3	FROTHER X_4 $(X_1 X_2 X_3)$	% -200M X_5 $(-X_2 X_3)$
1	21	-1	-1	-1	-1	-1
2	18	+1	-1	-1	+1	-1
3	17	-1	+1	-1	+1	+1
4	22	+1	+1	-1	-1	+1
5	19	-1	-1	+1	+1	+1
6	24	+1	-1	+1	-1	+1
7	20	-1	+1	+1	-1	-1
8	23	+1	+1	+1	+1	-1
cpt	12	0	0	0	0	0
cpt	13	0	0	0	0	0
cpt	25	0	0	0	0	0

Table 3.4 Experimental Design Matrix: Uncoded Levels

| | | | FACTORS | | |
RUN	TEST NO.	DIESEL ml.	AIR l/min.	RPM	FROTHER ml(1%sn)	% -200 MESH
1	21	0.1	3	950	2	20
2	18	1.5	3	950	10	20
3	17	0.1	7	950	10	50
4	22	1.5	7	950	2	50
5	19	0.1	3	1250	10	50
6	24	1.5	3	1250	2	50
7	20	0.1	7	1250	2	20
8	23	1.5	7	1250	10	20
cpt		0.8	5	1100	6	35

c_m is the percent assayed element in the mineral being concentrated. For PbS, $c_m = 207/207+32 \times 100 = 87$. For coal, $c_m = 100$,

f is percentage of combustibles in feed,

c is percentage of combustibles in concentrate

The value of Es changes with time (or position along the cell bank). Initially, the concentrate consists chiefly of "pure" coal (the fast floating fraction) plus some by-passed feed. With time, the proportion of combustibles in the concentrate stream diminishes until at some point, it is the same as the initial feed. At this point, Es is maximum and continuance of the separation process contaminates the product (Es declines). Although Es is concerned with technical aspects as opposed to economic, it is obvious that maintenance of the flotation operation at optimal values of Es ensures production of high quality concentrates. Ash penalties are avoided and profits maintained.

A sink-float analysis was performed on the sized concentrate products of test number 12 (centre point run). The densities of separation were: 1.3, 1.4, 1.5, and 1.8. The media, prepared with combinations of varsol (SG=0.8), perluxe (SG=1.6), and ethylene dibromide (SG=2.2) was held in a 2 litre separatory funnel. Extremely long settling times were required for the size fraction finer than 200 mesh. Separations were painstakingly performed in order to obtain representative data. This data was used to generate partition or Tromp curves for each of the size fractions.

4. RESULTS AND DISCUSSION

4.1 Centre Point Runs

Model parameters for composite flotation feed obtained for conditions simulating plant practice are given in Table 4.1. The means of these parameters were input to the model with the results shown in Table 4.2. The model predictions compare favourably with averaged plant data obtained for a 30 day period in June-July 1979 (Flintoff and Plitt [57], Table 1.1). This illustrates the accuracy of the three parameter model. Test 12 data was regressed by the two parameter model (Eq.2.38) as a laboratory project for fourth year Mineral Engineering students in October 1980. The residual mean sum of squares between observed and predicted yields determined the goodness of fit. Table 4.3 indicates the minimum residual was associated with the three parameter model for the two cases of combustibles and incombustibles.

A mass balance was performed with data collected from the number 4 flotation bank in August 1979 [57]. Yield and concentrate ash levels were computed for each cell. This data along with model predictions generated for centre point runs is presented in Figures 4.1 and 4.2.

Similarity exists between actual and predicted cumulative yield curves presented in Figure 4.1. The model consistently underpredicts actual data for a variety of reasons. It is possible that froth is transferred more

Table 4.1 Model Parameters for Centre Point Conditions

RUN	SPECIES	ϕ	$Ks(\text{sec}^{-1})$	$Kf(\text{sec}^{-1})$
	TOTAL MASS	0.240	9.27×10^{-4}	2.24×10^{-3}
12	INCOMBUSTIBLES	0.595	3.78×10^{-4}	1.67×10^{-3}
	WATER	0.875	1.46×10^{-3}	2.24×10^{-3}
	TOTAL MASS	0.196	5.02×10^{-4}	1.89×10^{-3}
13	INCOMBUSTIBLES	0.485	5.70×10^{-4}	1.15×10^{-4}
	WATER	0.562	3.34×10^{-3}	3.34×10^{-3}
	TOTAL MASS	0.360	2.89×10^{-4}	8.54×10^{-3}
26	INCOMBUSTIBLES	0.675	1.75×10^{-4}	6.56×10^{-3}
	WATER	0.874	7.62×10^{-4}	1.67×10^{-3}
	TOTAL MASS	0.265	5.73×10^{-4}	1.66×10^{-3}
MEAN	INCOMBUSTIBLES	0.585	3.12×10^{-4}	1.16×10^{-3}
	WATER	0.770	1.85×10^{-3}	1.41×10^{-3}

Table 4.2 Modelled Performance vs. Plant Data

	FLOTATION FEED ASH (%)	CONC. YIELD (%)	CONC. ASH (%)	E_s
PLANT DATA JUNE/JULY 1979	17.8	74.0	9.0	45.5
MODELLED PERFORMANCE	17.3	74.3	9.4	43.4

Table 4.3 Comparison Between Two and Three Parameter Model
Forms

MODEL FORM	SPECIES	SUM OF RESIDUALS SQUARED (SRS)	RESIDUAL MEANS SQUARE (RMS)
3-PARAMETER	TOTAL MASS	1.955	0.652
(EQ. 2.27)	INCOMBUSTIBLES	0.923	0.307
2-PARAMETER	COMBUSTIBLES	8.883	2.221
(EQ. 2.38)	INCOMBUSTIBLES	1.251	0.313

efficiently to the concentrate launder in plant equipment because of higher momentum accompanying higher volumetric flows. It is the objective at both scales to ensure that froth removal does not become the rate determining step. Yield is a function of froth bed thickness and volumetric flow rate of water into the froth. Moys [64] emphasized this together with the concept that optimal concentrate grades are attained if froth phase mixing is restricted to piston flow. This requires froth removal in the vertical plane, a system yet to be incorporated with plant equipment. Another aspect promoting discrepancies is omission of the observed piston flow component of pulp phase mixing from the model. Implicit with piston flow is a zero value of the countercurrent diffusion coefficient. Non-zero values associated with ideal mixing are responsible for comparatively lower yields. This is one reason why batch tests generate higher yields than continuous tests. The flotation column [65] is an attempt to provide piston flow in the pulp phase. The cost of improved recovery, however, is borne by reduced flotation rates which in turn implies higher capital equipment costs to maintain concentrate production levels. These units are also larger; impellers are displaced by increased tank volume and construction material requirements. It is ironic that the froth phase behaves as an ideal mixer since froth moves transversely into the concentrate launder (the traditional mode).
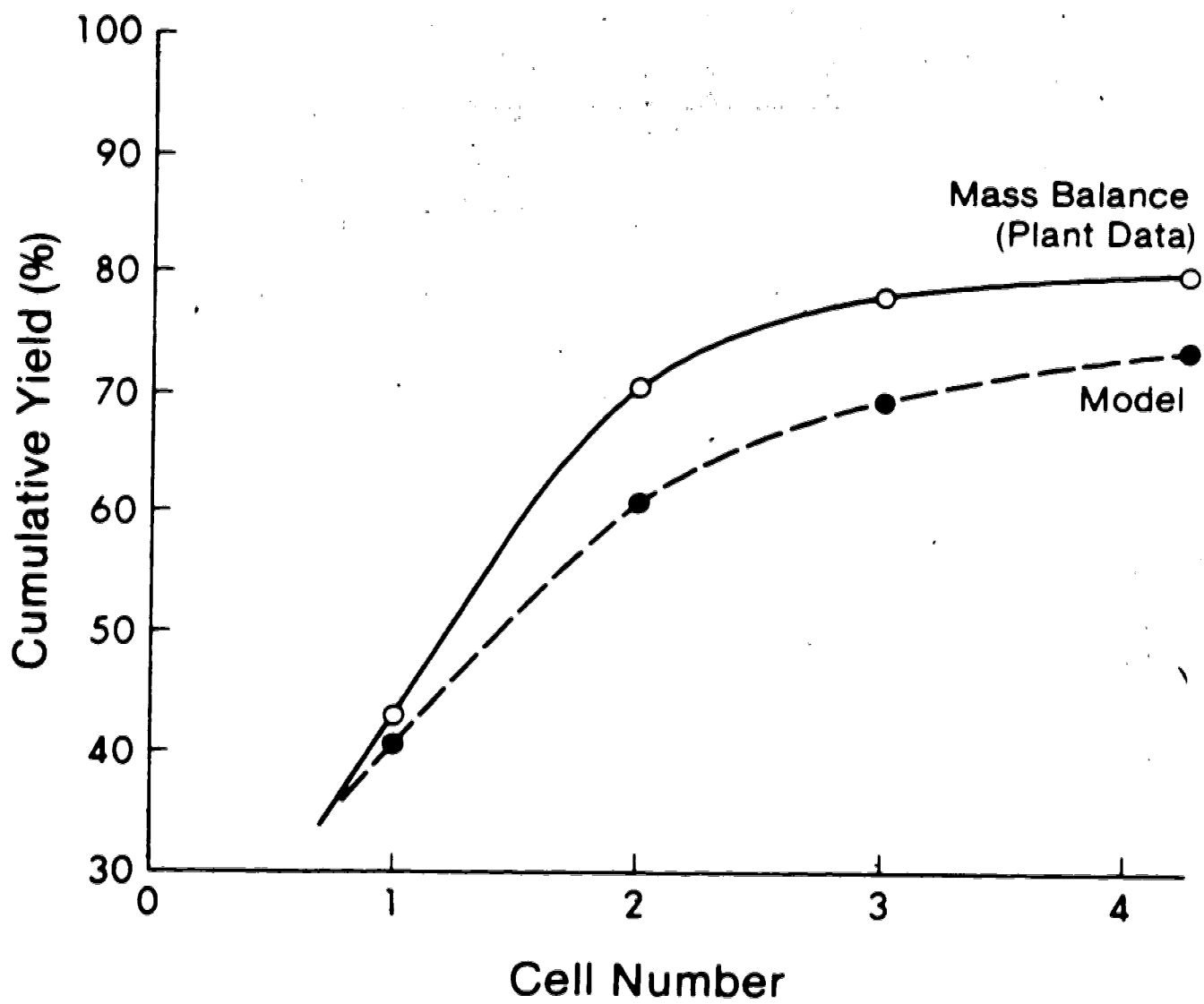
Fig. 4.1 Cumulative Yield Along Flotation Bank
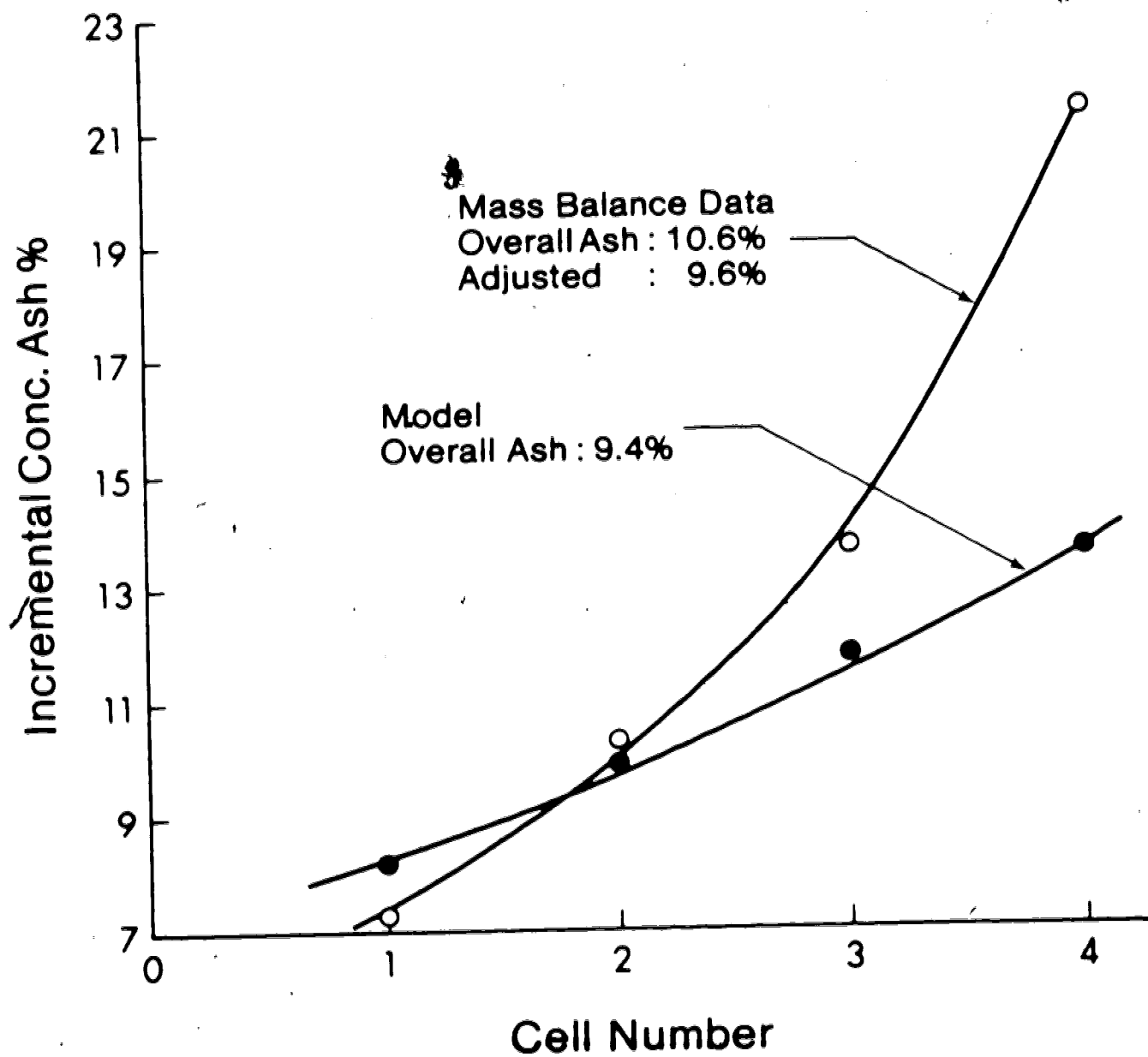
Fig. 4.2   Incremental Ash Along Flotation Bank

A third explanation for discrepancies is provided in Klimpel's suggestion for process optimization described above. To attain the plant yield, adjustments are required to increase Rf associated with laboratory conditions. This is achieved by improving the chemical environment. Since reagent dosage records did not accompany the mass balance data, it is possible that collector and frother dosages were significantly higher than laboratory values.

Differences in the maceral distribution of laboratory and plant feeds also contributes to discrepancies. Perhaps the laboratory samples were rich in the inertinite (slow floating) maceral. Petrographic analysis is required for confirmation. Regulation of maceral distribution is not possible since it is a disturbance process variable.

Final tailings samples were obtained at two locations for the mass balance. One was at the downstream wall of the number 4 cell while the other was at the dart valve of the tailings discharge box adjacent to the number 4 cell. Statistical analysis showed superiority of the dart valve sample. A comparison between measured and mass balanced predictions (dart valve) of the sampling campaign is given in Table 4.4. With this sample as a standard for comparison, the overall concentrate ash level regressed by the model was 9.4 percent, 1.2 units less than plant data. Flotation feed ash was 20.6 percent. Separation efficiency determined with the mass-balanced ash level is 58.6, well above the mean experienced during the 30 day monitoring period (45.5).

Table 4.4 Sampling Campaign of number 4 Flotation Bank

		CELL	NO.			FINAL
		1	2	3	4	CONC
MEASURED FEED ASH 20.6%	YIELD(%)	43.4	25.9	13.6	2.0	84.9
	CONC ASH (%)	7.4	10.2	13.6	21.1	10.6
MASS BAL FEED ASH 21.73%	YIELD(%)	43.?	27.4	6.9	2.5	79.9
	ASH (%) CONC	7.5	10.7	13.8	21.1	9.6

Separation efficiencies were compared for conditions of approximately 20 percent feed ash for two days during this period. For day number 1, feed and concentrate ash levels were 20.4 and 8.6 percent respectively with a yield of 58.2 percent for an ES value of 43.5. On day number 20, feed and concentrate ash levels of 19.9 and 9.4 percent combined with a 57.8 percent yield to produce an ES value of only 39.2. This indicates that the overall concentrate ash determined by the mass/balance is questionable. It is desirable to perform replicate sampling campaigns and mass balances to resolve this situation.

The data from the monitoring period is incomplete since reagent consumption and aeration rates were not recorded. Optimal matching of reagent dosage to feed coal occurs by chance since on-line ash monitoring is not yet available. Future installation of this equipment will assist control of reagent additions.

Figure 4.2 suggests that concentrate ash level is overestimated at the first cell and then underestimated at the third and fourth cells. For cell number 1 it is possible that the laboratory procedure generates a higher than actual value of Kf for incombustibles. It is also possible that variable maceral distributions and inherent ash levels promote discrepancy. The froth structure at extended flotation times may be different for each scale of investigation. If the froth is thinner in the plant, recovery increases at the expense of secondary cleaning. The

higher ash level of the plant feed also promotes higher
concentrate ash levels at latter cells of the bank.
Comparison of data obtained for similar feed ash levels is
desirable.

The recovery of water to the concentrate was predicted
by the model using test 12 parameters. Figure 4.3 details
the relationship between recovery of ash versus recovery of
water. Ash accumulates in the concentrate stream faster than
water, downplaying the entrainment mode of recovery. For the
ash component, bubble attachment is more significant. Hence,
concentrate ash is controlled by two factors: the "degree of
liberation" effected by the rotary breaker and the inherent
ash level.

The ash content of the fourth cell concentrate (mass
balance data) is marginally higher than the feed ash level.
In the context of Es, the current bank length appears to be
ideal. Model predictions, however, indicate increased
efficiency by addition of a fifth cell to each bank. Overall
yield would rise to 76.9 percent at a concentrate ash level
of 9.6 percent. These results, however, may not be
realizable due to the divergence between the model and
actual plant at extended flotation times. A continuous pilot
plant test would be useful at this stage; the model has
identified the proper bank length (plus or minus one cell)
to be investigated.
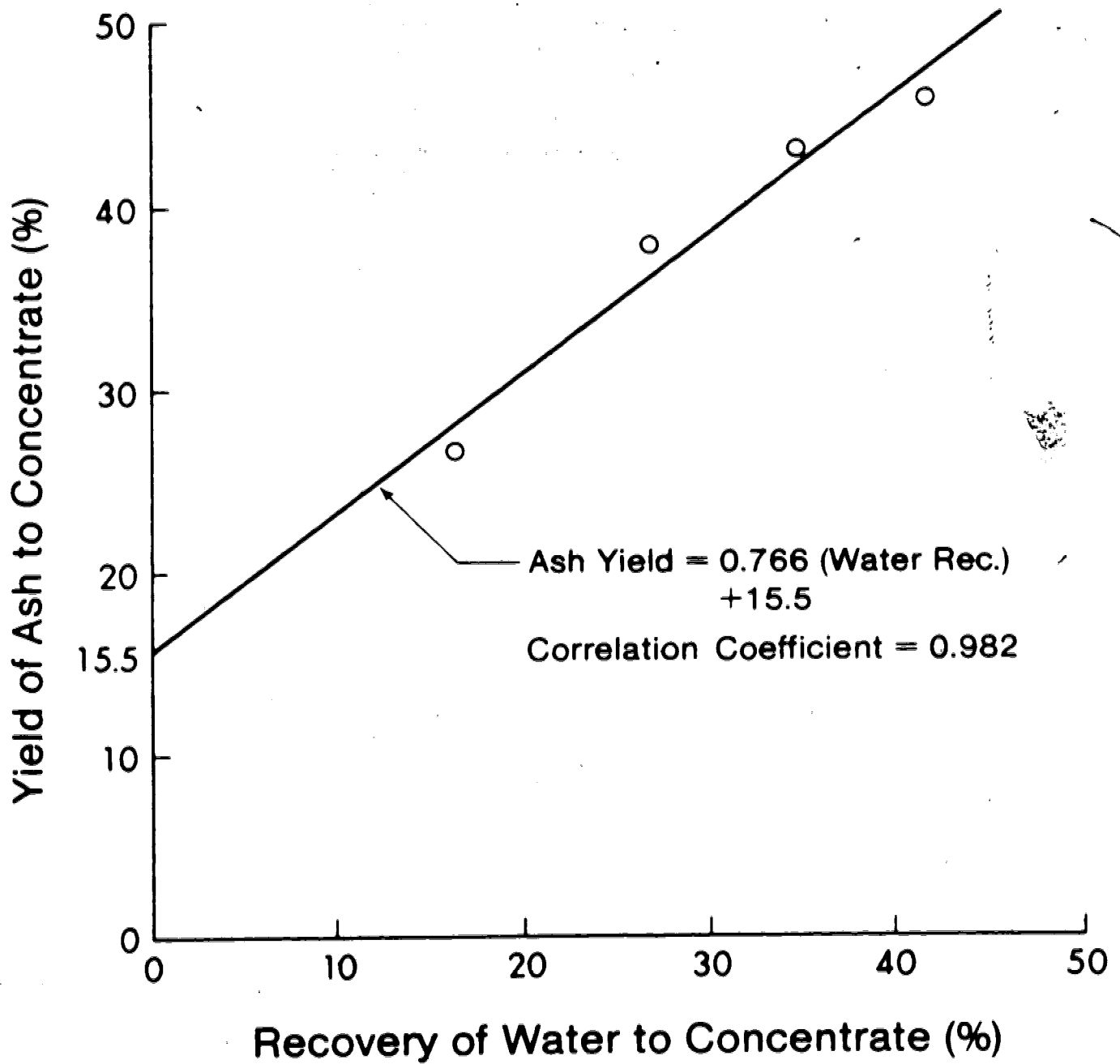
Fig. 4.3 Recovery of Ash vs. Recovery of Water – Test 12

4.1.1 Optimization of Flotation Plant Design

The flotation model can be utilized to suggest methods of optimizing plant design. Based on the centre point or current plant environment, three alternate processing schemes are presented. Model predictions for these alternatives are tabulated in **Table 4.5**.

4.1.1.1 Variation 1

<u>Principle</u> - Increase cell nominal residence time by distributing feed to 5 parallel, identical banks. Maintain current throughput. Expansion of flotation capacity not permitted. Model parameters are means of centre point runs.

```
Current installed flotation capacity = 4 banks x 4
cells/bank x 300ft³/cell = 4800ft³
Current bank nominal residence time = 289sec

Each bank is composed of 3, 300ft³ cells.
Total installed flotation capacity = 4500ft³
Bank residence time = (4500ft³/4800ft³) x 289sec = 271sec
Cell residence time = 271sec/3 cells = 90.3sec
```

4.1.1.2 Variation 2

<u>Principle</u> - Same as per variation 1 except expansion of flotation capacity is permitted.

```
Each bank is composed of 4, 300ft³ cells
Total installed flotation capacity = 6000ft³
Bank residence time = (6000ft³/4800ft³) x 289sec = 361sec
Cell residence time = 361sec/4 cells = 90.3sec
```

4.1.1.3 Variation 3

Principle - Increase cell nominal residence time by installing larger cells. Maintain current throughput, distributed to 4 parallel, identical banks.

Each bank is composed of 3, 500ft³ cells (Wemco 144)
Total installed flotation capacity = 6000ft³
Cell residence time = 361sec/3 cells = 120.3sec

The average daily flotation feed throughput determined during the monitoring period was 2800 tons. Based on 350 operating days per year and a selling price of $65 per ton of clean coal, one unit of yield is worth $650,000 annually. On this basis, the predicted increase of 2.2 units of yield over current performance implies that variation 2 generates additional annual revenue of $1.43 million. By similar analysis, the yield improvement of 1.3 units offered by variation 3 translates to the annual revenue gain of $850,000. Observe that the highest value of ES coincides with the most profitable plant configuration. Both alternatives appear to be economically viable but which is preferred? Variation 3 conforms to the current design trend of the "rationalized concentrator". Maintenance costs would be lower; only 12 impeller drive motors are required compared to 20 for variation 2. The ratio of froth area to cell volume is 0.22 and 0.19 for the Wemco 120 and 144 models respectively. On this basis, it is more proper to

TABLE 4.5 - MODEL PREDICTIONS FOR ALTERNATE FLOTATION PLANT DESIGNS

		FLOTATION CELL NO.				OVERALL CONCENTRATE	E_s
		1	2	3	4		
VARIATION 1	YIELD (%)	TOTAL MASS	45.4	18.9	8.2		72.5	
		INCOMBUSTIBLES	22.0	11.1	5.8		38.9	41.5
		CONCENTRATE ASH CONTENT (%)	8.4	10.2	12.2		9.3	
VARIATION 2	YIELD (%)	TOTAL MASS	45.4	18.9	8.2	4.0	76.5	
		INCOMBUSTIBLES	22.0	11.1	5.8	3.2	42.1	42.7
		CONCENTRATE ASH CONTENT (%)	8.4	10.2	12.2	14.0	9.5	
VARIATION 3	YIELD (%)	TOTAL MASS	50.7	17.9	7.0		75.6	
		INCOMBUSTIBLES	25.2	11.1	5.2		41.5	42.2
		CONCENTRATE ASH CONTENT (%)	8.6	10.7	12.7		9.5	

NOTE = FEED ASH = 17.3% FOR ALL CASES.

utilize the model 120 cells in order to facilitate transport from pulp to froth. Operating circumstances posed by both design variations must be considered prior to final selection.

4.1.2 Partition Curves

The partition or Tromp curve relates the fraction of feed material to a separator which reports to the underflow or dense product stream over a range of separating densities. An example of a Tromp curve is given in Figure 4.4. Flotation can be considered as a specific gravity separation process; the underflow is the tailings stream while the overflow is the froth concentrate. Two essential parameters derived from the Tromp curve are the cut point (dp) and probable error (Ep). The former is the specific gravity at which particles have an equal chance of reporting to either product stream. The latter indicates the lack of sharpness of separation. Low Ep values are indicative of efficient separations. The partition curve can be represented by a straight line running between $d_{,,}$ and $d_{,,}$ with attached tail section [66]. This approach was utilized for the size fractions of test 12 flotation concentrate. The raw data is assembled in Appendix II. The method of least squares was used to obtain the best fit straight line. The Tromp curve separating densities were 1.45, 1.65, and 1.825. The first two values are midpoints of the actual separating densities (1.4, 1.5, and 1.8). The final value represents

$$E_p = \frac{d_{75} - d_{25}}{2}$$
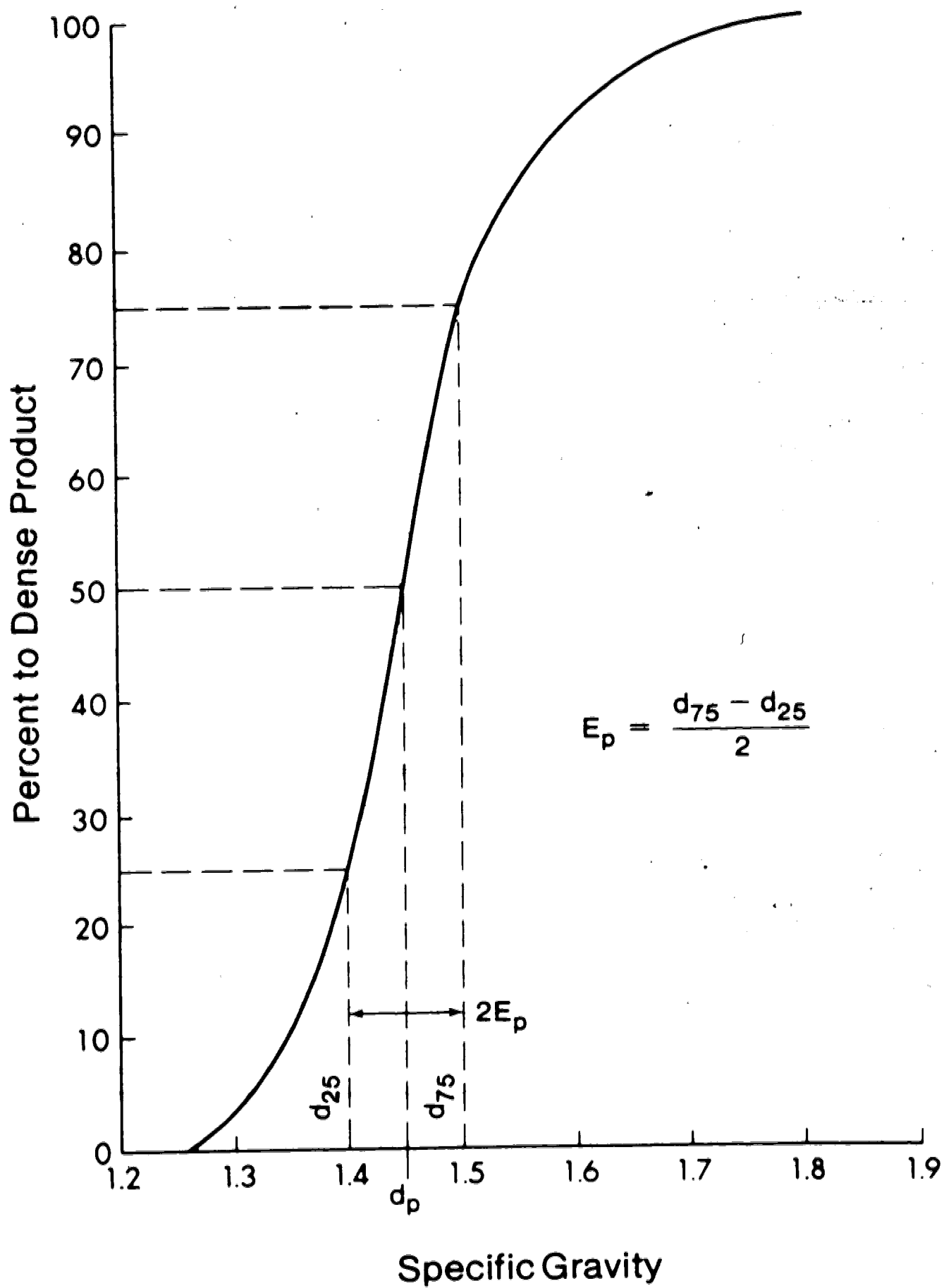
Fig. 4.4 A Typical Partition Curve
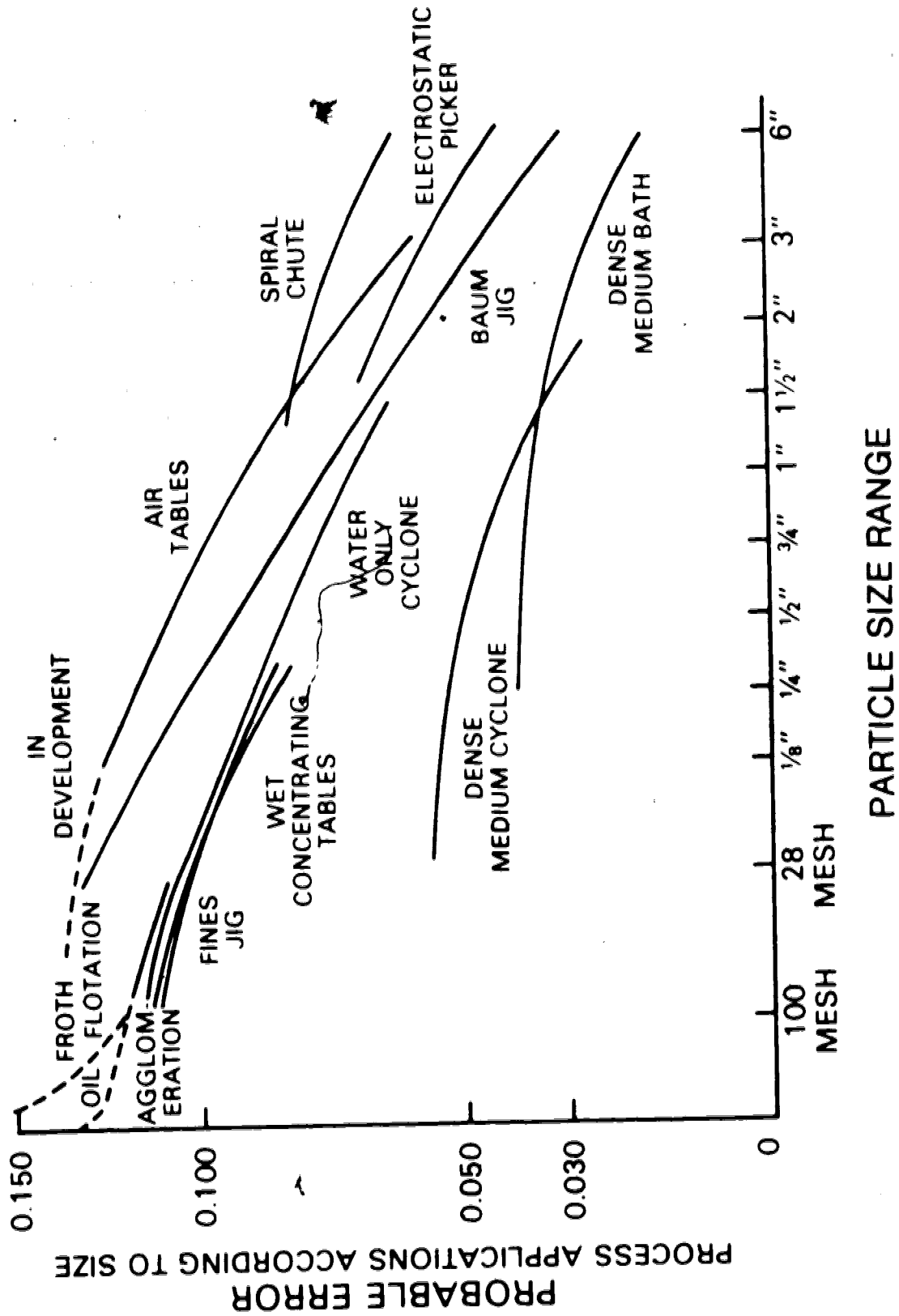
Fig. 4.5   Ep as a Function of Particle Size

the mean between the highest separating density and the heaviest particle present. In this case, 1.85 was considered as maximum density. This value is low, however, at the separating density of 1.8, nearly 85 percent of feed reports to underflow for all size ranges. The dp and Ep values for each size fraction are presented in Table 4.6. These results indicate the excellent selectivity of the flotation process for the finer sizes of the McIntyre coal. The Ep values are in agreement with data amassed by Elk [67] relating Ep to particle size for various coal separators (Figure 4.5).

4.2 Analysis of Factorial Design

The factorial design presented in Table 3.2 was evaluated according to Yates method as described by Mular and Bull [59]. The calculations are detailed in Table 4.7. The significant factors arising from this design are: aeration rate, frother dosage, and fraction of feed finer than 200 mesh. The linear model of Es in terms of coded levels of significant factors is given by Equation 4.1. Values of Es regressed by this model are included in Table 4.7.

$$\widehat{Es} = 28.9 + 4.7(x_1) + 8.5(x_4) + 6.5(x_3)$$

$$(4.1)$$

where:

$\widehat{Es}$ is the regressed value of Es,

Table 4.6 Tromp Curve Parameters: Test 12

SIZE RANGE (Mesh)	LINEAR SLOPE	REGRESSION Y INTERCEPT	DATA CORR. COEF.	E_p	d_p
20x48	205	-283	0.970	0.122	1.62
48x100	173	-247	0.915	0.144	1.72
100x200	166	-238	0.891	0.151	1.74
200x270	213	-315	0.854	0.117	1.71
-270	216	-300	0.998	0.116	1.62
Composite	193	-273	0.960	0.129	1.67

Table 4.7 - Analysis of Factorial Design by Yates Method

Run	Test No.	E_s	1	2	3 Effects Total	4 Effects	5 Co-efficients	6 Sum of Squares	Associated Factor(s)	$\hat{E}_s$	PI (K_w/m^3)	M_a $(\times 10^{-2})$
1	21	8.0	39.6	124.2	230.9	57.7	28.9	-	-	9.2	2.11	2.38
2	18	31.6	84.6	106.7	17.3	4.3	2.2	37.4	x_1	26.2	2.43	2.41
3	17	48.0	57.0	11.0	37.7	9.4	4.7	177.7	x_2	48.6	2.27	5.67
4	22	36.0	49.7	6.3	-4.3	-1.1	-0.5	2.3	$x_{12} + x_{34}$	31.6	2.11	5.68
5	19	34.9	23.6	45.0	-17.5	-4.4	-2.2	38.3	x_3	39.2	5.02	1.83
6	24	22.1	-12.6	-7.3	-8.7	-1.2	-0.6	2.8	x_{13}	22.2	4.88	1.82
7	20	15.3	-12.8	-36.2	-52.3	-13.1	-6.5	341.9	$-x_5$	18.6	5.15	4.29
8	23	34.4	19.1	31.9	68.1	17.0	8.5	579.7	x_4	35.6	4.83	4.32
Centre Point	12	43.5									3.37	3.48
Centre Point	13	40.5									3.41	3.96
Centre Point	25	46.3									3.33	3.41

Yates Method Columns

$\bar{E}_s = 43.4$ at 95% confidence level, $F_{1,2}$, $\alpha = 18.51$

$F \times S_e^2 = 18.51 \times 8.4 = 155.5$

$S_e^2 = 8.4$ ∴ Effect is significant if column 6 value exceeds 155.5

∴ Significant factors at 95% confidence level are: x_2, $-x_5$, x_4

∴ $\hat{E}_s = 28.9 + 4.7x_2 - (-6.5)x_5 + 8.5x_4$

x_2 is aeration level (coded),

x_4 is frother dosage (coded),

x_5 is fraction of feed finer than 200 mesh (coded)

Collector (diesel) dosage and impeller speed are not significant at their selected factor levels. This implies that the flotation process could be efficiently performed at the -1 factor level of collector dosage (20cc diesel/ tonne of coal), and impeller speed providing that the other factors are maintained at levels bounded by the factorial design.

Separation efficiencies for tests 17 and 19 either exceed or are close to the mean for centre point conditions. Examining the factor levels, the high value of Es for test 17 is partially attributable to the higher aeration rate. Air is an inexpensive flotation reagent which must be carefully controlled. The final aeration control element for the Wemco 120 machine is a sliding blind which throttles air intake through the standpipe. Factorial design results indicate that benefits will accrue from plant operation at increased aeration rates. Current plant practice is well above the 1-s suspension criterion, in the upper left quadrant of the hydraulic performance map. Supercharging, by installation of a turbine blower, must be considered in an optimization program. Adopting the scaling procedure practiced in section 3.1.2.2, plant aeration should be increased from 6.8 m³/minute to 9.6 m³/minute, an increase of 40 percent. Test 17 impeller speed is scaled to 192 rpm

at the plant level, 13 percent lower than present speed (scaling relationship in section 3.1.2.1). Preparation plant personnel were of the opinion that impeller speed should be reduced, prior to this study. Table 4.9 itemizes operating parameters for both machine scales. Observe the similarity of Np and PI for both scales at centre point conditions. Given this, it can be said that the scaled model duplicated the particle dispersion characteristics of the plant machine [10]. In terms of the probabilistic model, Pc was equivalent at both scales.

The froth phase of test 17 was approximately 1.5 inches thick, elastic in nature, and very mobile. In contrast, the froth of test 22 (-1 frother dosage level) was brittle and rigid; Plateau borders were dry and the froth could be blown away. Centre point froths were approximately 1.5 inches thick, however, they did not flow as readily as test 17 and tended to adhere to available structural surfaces.

Consideration should be given to restricting flotation feed to particles finer than 48 mesh (300 microns). The 20x48 mesh fraction currently handled by flotation could be more efficiently processed by automedium cyclones. The Ep values for the 14x28 mesh and 28x48 mesh ranges for an 8 inch automedium cyclone are 0.064 and 0.087 respectively [68]. The nominal bank residence time increases because scalping reduces the feed flowrate. Maintaining flotation feed pulp consistency at 9.1 weight percent solids, scalping the 20x48 mesh fraction increases nominal residence time by

TABLE 4.8 - WEMCO 120 FLOTATION MACHINE: OPERATING PARAMETERS FOR TWO SCALES

STRATEGY	SCALE	SIZE (M^3)	FROTH AREA (M^2)	IMPELLER DIA. (M)	IMPELLER SPEED (RPM)	AERATION RATE (M^3/MIN)	CONSUMED POWER (KW)	P I (KW/M^3)	N_p	N_q'
CENTRE POINT (TEST 12)	LABORATORY	6.51×10^{-3}	5.68×10^{-2}	5.09×10^{-2}	1100	5×10^{-3}	1.91×10^{-2}	2.92	8.85	1.58×10^{-3}
	PLANT	7.22	6.13	.558	220	6.8	17.9	2.48	6.44	9.02×10^{-3}
SCALPED FEED (TEST 17)	LABORATORY	6.5×10^{-3}	5.68×10^{-2}	5.09×10^{-2}	950	7×10^{-3}	1.28×10^{-2}	1.97	9.23	2.55×10^{-3}
	PLANT	7.22	6.13	.558	196	9.6	17.9	2.48	9.11	1.43×10^{-2}

NOTE - CONSUMED POWER (PLANT SCALE) NOT ADJUSTED FOR SCALPED FEED STRATEGY. IT IS ANTICIPATED THAT THIS VALUE WOULD BE

LOWER THAN FOR CURRENT PRACTICE

30.8 percent (refer to Table 3.2) to 94 seconds. This residence time and parameters for size ranges finer than 48 mesh obtained for test 17 conditons were processed by the model. The results are presented in Table 4.9. The extended residence time associated with the narrower feed size distribution increases yield by 3.4 units. This translates to additional annual revenues of $2.2 million, assuming that yield of the 20x48 mesh fraction by automedium cyclone is equivalent to flotation. The fact that projected improvement in yield associated with the narrow feed size spectrum is obtained at a lower Es value than test 17 suggests that the relationship between technical and economic efficiency is not linear. Considering the modelled performance of test 17 it is apparent that concentrate ash level must increase to the target level in order to maximize yield. This target is currently 8.5 perc██ for average feed ash of 17.8 percent. At a feed ash of 1█percent, concentrate ash target of approximately 8 percent would be more reasonable. In this case, increased yield occurred at the expense of Es; the value near the 8 percent ash target (42.8) is lower than the cleaner test 17 product (48.6). Schulz insists that Es is independent of economic considerations. Certainly, operation at high Es values ensures near optimum performance, however, economics must precisely identify desirable factor levels.

The high performance of the narrow size spectrum strategy is accomplished with reduced diesel collector consumption. Gaudin [69] suggested that coarse particles

Table 4.9 Modelled Performance of the Narrow Size Spectrum
Strategy

SIZE RANGE (Mesh)	FEED ASH (%)	MODIFIED SIZE CONSIST (%)	YIELD (%)	CONCENTRATE ASH (%)	Es
48x100	13.9	30.6	76.8	6.7	47.3
100x200	15.1	19.3	80.4	7.6	47.7
200x270	14.5	7.0	83.2	8.1	43.6
-270	13.6	43.1	86.6	9.0	34.6
Composite	14.1	100.0	82.2	7.9	42.8

require a higher density of collecter molecule coverage than fines of the same mineral species. Trahar [1] uses separate conditioning stages for fine and coarse size fractions. The bulk of the collector dosage is given to the coarse while the fines are handled with starvation amounts to ensure selectivity (grade considerations). Although the dramatic savings in collector indicated above may not be fully realized at the plant scale, test results indicate that it is expensive to treat 20x48 mesh particles by flotation. To ensure effective implementation of the narrow feed size spectrum strategy, the operator must emphasize efficient screening operation to minimize misplacement of coarse particles in flotation feed. Costs incurred by establishment of a screen monitoring and maintenance program will be recovered at the flotation section of the plant.

Multivariable regression analysis performed for this factorial design indicated that $\emptyset$ was strongly correlated with feed ash content. Kf was influenced by aeration rate and feed ash, however, KS was not strongly dependent on any factor. This is not surprising as KS accounts for departure from first order behaviour at extended times.

4.2.1 Effects of Particle Size

Model parameters for sized fractions of total mass and incombustibles species for tests 12 and 17 are given in Tables 4.10 and 4.11. Three features are apparent from these data. Firstly, the distribution of parameter

Table 4.10 Model Parameters for Sized Fractions: Test 12

SIZE RANGE (Mesh)	SPECIES	$\emptyset$	Ks (sec^{-1})	Kf (sec^{-1})
20x48	Total Mass	0.277	5.27×10^{-4}	2.26×10^{-2}
	Incombustibles	0.671	6.45×10^{-4}	1.57×10^{-2}
48x100	Total Mass	0.283	1.37×10^{-3}	2.67×10^{-2}
	Incombustibles	0.633	2.68×10^{-4}	1.88×10^{-2}
100x200	Total Mass	0.226	1.27×10^{-3}	2.34×10^{-2}
	Incombustibles	0.545	4.24×10^{-4}	1.66×10^{-2}
200x270	Total Mass	0.091	3.31×10^{-4}	2.12×10^{-2}
	Incombustibles	0.289	1.01×10^{-9}	1.67×10^{-2}
-270	Total Mass	0.234	9.97×10^{-4}	1.79×10^{-2}
	Incombustibles	0.680	1.21×10^{-3}	1.67×10^{-2}

Table 4.11 Model Parameters for Sized Fractions: Test 17

SIZE RANGE (Mesh)	SPECIES	$\varnothing$	K_s (sec⁻¹)	K_f (sec⁻¹)
	Total Mass	0.278	1.07×10^{-4}	1.16×10^{-2}
35x48				
	Incombustibles	0.708	2.22×10^{-4}	5.77×10^{-3}
	Total Mass	0.204	5.11×10^{-4}	1.40×10^{-2}
48x100				
	Incombustibles	0.589	7.81×10^{-14}	7.97×10^{-3}
	Total Mass	0.172	8.03×10^{-14}	1.50×10^{-2}
100x200				
	Incombustibles	0.560	8.13×10^{-14}	9.28×10^{-3}
	Total Mass	0.156	1.59×10^{-4}	2.02×10^{-2}
200x270				
	Incombustibles	0.520	2.35×10^{-3}	1.58×10^{-2}
	Total Mass	0.174	1.34×10^{-3}	1.47×10^{-2}
-270				
	Incombustibles	0.523	6.95×10^{-4}	1.03×10^{-2}

values over size is similar for both species. This reinforces the concept that combustibles and incombustibles are both recovered by the bubble attachment mechanism. Lower Kf values for incombustibles indicate a slower reaction rate. Secondly, the distribution of Kf over particle size is similar to suggestions by Imaizumi and Inoue [43], and Lynch [49]. The fast floating component extends over the size range 74-225 microns whereas the slow floating fines and coarse middling particles will be recovered at extended flotation times. Thirdly, the slightly lower rate constants associated with test 17 are offset by lower values of $\emptyset$. Although the flotation reaction is slower, it proceeds to a higher degree of completion because of the lower ash content of test 17 feed. A possible method of increasing test 17 flotation rates is dispersion of air into finer bubbles. This is accomplished by selection of an appropriate impeller design and regulation of frother dosage.

Model results for discrete size ranges for tests 12 and 17 are presented in Tables 4.12 and 4.13. Comparison of Es values indicate either superiority of the narrow size spectrum strategy (ie 200x270 mesh) or its similarity to the present operating regime (ie 48x100 mesh). Variation exists, in feed ash of the same size range for these tests. It was hoped that this would be circumvented by the sample preparation procedure. Also contributing to this variance was sampling bias associated with ash analysis of test products. Reliance on Es is beneficial given these

TABLE 4.12 - MODEL PREDICTIONS FOR SIZED FRACTIONS: TEST 12

SIZE RANGE (MESH)	FEED ASH %		PLOTATION CELL NO.				FINAL CONCENTRATE	E_s
			1	2	3	4		
20x48	16.7	YIELD (%)	46.0	17.9	7.4	3.3	74.6	52.8
		CONCENTRATE ASH (%)	6.37	7.65	8.65	9.39	7.04	
48x100	18.0	YIELD (%)	49.9	18.4	7.6	3.7	79.6	49.1
		CONCENTRATE ASH (%)	8.08	9.89	11.71	13.24	9.08	
100x200	17.9	YIELD (%)	50.7	19.7	8.3	3.9	82.6	40.9
		CONCENTRATE ASH (%)	9.37	15.28	14.34	17.44	10.79	
200x270	15.5	YIELD (%)	55.1	21.7	8.5	3.4	88.7	24.8
		CONCENTRATE ASH (%)	10.94	11.39	11.69	16.47	11.87	
-270	18.2	YIELD (%)	44.9	20.2	9.6	4.8	79.5	36.9
		CONCENTRATE ASH (%)	9.35	11.70	15.50	22.29	11.48	

NOMINAL CELL RESIDENCE TIME = 72.3 SECONDS

TABLE 4.13 - MODEL PREDICTIONS FOR SIZED FRACTIONS: TEST 17

SIZE RANGE (MESH)	FEED ASH %		FLOTATION CELL NO.				FINAL CONCENTRATE	E_s
			1	2	3	4		
35x48	16.0	YIELD (%)	33.0	17.9	9.7	5.3	65.9	53.3
		CONCENTRATE ASH(%)	4.18	5.43	6.99	9.10	5.33	
48x100	14.0	YIELD (%)	40.2	19.8	9.9	4.9	74.8	47.6
		CONCENTRATE ASH(%)	5.24	6.69	8.54	10.85	6.43	
100x200	15.1	YIELD (%)	43.2	20.6	9.9	4.7	78.4	48.0
		CONCENTRATE ASH(%)	6.18	7.70	9.65	12.07	7.37	
200x270	14.5	YIELD (%)	50.2	20.3	8.3	3.3	82.1	43.3
		CONCENTRATE ASH(%)	7.40	8.51	9.71	11.16	8.06	
-270	13.6	YIELD (%)	44.2	22.0	11.2	6.0	83.4	35.7
		CONCENTRATE ASH(%)	7.59	8.82	10.49	12.67	8.67	

NOMINAL CELL RESIDENCE TIME = 72.3 SECONDS

circumstances because ES, by definition, accounts for changes in feed ash. If yield was the objective criterion, interpretation of results would have been complicated by the fact that yield is inversely related to feed ash (refer to Flintoff and Plitt [57].)

4.2.2 Flotation Control Strategy for McIntyre Mines

Maximization of recovery is the objective of rougher stage flotation in a sulphide mineral concentrator. Hence, control strategy emphasizes proper matching of collector reagent dosage to feed grade. The role of the cleaner flotation section is maintenance of concentrate grade targets through control of aeration and froth bed thickness. This distributed control strategy is not available at McIntyre Mines. Concentrate yield and grade must be controlled at the same process location.

The forthcoming on-stream ash monitor [70] will play a vital role in the flotation control strategy. A block diagram of a possible strategy is given in Figure 4.6. Operating in conjunction with a computer, changes in feed ash will be interpreted as changes in $\emptyset$. The computer will signal flow adjustments to diesel collector in order to maintain reasonable values of Kf and yield. Concentrate ash level would determine froth bed thickness through aeration rate control. Yield and ES would be calculated by the computer, however, process lag (ie nominal bank residence time) must be considered to obtain proper pairing of feed
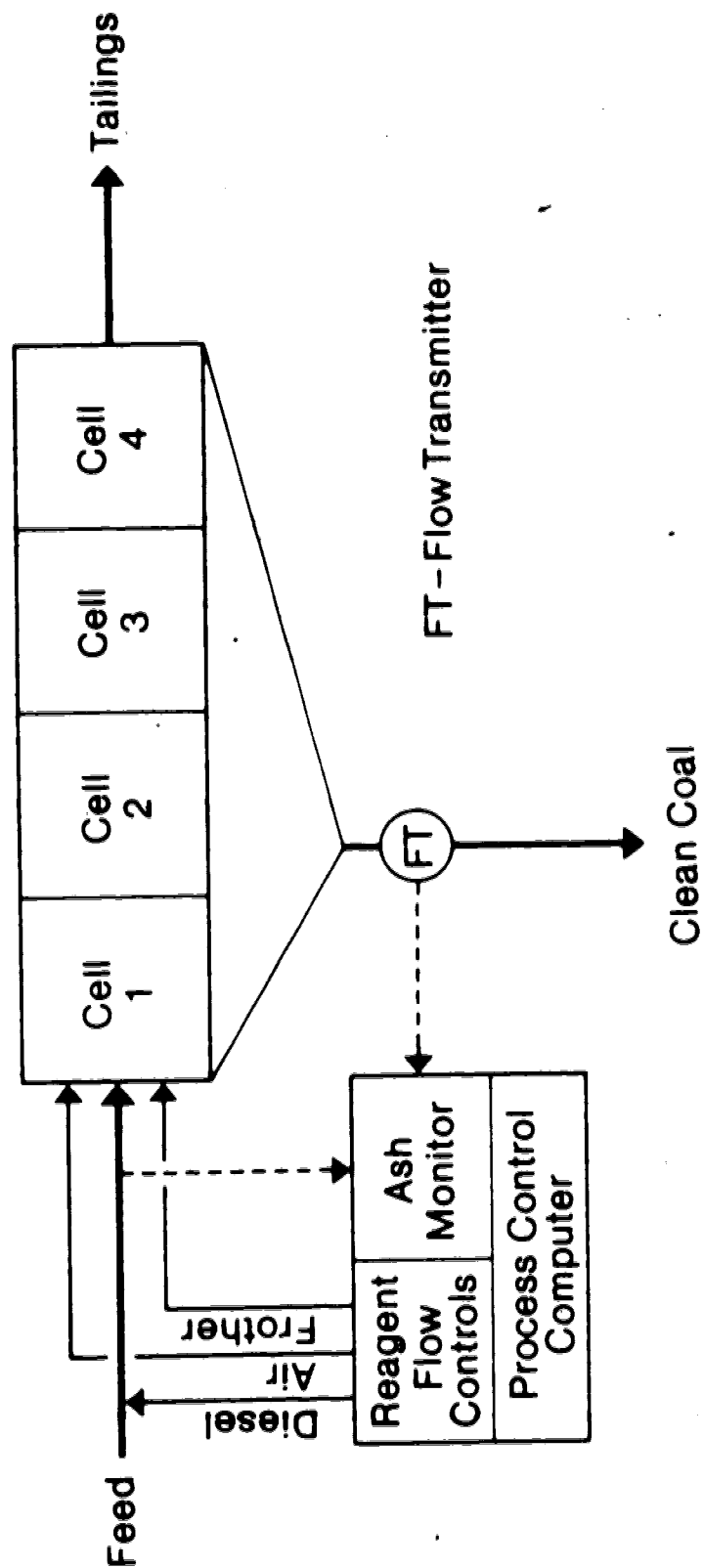
Fig. 4.6 Flotation Control Block Diagam

and concentrate sample assays. The sampling frequency must
be selected to prevent over-control (sampling frequency too
high, resulting in severe, undamped control actions) or
under-control (sampling frequency too low resulting in
mismatching of flotation environment to feed
characteristics.)

Frother dosage can be correlated to concentrate
flowrate. This quantifies froth nature, permitting
identification of froth overloading by the computer. Froth
bed thickness must be taken into account as thick, yet not
overloaded froths, generate low concentrate flowrates.

The process computer establishes factor levels in terms
of the set point. The set point reflects efficiency in
either technical or economic terms. It is possible to
utilize ES as the set point, however, profit targets may be
preferrable for reasons given above. The operator must
determine which criterion is more desirable.

4.3 Evaluation of the Lynch Flotation Control Strategy

A laboratory procedure was developed to evaluate the
Lynch flotation control strategy (Figure 2.12) for the
McIntyre coal. The rougher portion of the cell bank was
restricted to the first cell. Procedurally, this was
represented by the first three froth increment periods. The
object of the remaining periods was to assess performance of
the scavenger section (last three cells in the bank). Diesel

collector was added at both stages, the rougher receiving
the bulk of the dosage. This divergence from the Lynch
format in which collector dosage emphasis is placed on the
scavenger section is justified because the short bank length
necessitates rapid yield maximization. This is also
supported by the probablistic flotation model: it is
sensible to recover valuable particles as soon as stable
bubble-particle aggregates are formed. Frother concentration
was held constant in both flotation sections as frother was
introduced via the water replenishment system.

The feed size range studied was 20x0 mesh. The narrow
feed size-spectrum strategy was not evaluated. A 2^2
factorial design was utilized in this investigation. Factors
selected for study were diesel collector dosage at the
scavenger section, and frother dosage. Collector dosage at
the rougher section was established at 0.8 ml per 500 g coal
(1.6 litres/tonne). Impeller speed was set at 975 rpm and
aeration maintained at 7.75 litres/minute. This provided
power intensity and air flow number of 2.3 kW/m³ and 0.06
respectively. One set of model parameters was required for
each flotation section. The model was executed twice for
each species and the results rearranged to predict overall
performance. Essentially, the disappearance kinetics
analysis is reset for each staged addition of collector. The
experimental design, in coded and uncoded forms, is given in
Table 4.14.

Table 4.14 Experimental Design for Evaluation of Lynch Strategy

RUN	TEST NO.	CODED LEVELS SCAVENGER COLLECTOR X_1	LEVELS FROTHER X_2	UNCODED X_1 ml.	LEVELS X_2 ml. 1% sol.
1	53	-1	-1	0.2	8
2	55	+1	-1	0.6	8
3	52	-1	+1	0.2	12
4	50	+1	+1	0.6	12
cp	40 41	0	0	0.4	10

Evaluation of the experimental design by Yates method is given in Table 4.15. Time constraints limited the number of centre point runs to two. Because of this, a significant factor was not identified. It is suggested, however, that frother dosage would emerge as significant with performance of a third centre point run.

Optimum conditions for the Lynch strategy are provided at the centre point. Comparison of yield, concentrate ash, and Es for the centre point with either the current operating practice or the narrow size spectrum strategy indicates the inferiority of the Lynch scheme for this coal. The difference in operating cost between the Lynch and the narrow size strategy is exceptionally large as the former consumes twelve times as much diesel collector.

Table 4.15 - <u>Analysis of Second Factorial Design by Yates Method</u>

| | | | Yates Method Columns | |
Run	Test No.	$\bar{E}_s$	1	2 Effects Totals	3 Effects	4 Co-efficients	5 Sum of Squares	Associated Factors
1	53	19.5	44.2	111.8	55.9	28.0	-	-
2	55	24.7	67.6	1.2	0.6	0.3	0.4	X_1
3	52	35.8	5.2	23.4	11.7	5.8	136.9	X_2
4	50	31.8	-4.0	-9.2	-4.6	-2.3	21.2	X_3
Centre Points	40	39.8						
Centre Points	41	42.8						

$\bar{E}_s = 41.3$ at 90% confidence level, $F_{1,1,\alpha} = 39.86$

$S_e^2 = 4.8$ $F \times S_e^2 = 39.86 \times 4.8 = 191.3$

∴ No effects are significant

138

5. CONCLUSIONS AND SUGGESTIONS FOR FURTHER WORK

A scaled laboratory model of the Wemco 120 flotation cell, utilized by McIntyre Mines Ltd., has been designed and fabricated. The desired flotation environment can be precisely established to estimate the effects of procedural modifications on plant performance. This equipment is a valuable screening tool; conditions which should be investigated at the pilot and operating plant levels are quickly identified. Inappropriate operating conditions can be discarded in the laboratory thus eliminating production losses associated with plant testing. The following conclusions pertain to the laboratory investigation of the flotation of a low volatile bituminous coal from the mountain region of Alberta:

1. Similarity between laboratory and plant scales exists for: geometric aspects, modified air flow number and power intensity. This suggests that both machine scales exhibited similar particle suspension/dispersion patterns.

2. The three parameter heuristic flotation model expressed by Lynch (equation 2.27) accurately describes the flotation response of the studied coal. Klimpel's two parameter model (equation 2.38) fitted with the same data was not as accurate as the three parameter model.

3. Feed ash level influences the magnitude of $\emptyset$, the fraction of material which is slow floating. As feed ash increases, $\emptyset$ also increases. The rate constant

139

associated with fast floating, liberated, intermediate size particles, Kf, is directly proportional to aeration rate and inversely proportional to feed ash level. The slow floating fraction rate constant, KS, was not associated with any process variable.

4. Aeration rate at the plant scale should be evaluated at an increased level (9.6 m³/minute), with a commensurate decrease of impeller speed from 220 rpm to 196 rpm. At these new levels, Nq' is 1.43×10^{-1}, and PI is 2.48 kW/m³.

5. Addition of a fifth bank of Wemco 120 cells would increase nominal cell residence time by 25 percent providing throughput is not increased. Model results indicate an increase in yield of 2.2 units is available with this expansion.

6. Flotation practice at McIntyre Mines should be restricted to particles finer than 48 mesh (300 microns). Coarser particles presently handled by flotation (20x48 mesh) are more efficiently processed with automedium cyclones. Two benefits accrue from the narrow feed size spectrum strategy. Firstly, nominal residence time is increased by 30 percent at current throughput and feed pulp density. Extended flotation time enhances recovery of slow floating fines. Secondly, coarser particles consume disproportionately larger amounts of diesel collector to increase hydrophobicity and bubble attachment. Laboratory results indicate that

application of the narrow size spectrum strategy could reduce consumption of diesel to one eighth of present demand.

7. The operating strategy developed by Lynch for Australian coals was evaluated, with minor modifications. It was determined that this strategy is inappropriate for the Alberta coal. The heterogeneous nature of coal requires the tailoring of control strategies by each operator.

The following aspects of coal flotation are suggested as topics of future investigations:

1. The coal operator should establish the relationship between technical and economic efficiency of the flotation operation.

2. The process control strategy should be developed in terms of the on-line ash monitor. Flexibility is a desirable feature which would permit efficient operation at all market conditions.

3. The narrow size spectrum strategy should be evaluated at the pilot and full plant levels. It is essential to monitor the performance of the scalped coarse particles in the cyclone section of the plant.

4. Flotation feed at Fording Coal Mine is sized at 100x0 mesh. It is possible that this is an excessively narrow size spectrum. Addition of 48x100 mesh particles could improve recovery of fines by a mechanism resembling carrier flotation.

References

1. Trahar, W. *The Selective Flotation of Galena from Sphalerite With Special Reference to the Effects of Particle Size*. Int. J. Min. Proc., v. 3, pp. 151-166, 1976.

2. Taggart, A. Handbook of Ore Dressing (2nd edition). J. Wiley and Sons, New York, 1942.

3. Gaudin, A.M. Flotation. McGraw-Hill, New York, 1932.

4. Sutherland, K.L. *Kinetics of the Flotation Process*. J. Phys. Chem., v. 25, pp. 394-425, 1948.

5. Woodburn, E.J., et al. *The Effect of Particle Size Distribution on the Performance of a Phosphate Flotation Process*. Metall. Trans., v. 2, pp. 3163-74, 1971.

6. Morris, T.M. *Measurement and Evaluation of the Rate of Flotation as a Function of Particle Size*. Trans. A.I.M.E., v. 193, pp. 794-798, 1952.

7. Bennett, A., et al. *Studies in Froth Flotation of Coal*. Proceedings, Proceedings, 3rd Int. Coal Preparation Congress, Liege, 1958.

8. Gaudin, A.M., et al. *Flotation Kinetics - The Effect of Size on the Behaviour of Galena Particles*. J. Phys. Chem., v .46, pp. 902, 1942.

9. Engelbrecht, J., and Woodburn, E. *The Effect of Froth Height, Aeration Rate, and Gas Precipitation on Flotation*. J.S. African I.M.M., v. 76, pp. 125-131, 1976.

10. Harris, C.C. *Flotation Machines in:* Flotation - A.M. Gaudin Memorial Volume. A.I.M.E., pp. 753-815, 1976.

11. Schubert, H., and Bischofberger, C. *On the Hydrodynamics of Flotation Machines*. Int. J. Min. Proc., v. 5, pp. 131-142, 1978.

12. Arbiter, N., et al. *The Air Flow Number in Flotation Machine Scale Up*. Int. J. Min. Proc., v. 3, pp. 257-286, 1976.

13. Harris, C.C., et al. *A Recycle Flow Flotation Machine Model*. Int. J. Min. Proc., v. 2, pp. 39-58, 1975.

14. Degner, V., and Treweek, H. *Large Flotation Cell Design and Development in:* Flotation - A.M. Gaudin Memorial Volume. A.I.M.E., pp. 816-837, 1976.

15. Fallenius, K. *Outokumpu Flotation Machines in:* Flotation - A.M. Gaudin Memorial Volume. A.I.M.E., pp. 838-853, 1976.

16. Meerman, P. *Interface - Active Chemicals in Coal Preparation - Practical Experience at the Dutch State Mines.* Proceedings, 2nd Int. Coal Preparation Congress, Leeds, 1957.

17. Poling, G. *Selection and Sizing of Flotation Machines in:* Mineral Processing Plant Design (2nd edition). A.I.M.E., pp. 887-906, 1979.

18. Sun, S.C. *Hypothesis for Different Floatabilities of Coals, Carbons, and Hydrocarbon Minerals.* Trans. A.I.M.E., v. 199, pp. 67-75, 1954.

19. Miller, F.G., et al. *Study of the Mechanism of Coal Flotation and Its Role in a System for Processing Fine Coal.* Trans. A.I.M.E., v. 238, pp. 276-281, 1967.

20. Pearson, D. *The Quality of Western Canadian Coking Coal.* Bulletin of the CIMM, v. 73, n. 813, pp. 70-84, 1980.

21. Aplan, F.F. *Coal Flotation in:* Flotation - A.M. Gaudin Memorial Volume. A.I.M.E., pp. 1235-1264, 1976.

22. Goncharova, G., et al. *Interaction Between Non-Polar and Heteropolar Reagents in Flotation.* Coke Chem. USSR, n. 12, pp. 6-8, 1974.

23. Iskra, J., and Laskowski, J. *New Possibilities for Investigating Air Oxidation of Coal Surfaces at Low Temperatures.* Fuel, v. 46, 1967.

24. Berkowitz, N., et al. *Behaviour Differences Between Carboniferous and Cretaceous Bituminous Coals of Similar Rank.* Fuel, v. 53, 1974.

25. Sun, S.C. *Effects of Oxidation of Coals on their Flotation Properties.* Trans. A.I.M.E., v. 199, pp. 396-401, 1954.

26. Wen, W.W. Electrokinetic and Flotation Behaviour of Oxidized Coal. PhD Thesis, Pennsylvania State University, 1977.

27. McIntyre, A. Flotation Behaviour of Oxidized Coal. BSc Thesis, University of Alberta, 1977.

28. Botha, P.H. *An Investigation of the Flotation of Three South African Coals*. J.S. African I.M.M., v. 80, n. 11, pp. 395-400, 1980.

29. Aplan, F.F. *Conference on Coal Preparation at Rindge N.H.*. Unpublished Proceedings, 1979.

30. Steiner, H.J. *Kinetic Aspects of the Flotation Behaviour of Locked Particles*. Proceedings 10th Int. Min. Proc. Congress, London, 1973.

31. Firth, B., et al. *The Influence of Feed Size Distribution on the Staged Flotation of Poorly Floating Coals*. Proc. Australasian I.M.M., n. 267, pp. 49-53, 1978.

32. King, R.P. *A Pilot Plant Investigation of a Kinetic Model for Flotation*. National Institute for Metallurgy (S. Africa), Report no. 1847, 1976.

33. Woodburn, E.T. *Mathematical Modelling of Flotation Processes*. Min. Sci. and Engineering, v. 5, n. 2, pp. 3-17, 1970.

34. Bushell, C.H. *Kinetics of Flotation*. Trans. A.I.M.E., v. 223, pp. 266-278, 1962.

35. Jowett, A., and Safvi, S. *Refinements in Methods of Determining Flotation Rates*. Trans. A.I.M.E., v. 217, pp. 351-357, 1960.

36. Lynch, A.J., et al. *The Behaviour of Minerals in Sulphide Flotation Processes*. J.S. African I.M.M., v. 74, pp. 349-361, 1974.

37. Schuhmann, R. *Flotation Kinetics - Methods for the Steady State Study of Flotation Problems*. J. Phys. Chem., v. 46, pp. 891-902, 1942.

38. Morris, T.M. *Measurement and Evaluation of the Rate of Flotation as a Function of Particle Size*. Trans, A.I.M.E., v. 193, pp. 794-798, 1952.

39. Brown, D., and Smith, H. *Flotation of Coal as a Rate Process*. Trans. Inst. Min. Eng., v. 113, pp. 1001-1019, 1954.

40. Arbiter, N. *Flotation Rates and Flotation Efficiency*. Trans. A.I.M.E., v. 190, pp. 791-796, 1951.

41. deBruyn, P., and Modi, H. *Particle Size and Flotation Rate of Quartz*. Trans. A.I.M.E., v. 205, pp. 415-419, 1956.

42. Tomlinson, H., and Fleming, M. *Flotation Rate Studies*. Proceedings, 6th Int. Min. Proc. Congress, Cannes, pp. 563-579, 1963.

43. Imaizumi, T., and Inoue, I. *Kinetic Consideration of Froth Flotation:* Proceedings, 6th Int. Min. Proc. Congress, Cannes, pp. 581-593, 1963.

44. Jowett, A. *Formation and Disruption of Particle - Bubble Aggregates in Flotation.* Proceedings, Int. Symposium on Fine Particles Processing, A.I.M.E., Las Vegas, 1980.

45. Kelsall, D.F. *Application of Probability in the Assessment of Flotation Systems.* Trans. I.M.M., v. 70, pp. 191-204, 1960.

46. Jowett, A., et al. *Application of Mathematical Models of Flotation.* Proceedings, Symposium in Automatic Control Systems in Mineral Processing Plants, Brisbane, 1971.

47. Lynch, A.J., et al. *Modelling of Industrial Sulphide Flotation Circuits in:* Flotation - A.M. Gaudin Memorial Volume. A.I.M.E., pp. 725-752, 1976.

48. Flint, L.R. *Factors Influencing the Design of Flotation Equipment.* Min. Sci. and Eng., v. 5, n. 3, pp. 232-241, 1973.

49. Lynch, A.J., et al. *Automatic Control of Coal Flotation Circuits.* Proceedings, 8th Int. Coal Prep. Congress, Donetsk, 1979.

50. Lynch, A.J., et al. *Computer Control of Chalcopyrite Flotation at Mount Isa Mines Ltd. in:* Flotation - A.M. Gaudin Memorial Volume. A.I.M.E., pp. 994-1026, 1976.

51. Harris, C.C. *Multiphase Models of Flotation Machine Behaviour.* Int. J. Min. Proc., v. 5, pp. 107-129, 1978.

52. Klimpel, R.R., et al. *Laboratory Characterization of the Influence of Reagent Changes on Coal Flotation.* A.I.M.E., Annual Meeting, New Orleans, 1979.

53. Klimpel, R.R. *The Engineering Analysis of Dispersion Effects in Selected Mineral Processing Operations.* Proceedings, Int. Symposium on Fine Particles Processing, A.I.M.E., Las Vegas, 1980.

54. Trahar, W., and Warren, L. *The Floatability of Very Fine Particles - A Review.* Int. J. Min. Proc., v. 3, pp. 103-131, 1976.

55. Wemco Information Bulletin, no. FS-B54.

56. Dell, C.C., and Bunyard, M.J. *Development of an Automatic Flotation Cell for the Laboratory*. Trans. I.M.M., v. 81, pp. C245-248, 1972.

57. Flintoff, B.C., and Plitt, L.R. *A Preliminary Study of the Flotation Circuit at McIntyre Mines Ltd.*, Grande Cache Alta. University of Alberta - Dept. of Mineral Engineering Report, 1979.

58. Nelder, J., and Mead, R. *A Simplex Method for Function Minimization*. Computer Journal, v. 7, pp. 308-312, 1965.

59. Mular, A., and Bull, W. Mineral Processes - Their Analysis, Optimization, and Control. Colorado School of Mines, 1969.

60. Agar, G., et al. *Ilmenite Concentration from the Laurentian Titanium Deposit*. Bulletin of the CIMM, v. 73, n. 816, pp. 140-147, 1980.

61. Malhotra, D., et al. *Effect of Agitation and Aeration on Flotation of Molybdenite*. Mining Engineering, v. 32, n. 9, pp. 1392-1397, 1980.

62. Somasundaran, P., and Prickett, G. *Optimization of a Flotation Operation Using Statistical Methods*. Trans. A.I.M.E., v. 244, pp. 369-377, 1969.

63. Schulz, N.F. *Separation Efficiency*. Trans. A.I.M.E., v. 247, pp. 81-87, 1970.

64. Moys, M.H. *A Study of a Plug Flow Model for Froth Behaviour*. Int. J. Min. Proc., v. 5, pp. 21-38, 1978.

65. Sastry, K., and Fuerstenau, D. *Theoretical Analysis of a Countercurrent Flotation Column*. Trans. A.I.M.E., v. 247, pp. 46-52, 1970.

66. Walters, A., and Ramini, R. *The Optimization of Coal Preparation Plant Yields Using Computer Programming*. Proceedings, 7th Int. Coal Preparation Congress, Sydney, 1976.

67. Elk, F. *Common Sense Coal Preparation*. Coal Min. Proc., v. 16, n. 3, p. 58, 1978.

68. Picard, J., et al. *Improved Compound Water Cyclone for Cleaning Coal Slimes*. WRL/Canmet Report ERP/ERL 75-143(IR), 1975.

69. Gaudin, A.M., et al. *Effects of Flotation*. A.I.M.E., Tech. Publication no. 44, 1931.

70. Flintoff, B.C. An On-stream Ash Monitor. PhD Thesis, University of Alberta, In preparation, 1981.

Appendix I

Raw Data : Flotation Tests

TEST NUMBER 12

1. CONDITIONS

COLLECTOR: 0.8cc = 1.6 l/tonne   RPM: 1100

FROTHER: 6cc(1% sol) = 0.12 l/tonne   % -200 MESH: 35

AERATION RATE: 5 l/min   FEED ASH: 17.3%

2. DATA

FROTH INCREMENT	WT(g)	ASH(%)
1	97.2	7.67
2	81.0	9.13
3	90.3	10.35
4	72.0	12.50
5	22.3	17.05
6	11.9	20.30
TAILINGS	90.6	58.36
TOTAL	465.3	

3. ANALYSIS

	$\emptyset$	K_S(sec^{-1})	K_f(sec^{-1})
TOTAL MASS	0.240	9.27×10^{-4}	0.0224
INCOMBUSTIBLES	0.595	3.78×10^{-4}	0.0167

PI: 2.93 kW/m^3 N_q': 1.58×10^{-3} N_p: 8.85

MODEL OUTPUT

CELL NO.	CUMULATIVE YIELD(%)	CUMULATIVE CONCENTRATE ASH (%)
1	48.5	8.5
2	67.8	9.0
3	74.7	9.6
4	79.4	9.8

TEST NUMBER 13

1. CONDITIONS

COLLECTOR: 0.8cc = 1.6 1/tonne   RPM: 1100

FROTHER: 6cc(1% sol) = 0.12 1/tonne   % -200 MESH: 35

AERATION RATE: 5 1/min   FEED ASH: 17.4%

2. DATA

FROTH INCREMENT	WT(g)	ASH(%)
1	94.5	6.28
2	70.1	6.93
3	97.2	7.79
4	85.4	10.68
5	28.1	15.15
6	12.8	17.96
TAILINGS	85.5	46.60
TOTAL	473.6	

3. ANALYSIS

	$\emptyset$	$Ks(sec^{-1})$	$Kf(sec^{-1})$
TOTAL MASS	0.196	5.02×10^{-4}	0.0189
INCOMBUSTIBLES	0.485	5.70×10^{-3}	0.0115

PI: 2.85 kW/m³   Nq': 1.58×10^{-3} Np: 8.61

MODEL OUTPUT

CELL NO.	CUMULATIVE YIELD(%)	CUMULATIVE CONCENTRATE ASH (%)
1	47.2	8.7
2	67.4	9.4
3	76.3	10.0
4	80.5	10.3

TEST NUMBER 17

1. CONDITIONS

COLLECTOR: 0.1cc = 0.2 1/tonne   RPM: 950

FROTHER :10cc(1% sol) = 0.2 1/tonne   % -200 MESH: 50

AERATION RATE: 7 1/min   FEED ASH: 14.2%

2. DATA

FROTH INCREMENT	WT(g)	ASH(%)
1	76.1	4.78
2	63.6	5.39
3	100.0	6.17
4	96.4	7.19
5	37.6	9.95
6	20.1	12.34
TAILINGS	92.0	37.60
TOTAL	485.8	

3. ANALYSIS

	θ	$Ks(sec^{-1})$	$Kf(sec^{-1})$
TOTAL MASS	0.165	8.38×10^{-10}	0.0145
INCOMBUSTIBLES	0.580	8.98×10^{-4}	0.0103

PI: 1.97 kW/m³   Nq': 2.55×10^{-3} Np: 9.23

MODEL OUTPUT

CELL NO.	CUMULATIVE YIELD(%)	CUMULATIVE CONCENTRATE ASH (%)
1	42.9	6.0
2	63.7	6.3
3	73.8	6.6
4	78.8	6.8

TEST NUMBER 18

1. CONDITIONS

COLLECTOR: 1.5cc = 3.0 1/tonne   RPM: 950

FROTHER: 10cc(1 % sol) = 0.2 1/tonne   % -200 MESH: 20

AERATION RATE: 3 1/min   FEED ASH: 16.2%

2. DATA

FROTH INCREMENT	WT(g)	ASH(%)
1	24.5	3.88
2	26.0	4.35
3	64.5	4.57
4	52.7	5.17
5	39.2	6.97
6	32.0	6.53
TAILINGS	248.1	26.80
TOTAL	487.0	

3. ANALYSIS

	θ	$Ks(sec^{-1})$	$Kf(sec^{-1})$
TOTAL MASS	0.530	6.06×10^{-4}	0.00888
INCOMBUSTIBLES	0.712	1.05×10^{-3}	0.00653

PI: 2.10 kW/m³   Nq': 1.09×10^{-3} Np: 9.87

MODEL OUTPUT

CELL NO.	CUMULATIVE YIELD(%)	CUMULATIVE CONCENTRATE ASH (%)
1	20.7	7.3
2	34.0	7.5
3	42.8	7.6
4	48.9	7.6

TEST NUMBER 19

1. CONDITIONS

COLLECTOR: 0.1cc = 0.2 1/tonne   RPM: 1250

FROTHER: 10cc(1% sol) = 0.2 1/tonne   % -200 MESH: 50

AERATION RATE: 3 1/min   FEED ASH: 13.9%

2. DATA

FROTH INCREMENT	WT(g)	ASH(%)
1	51.8	6.08
2	44.5	5.43
3	86.6	5.99
4	109.7	4.66
5	55.8	11.25
6	28.2	15.08
TAILINGS	113.5	29.16
TOTAL	490.1	

3. ANALYSIS

	$\emptyset$	$Ks(sec^{-1})$	$Kf(sec^{-1})$
TOTAL MASS	0.128	9.09×10^{-1}	0.00930
INCOMBUSTIBLES	0.289	4.76×10^{-1}	0.00419

PI: 4.35 kW/m³   Nq': 8.32×10^{-4} Np: 8.95

MODEL OUTPUT

CELL NO.	CUMULATIVE YIELD(%)	CUMULATIVE CONCENTRATE ASH (%)
1	35.2	6.6
2	56.1	7.3
3	68.6	7.9
4	76.1	8.5

TEST NUMBER 20

1. CONDITIONS

COLLECTOR: 0.1cc = 0.2 l/tonne   RPM: 1245

FROTHER: 2cc(1% sol) = 0.04 l/tonne   % -200 MESH: 20

AERATION RATE: 7 l/min   FEED ASH: 18.5%

2. DATA

FROTH INCREMENT	WT(g)	ASH(%)
1	23.6	6.35
2	13.9	5.76
3	23.9	5.73
4	34.8	6.20
5	30.0	7.05
6	27.1	7.35
TAILINGS	333.7	23.88
TOTAL	487.0	

3. ANALYSIS

	$\emptyset$	$Ks(sec^{-1})$	$Kf(sec^{-1})$
TOTAL MASS	0.937	1.34×10^{-3}	0.0406
INCOMBUSTIBLES	0.968	8.18×10^{-4}	0.0510

PI: 4.46 kW/m^3 Nq': 1.95×10^{-3} Np: 9.30

MODEL OUTPUT

CELL NO.	CUMULATIVE YIELD(%)	CUMULATIVE CONCENTRATE ASH (%)
1	13.0	11.3
2	21.8	11.6
3	28.9	11.8
4	35.3	12.1

TEST NUMBER 21

1. CONDITIONS

COLLECTOR: 0.1cc = 0.2 l/tonne   RPM: 960

FROTHER: 2cc(1% sol) = 0.04 l/tonne   % -200 MESH: 20

AERATION RATE: 3 l/min   FEED ASH: 20.2%

2. DATA

FROTH INCREMENT	WT(g)	ASH(%)
1	4.3	5.65
2	3.3	5.16
3	7.4	5.19
4	11.4	5.32
5	7.8	6.15
6	8.3	5.81
TAILINGS	442.8	21.59
TOTAL	485.3	

3. ANALYSIS

	$\emptyset$	$Ks(sec^{-1})$	$Kf(sec^{-1})$
TOTAL MASS	0.914	1.09×10^{-4}	0.00548
INCOMBUSTIBLES	0.677	2.25×10^{-4}	0.000341

PI: 1.83 kW/m³   Nq': 1.08×10^{-3} Np: 8.32

MODEL OUTPUT

CELL NO.	CUMULATIVE YIELD(%)	CUMULATIVE CONCENTRATE ASH (%)
1	3.2	5.0
2	5.6	5.5
3	7.6	6.1
4	9.2	6.6

TEST NUMBER 22

1. CONDITIONS

COLLECTOR: 1.5cc = 3 l/tonne   RPM: 940

FROTHER: 2cc(1% sol) = 0.04 l/tonne   % -200 MESH: 50

AERATION RATE: 7 l/min   FEED ASH: 14.9%

2. DATA

FROTH INCREMENT	WT(g)	ASH(%)
1	50.4	4.98
2	44.1	5.35
3	73.7	5.33
4	67.5	6.14
5	35.6	6.58
6	12.0	6.81
TAILINGS	199.1	23.78
TOTAL	482.4	

3. ANALYSIS

	$\emptyset$	$Ks(sec^{-1})$	$Kf(sec^{-1})$
TOTAL MASS	0.385	3.32×10^{-7}	0.0135
INCOMBUSTIBLES	0.834	5.28×10^{-4}	0.0163

PI: 1.83 kW/m³   Nq': 2.58×10^{-3} Np: 8.86

MODEL OUTPUT

CELL NO.	CUMULATIVE YIELD(%)	CUMULATIVE CONCENTRATE ASH (%)
1	30.5	5.9
2	45.8	6.2
3	53.6	6.6
4	57.5	7.1

TEST NUMBER 23

1. CONDITIONS

COLLECTOR: 1.5cc = 3 l/tonne   RPM: 1235

FROTHER: 10cc(1 % sol) = 0.2 l/tonne   % -200 MESH: 20

AERATION RATE: 7 l/min   FEED ASH: 22.5%

2. DATA

FROTH INCREMENT	WT(g)	ASH(%)
1	51.5	5.42
2	22.0	5.35
3	41.5	5.57
4	59.8	6.61
5	39.1	8.14
6	31.5	9.27
TAILINGS	198.9	39.69
TOTAL	444.3	

3. ANALYSIS

	$\emptyset$	$Ks(sec^{-1})$	$Kf(sec^{-1})$
TOTAL MASS	0.849	2.70×10^{-3}	0.0429
INCOMBUSTIBLES	0.907	1.06×10^{-3}	0.0368

PI: 4.23 kW/m^3 Nq': 1.97×10^{-3} Np: 9.04

MODEL OUTPUT

CELL NO.	CUMULATIVE YIELD(%)	CUMULATIVE CONCENTRATE ASH (%)
1	25.4	11.8
2	39.7	11.9
3	50.1	12.2
4	58.4	12.5

TEST NUMBER 24

1. CONDITIONS

COLLECTOR: 1.5cc = 3 l/tonne   RPM: 1255

FROTHER: 2cc(1% sol) = 0.04 l/tonne   % -200 MESH: 50

AERATION RATE: 3 l/min   FEED ASH: 15.0%

2. DATA

FROTH INCREMENT	WT(g)	ASH(%)
1	37.5	8.33
2	29.8	8.21
3	50.4	8.40
4	82.7	9.00
5	56.6	10.58
6	29.7	11.88
TAILINGS	186.1	18.91
TOTAL	472.8	

3. ANALYSIS

	$\emptyset$	$Ks(sec^{-1})$	$Kf(sec^{-1})$
TOTAL MASS	0.248	1.41×10^{-7}	0.00691
INCOMBUSTIBLES	0.459	4.59×10^{-9}	0.00542

PI: 4.23 kW/m³   Nq': 8.29×10^{-4} Np: 8.61

MODEL OUTPUT

CELL NO.	CUMULATIVE YIELD(%)	CUMULATIVE CONCENTRATE ASH (%)
1	25.1	9.6
2	41.8	9.9
3	52.9	10.2
4	60.4	10.4

TEST NUMBER 25

1. CONDITIONS

COLLECTOR: 0.8cc = 1.6 l/tonne   RPM: 1120

FROTHER: 6cc(1% sol) = 0.12 l/tonne   % -200 MESH: 35

AERATION RATE: 5 l/min   FEED ASH: 17.5%

2. DATA

FROTH INCREMENT	WT(g)	ASH(%)
1	58.5	5.41
2	41.8	5.45
3	80.7	5.62
4	93.1	6.78
5	38.8	8.11
6	26.4	9 32
TAILINGS	142.6	39.12
TOTAL	481.9	

3. ANALYSIS

	$\emptyset$	$Ks(sec^{-1})$	$Kf(sec^{-1})$
TOTAL MASS	0.254	3.84×10^{-3}	0.0116
INCOMBUSTIBLES	0.781	4.86×10^{-4}	0.0134

PI: 2.86 kW/m³   Nq': 1.55×10^{-3} Np: 8.19

MODEL OUTPUT

CELL NO.	CUMULATIVE YIELD(%)	CUMULATIVE CONCENTRATE ASH (%)
1	34.1	6.9
2	52.6	7.1
3	62.6	7.4
4	68.1	7.8

TEST NUMBER 40

1. CONDITIONS

COLLECTOR: 0.8+0.4cc = 2.4 l/tonne   RPM: 970

FROTHER: 10cc(1% sol) = 0.2 l/tonne   % -200 MESH: 35

AERATION RATE: 7.75 l/min   FEED ASH: 18.1%

2. DATA

FROTH INCREMENT	WT(g)	ASH(%)
1	59.5	8.73
2	37.7	9.09
3	56.3	9.86
4	91.1	10.14
5	61.0	11.81
6	34.0	13.99
TAILINGS	130.3	38.15
TOTAL	469.9	

3. ANALYSIS

	θ	$Ks(sec^{-1})$	$Kf(sec^{-1})$
ROUGHER:			
TOTAL MASS	0.921	5.24×10^{-3}	0.0868
INCOMBUSTIBLES	0.785	4.10×10^{-4}	0.0191
SCAVENGER:			
TOTAL MASS	0.236	2.33×10^{-8}	0.00807
INCOMBUSTIBLES	0.508	1.76×10^{-7}	0.00522

PI: 2.06 kW/m³   Ng': 2.77×10^{-3} Np: 9.07

MODEL OUTPUT

CELL NO.	CUMULATIVE YIELD(%)	CUMULATIVE CONCENTRATE ASH (%)
1	32.1	8.3
2	51.3	9.3
3	63.4	9.7
4	71.0	10.0

TEST NUMBER 41

1. CONDITIONS

COLLECTOR: 0.8+0.4cc = 2.4 l/tonne   RPM: 965

FROTHER: 10cc(1% sol) = 0.2 l/tonne   % -200 MESH: 35

AERATION RATE: 7.75 l/min   FEED ASH: 17.8%

2. DATA

FROTH INCREMENT	WT(g)	ASH(%)
1	72.7	7.22
2	48.5	8.09
3	82.5	8.72
4	78.6	9.65
5	43.7	11.73
6	24.7	14.23
TAILINGS	124.6	41.61
TOTAL	475.3	

3. ANALYSIS

	θ	$Ks(\text{sec}^{-1})$	$Kf(\text{sec}^{-1})$
ROUGHER:			
TOTAL MASS	0.967	8.76×10^{-3}	0.601
INCOMBUSTIBLES	0.944	2.79×10^{-3}	0.0323
SCAVENGER:			
TOTAL MASS	0.378	3.12×10^{-4}	0.0101
INCOMBUSTIBLES	0.709	2.12×10^{-4}	0.00726

PI: 1.85 kW/m³   Nq': 2.78×10^{-3} Np: 8.30

MODEL OUTPUT

CELL NO.	CUMULATIVE YIELD(%)	CUMULATIVE CONCENTRATE ASH (%)
1	40.8	8.6
2	56.8	9.0
3	66.3	9.2
4	72.0	9.3

TEST NUMBER 50

1. CONDITIONS

COLLECTOR: 0.8+0.6cc = 2.8l/tonne   RPM: 975

FROTHER: 12cc(1% sol) = 0.24 1/tonne   % -200 MESH: 35

AERATION RATE: 7.75 1/min   FEED ASH: 18.0%

2. DATA

FROTH INCREMENT	WT(g)	ASH(%)
1	50.4	10.30
2	44.4	10.36
3	50.9	10.91
4	97.8	10.57
5	56.0	11.62
6	30.4	12.48
TAILINGS	155.8	32.92
TOTAL	485.7	

3. ANALYSIS

	$\emptyset$	$Ks(sec^{-1})$	$Kf(sec^{-1})$
ROUGHER:			
TOTAL MASS	0.549	8.12×10^{-4}	0.0184
INCOMBUSTIBLES	0.782	7.28×10^{-4}	0.0181
SCAVENGER:			
TOTAL MASS	0.340	2.12×10^{-3}	0.00958
INCOMBUSTIBLES	0.627	6.32×10^{-3}	0.00817

PI: 2.02 kW/m³   Nq': 2.76×10^{-3} Np: 8.79

MODEL OUTPUT

CELL NO.	CUMULATIVE YIELD(%)	CUMULATIVE CONCENTRATE ASH (%)
1	25.8	11.4
2	45.9	11.0
3	57.7	10.9
4	64.7	10.9

TEST NUMBER 52

1. CONDITIONS

COLLECTOR: 0.8+0.2cc = 2 l/tonne   RPM: 955

FROTHER: 12cc(1% sol) = 0.24 l/tonne   % -200 MESH: 35

AERATION RATE: 7.75 l/min   FEED ASH: 18.3%

2. DATA

FROTH INCREMENT	WT(g)	ASH(%)
1	74.7	10.16
2	38.0	9.36
3	67.5	10.09
4	89.7	11.08
5	52.4	13.10
6	22.3	14.37
TAILINGS	127.4	37.86
TOTAL	472.0	

3. ANALYSIS

	$\emptyset$	$Ks(sec^{-1})$	$Kf(sec^{-1})$
ROUGHER:			
TOTAL MASS	0.934	6.86×10^{-3}	0.964
INCOMBUSTIBLES	0.956	3.14×10^{-3}	0.884
SCAVENGER:			
TOTAL MASS	0.332	3.39×10^{-4}	0.0105
INCOMBUSTIBLES	0.619	9.28×10^{-14}	0.0831

PI: 1.69 kW/m³   Nq': 2.81×10^{-3} Np: 7.82

MODEL OUTPUT

CELL NO.	CUMULATIVE YIELD(%)	CUMULATIVE CONCENTRATE ASH (%)
1	37.5	10.5
2	55.6	10.8
3	65.8	10.9
4	71.6	11.0

TEST NUMBER 53

1. CONDITIONS

COLLECTOR: 0.8+0.2cc = 2 l/tonne   RPM: 965

FROTHER: 8cc(1% sol) = 0.16 l/tonne   % -200 MESH: 35

AERATION RATE: 7.75 l/min   FEED ASH: 17.4%

2. DATA

FROTH INCREMENT	WT(g)	ASH(%)
1	33.4	10.54
2	27.5	10.50
3	38.0	11.36
4	61.7	11.16
5	32.1	12.23
6	21.6	12.36
TAILINGS	264.3	22.40
TOTAL	478.8	

3. ANALYSIS

	θ	Ks(sec^{-1})	Kf(sec^{-1})
ROUGHER:			
TOTAL MASS	0.659	3.80×10^{-3}	0.0153
INCOMBUSTIBLES	0.779	9.90×10^{-3}	0.0137
SCAVENGER:			
TOTAL MASS	0.833	1.05×10^{-3}	0.0185
INCOMBUSTIBLES	0.876	4.7410^{-4}	0.0138

PI: 1.85 kW/m^2 Nq': 2.78×10^{-3} Np: 8.30

MODEL OUTPUT

CELL NO.	CUMULATIVE YIELD(%)	CUMULATIVE CONCENTRATE ASH (%)
1	18.1	11.1
2	30.8	11.1
3	38.6	11.1
4	44.2	11.2

TEST NUMBER 55

1. CONDITIONS

COLLECTOR: 0.8+0.6cc = 2.8l/tonne   RPM: 960

FROTHER: 8cc(1% sol) = 0.16 l/tonne   % -200 MESH: 35

AERATION RATE: 7.75 l/min   FEED ASH: 17.1%

2. DATA

FROTH INCREMENT	WT(g)	ASH(%)
1	43.7	10.80
2	34.0	10.64
3	30.8	11.60
4	92.3	10.48
5	47.0	11.56
6	33.9	11.70
TAILINGS	215.7	25.04
TOTAL	497.4	

3. ANALYSIS

	$\emptyset$	$Ks(sec^{-1})$	$Kf(sec^{-1})$
ROUGHER:			
TOTAL MASS	0.729	5.73×10^{-3}	0.0275
INCOMBUSTIBLES	0.919	1.21×10^{-3}	0.0492
SCAVENGER:			
TOTAL MASS	0.835	2.29×10^{-3}	0.0259
INCOMBUSTIBLES	0.792	5.78×10^{-4}	0.0115

PI: 1.86 kW/m³   Nq': 2.80×10^{-3} Np: 8.48

MODEL OUTPUT

CELL NO.	CUMULATIVE YIELD(%)	CUMULATIVE CONCENTRATE ASH (%)
1	18.0	13.0
2	36.6	11.4
3	48.0	11.1
4	56.2	11.0

Appendix II

Raw Data : Sink-Float Analysis of Clean Coal Concentrate

PARTITION CURVE DATA: TEST 12 (SIZED FRACTIONS)

SIZE RANGE: Composite   CONCENTRATE YIELD: 79.9%

                               TAILINGS YIELD: 20.1%

DISTRIBUTION (WT %)

SPECIFIC GRAVITY	CONCENTRATE	TAILINGS	PARTITION NUMBER
-1.3	27.14	8.06	6.95
+1.3-1.4	48.98	13.86	6.65
+1.4-1.5	13.48	8.11	13.15
+1.5-1.8	8.31	16.91	33.86
+1.8	2.10	53.07	86.41
Total	100.00	100.00	

SIZE RANGE: 20x48 mesh   CONCENTRATE YIELD: 74.6%

                               TAILINGS YIELD: 25.4%

DISTRIBUTION (WT %)

SPECIFIC GRAVITY	CONCENTRATE	TAILINGS	PARTITION NUMBER
-1.3	47.33	12.34	8.14
+1.3-1.4	34.73	12.68	11.05
+1.4-1.5	10.85	7.51	19.10
+1.5-1.8	6.47	14.78	43.71
+1.8	0.62	52.70	96.68
Total	100.00	100.00	

SIZE RANGE: 48x100 mesh   CONCENTRATE YIELD: 79.6%

TAILINGS YIELD: 20.4%

DISTRIBUTION (WT %)

SPECIFIC GRAVITY	CONCENTRATE	TAILINGS	PARTITION NUMBER
-1.3	41.70	10.16	5.87
+1.3-1.4	42.24	14.81	8.25
+1.4-1.5	11.84	6.12	11.72
+1.5-1.8	10.34	11.48	22.13
+1.8	4.22	57.43	77.74
Total	100.00	100.00	

SIZE RANGE: 100x200 mesh   CONCENTRATE YIELD: 82.6%

TAILINGS YIELD: 17.4%

DISTRIBUTION (WT %)

SPECIFIC GRAVITY	CONCENTRATE	TAILINGS	PARTITION NUMBER
-1.3	24.62	6.85	5.53
+1.3-1.4	48.00	15.69	6.44
+1.4-1.5	12.61	7.65	11.33
+1.5-1.8	10.55	10.72	17.67
+1.8	4.21	59.09	74.70
Total	100.00	100.00	

SIZE RANGE: 200x270 mesh   CONCENTRATE YIELD: 79.6%

TAILINGS YIELD: 20.4%

DISTRIBUTION (WT %)

SPECIFIC GRAVITY	CONCENTRATE	TAILINGS	PARTITION NUMBER
-1.3	9.75	4.69	5.77
+1.3-1.4	61.42	21.55	4.29
+1.4-1.5	16.36	10.17	7.34
+1.5-1.8	11.63	8.70	8.68
+1.8	0.84	54.89	89.18
Total	100.00	100.00	

SIZE RANGE: -270 mesh   CONCENTRATE YIELD: 82.6%

TAILINGS YIELD: 17.4%

DISTRIBUTION (WT %)

SPECIFIC GRAVITY	CONCENTRATE	TAILINGS	PARTITION NUMBER
-1.3	2.17	0.74	7.93
+1.3-1.4	72.57	10.58	3.54
+1.4-1.5	18.94	10.58	12.34
+1.5-1.8	5.49	33.14	60.27
	0.83	44.98	74.70
Total	100.00	100.00	

Appendix III

Computer Program for the Nelder-Mead SIMPLEX

```
C*********************************************************************
C
C
C          A SIMPLEX METHOD FOR FUNCTION MINIMIZATION
C
C      VERSION NO. 1          NOV. 29/77        B. FLINTOFF
C
C*********************************************************************
C      REFERENCE:  NELDER,J.A.,MEAD,R.
C                  A SIMPLEX METHOD FOR FUNCTION MINIMIZATION
C                  COMPUTER JOURNAL,  VOL7
C                  PP 308, 1965
C
C      ALTERNATE:  MULAR,A.L.,BULL,W.R.
C                  MINERAL PROCESSES:ANALYSIS, OPTIMAIZATION
C                  AND CONTROL.
C                  UBC PRESS, CHAP 13
C                  1969
C*********************************************************************
C
C          VARIABLE DEFINITION:
C          *******************
C
C      NAME         DIMENSION                    FUNCTION
C      ....         .........                    ........
C      ALPHA                       COEFFICIENT OF REFLECTION
C      BETA                        COEFFICIENT OF CONTRACTION
C      CENTRO          50          CENTROID COORDINATES
C      CYCCNT                      NO. OF OBJECTIVE EVALUATIONS
C      CYCLES                      MAXIMUM NO. OF CYCCNT ALLOWED
C      GAMMA                       COEFFICIENT OF EXPANSION
C      GENMAT       51 X 50        MATRIX OF COORDS IN HYPERSPACE
C      GUESS           50          INITIAL GUESS VECTOR FOR GENMAT
C      H                           ROW POINTER FOR HIGHEST OBJECTIVE
C      L                           ROW POINTER FOR LOWEST OBJECTIVE
C      N                           NUMBER OF ELEMENTS IN A ROW
C      OBJVAL          51          VECTOR OF OBJECTIVE VALUES
C      R                           WORK VARIABLE
C      REFLCT          50          VECTOR OF COORDS FOR REFLECTION
C      S                           ROW POINTER FOR SECOND HIGHEST OBJECTI'
C        STDERR                     STANDARD ERROR OF OBJVAL ABOUT LOWEST
C VALUE
C        STEP          50          STEP SIZES FOR GUESS TO GIVE INITIAL
C GENMAT
C        STEPNO                    COUNTER FOR NUMBER OF SIMPLEX SIZE
C REDUCTIONS
C      STOP                        CONVERGENCE CRITERION FOR STDERR
C      T1                          WORK VARIABLE
C      T2                          WORK VARIABLE
C      TEMP1           50          WORK VECTOR
C      TEMP2           50          WORK VECTOR (NOT IN USE WITH THIS LIST
C      TEMP3                       WORK VARIABLE
C      U                           WORK VARIABLE
C      Y                           CALCULATED OBJECTIVE VALUE FOR ROW H
C*********************************************************************
C
C      USAGE:  THE PROGRAM EXPECTS DATA ENTRY TO HAVE THE FOLLOWING
C      ......  STRUCTURE. CARD 1:NUMBER OF SEARCH ELEMENTS.(1<N<52)
C              CARD 2:A VECTOR OF N ELEMENTS (FIRST GUESSES) FROM WHI
C              THE INITIAL SIMPLEX IS GENERATED. CARD 3:A VECTOR OF N
```

```
C            ELEMENTS WHICH REPRESENT THE STEP SIZE FOR PERTURBATION
C            OF THE FIRST GUESSES IN INITIALLIZATION OF THE SIMPLEX.
C            NOTE: DATA IS FREE FORMAT AND MUST BE SEPARATED BY A COMMA
C
C     ***********************************************************************
C ******
C     DIMENSION CENTRO(50), GENMAT(51,50), GUESS(50), STEP(50),
     1           REFLCT(50)
      DIMENSION OBJVAL(51), TEMP1(50), TEMP2(50)
      INTEGER CYCLES, H, STEPNO, CYCCNT, S, OUTPUT
      COMMON GENMAT, S, L, H, Y, OBJVAL, CYCCNT, N, NPLUS1, OUTPUT
C*************************************************************************
C
C        VARIABLE INITIALLIZATION
C
C*************************************************************************
C SET UP STOPPING CRITERION AND CYCLE LIMIT
      STOP = 1E-03
      CYCLES = 1000
      OUTPUT = 0
C SETUP REFLECTION,EXPANSION,AND CONTRACTION COEFFICIEMTS
      ALPHA = 1
      GAMMA = 2
      BETA = .5
C READ IN NUMBER OF ELEMENTS PER SIMPLEX ROW
      READ (5,10) N
   10 FORMAT (I2)
C READ IN FIRST GUESS VECTOR FOR SIMPLEX GENERATION
      READ (5,20) (GUESS(I),I=1,N)
   20 FORMAT (10F5.2)
C READ IN STEP SIZES ASSOCIATED WITH GUESS(I)
      READ (5,20) (STEP(I),I=1,N)
C CALCULATE INITIAL SIMPLEX FROM GUESS AND STEP
      NPLUS1 = N + 1
      DO 60 J = 1, N
         DO 30 I = 1, NPLUS1
            IF (I .EQ. J + 1) GO TO 40
            GENMAT(I,J) = GUESS(J) - (2/(FLOAT(J) + 1)) * STEP(J)
   30    CONTINUE
   40    GENMAT(I,J) = GUESS(J) + ((2/(FLOAT(J) + 1))*STEP(J)) * FLOAT(J)
         IF (J .EQ. N) GO TO 70
         JPLUS2 = J + 2
         DO 50 I = JPLUS2, NPLUS1
            GENMAT(I,J) = GUESS(J)
   50    CONTINUE
   60 CONTINUE
C SETUP CYCLE COUNTER FOR OBJECTIVE EVALUATIONS
   70 CYCCNT = 0
C SETUP CYCLE COUNTER FOR SIZE REDUCTIONS
      STEPNO = 0
C*************************************************************************
C
C        BEGIN SIMPLEX CALCULATIONS
C
C*************************************************************************
C
C EVALUATE OBJECTIVE FOR ALL ROWS IN GENMAT
   80 DO 90 I = 1, NPLUS1
         H = I
         CALL OBJECT
```

```
        OBJVAL(I) = Y
   90 CONTINUE
C RANK THE OBJECTIVES ACCORDING TO THEIR MAGNITUDE
  100 CALL RANK
C CALCULATE THE STANDARD ERROR OF THE OBJECTIVE VALUES
      T1 = 0
      T2 = 0
      DO 110 I = 1, NPLUS1
         U = OBJVAL(I) - OBJVAL(L)
         T1 = T1 + U ** 2
         T2 = T2 + U
  110 CONTINUE
      STDERR = SQRT((T1 - (T2**2/NPLUS1))/N)
      IF (STDERR .LT. STOP) GO TO 290
      IF (CYCCNT .GT. CYCLES) GO TO 270
C********************************************************************
C                 REFLECTION
C********************************************************************
C SAVE ROW CORRESPONDING TO HIGHEST OBJECTIVE VALUE
      DO 120 I = 1, N
         TEMP1(I) = GENMAT(H,I)
  120 CONTINUE
C CALCULATE THE CENTROID OF THE HYPERPLANE
      DO 130 J = 1, N
         CENTRO(J) = 0
         DO 130 I = 1, NPLUS1
            IF (I .EQ. H) GO TO 130
            CENTRO(J) = CENTRO(J) + GENMAT(I,J) / N
  130 CONTINUE
C CALCULATE REFLECTED VALUE COORDINATES
      DO 140 J = 1, N
         REFLCT(J) = (1 + ALPHA) * CENTRO(J) - ALPHA * TEMP1(J)
         GENMAT(H,J) = REFLCT(J)
  140 CONTINUE
C CALCULATE OBJECTIVE ASSOC. WITH REFLECTED COORDS.
      CALL OBJECT
      TEMP3 = Y
C REPLACE REFLECTED ROW WITH ORIGINAL H ROW
      DO 150 J = 1, N
         GENMAT(H,J) = TEMP1(J)
  150 CONTINUE
C COMPARE OBJECTIVE VALUES OF LOWEST ROW AND REFLECTED COORDS
      IF (TEMP3 .GE. OBJVAL(L)) GO TO 170
C********************************************************************
C                 EXPANSION
C********************************************************************
      DO 160 J = 1, N
         GENMAT(H,J) = (1 + GAMMA) * REFLCT(J) - GAMMA * CENTRO(J)
  160 CONTINUE
C CALCULATE OBJECTIVE ASSOCIATED WITH EXPANSION COORDS.
      CALL OBJECT
C COMPARE OBJECTIVES OF EXPANDED WITH LOWEST ROW
      IF (Y .GT. OBJVAL(L)) GO TO 180
C IF EXPANSION WAS A SUCCESS REPLACE ROW H
      OBJVAL(H) = Y
      GO TO 100
C COMPARE OBJECTIVES OF REFLECTED WITH SECOND HIGHEST ROW
  170 IF (TEMP3 .GT. OBJVAL(S)) GO TO 200
C IF REFLECTION WAS A SUCCESS REPLACE ROW H
  180 OBJVAL(H) = TEMP3
```

```fortran
      DO 190 J = 1, N
         GENMAT(H,J) = REFLCT(J)
  190 CONTINUE
      GO TO 100
C COMPARE OBJECTIVES OF REFLECTION AND HIGHEST ROW
  200 IF (TEMP3 .GT. OBJVAL(H)) GO TO 220
C REPLACE ROW H WITH REFLECTED COORDS.
      DO 210 J = 1, N
         GENMAT(H,J) = REFLCT(J)
  210 CONTINUE
      OBJVAL(H) = TEMP3
C*************************************************************
C                   CONTRACTION
C*************************************************************
C SAVE ROW H AND CALCULATE CONTRACTION COORDS.
  220 DO 230 J = 1, N
         TEMP1(J) = GENMAT(H,J)
         GENMAT(H,J) = BETA * GENMAT(H,J) + (1 - BETA) * CENTRO(J)
  230 CONTINUE
C CALCULATE OBJECTIVE ASSOC. WITH CONTRACTED COORDS.
      CALL OBJECT
C COMPARE OBJECTIVES OF CONTRACTED COORDS. AND ROW H
      IF (Y .GT. OBJVAL(H)) GO TO 240
C IF CONTRACTION WAS A SUCCESS REPLACE ROW H
      OBJVAL(H) = Y
      GO TO 100
C*************************************************************
C          STEP CHANGE-----SIZE REDUCTION
C*************************************************************
C REPLACE CONTRACTED COORDS WITH ORIGINAL ROW H AND REDUCE SIZE
  240 DO 250 J = 1, N
         GENMAT(H,J) = TEMP1(J)
         DO 250 I = 1, NPLUS1
            GENMAT(I,J) = (GENMAT(I,J) + GENMAT(L,J)) / 2
  250 CONTINUE
C INCREMENT STEP CHANGE COUNTER AND PRINT DATA
      STEPNO = STEPNO + 1
      WRITE (6,260) STEPNO, CYCCNT
  260 FORMAT (' ', 'STEP CHANGE NUMBER ', I4, ' OCCURRED NEAR CYCLE ',
     1        I4)
      GO TO 80
C*************************************************************
C              END OF SIMPLEX CALCULATIONS
C*************************************************************
C
C
C
C*************************************************************
C
C
C          OUPUT SECTION
C
C    THIS SECTION IS USER MODIFIED SUBJECT TO OUPUT REQUIREMENTS
C
C*************************************************************
  270 WRITE (6,280) CYCCNT
  280 FORMAT (' ', 'SIMPLEX FAILED TO CONVERGE IN ', I4, ' CYCLES')
      GO TO 310
  290 WRITE (6,300)
  300 FORMAT (' ', 'CONVERGENCE INFORMATION.......')
```

```
310 WRITE (6,320)
320 FORMAT (' ', 'SIMPLEX ROW L FOLLOWS')
    WRITE (6,330) (GENMAT(L,J),J=1,N)
330 FORMAT (' ', 8(E12.5,3X))
    WRITE (6,340) OBJVAL(L), OBJVAL(H)
340 FORMAT (' ', 'LOWEST AND HIGHEST OBJECTIVES ARE ', E12.5, ' AND ',
   1        E12.5)
    WRITE (6,350) CYCCNT
350 FORMAT (' ', 'NUMBER OF CYCLES =', I4)
    H = L
    OUTPUT = 1
    CALL OBJECT
    STOP
    END
C
C*************************************************************************
C
C
C
C
C*************************************************************************
C
C
    SUBROUTINE RANK
    DIMENSION GENMAT(51,50), OBJVAL(51)
    INTEGER CYCLES, H, STEPNO, CYCCNT, S, OUTPUT
C
C*************************************************************************
C
C
    THE FUNCTION OF THIS SUBROUTINE IS TO DETERMINE WHICH ROWS
C   OF THE SIMPLEX CORRESPOND TO THE HIGHEST,SECOND HIGHEST AND LOWEST
C   OBJECTIVE VALUES
C
C
C   *************************************************************************
C
C ***
C
    COMMON GENMAT, S, L, H, Y, OBJVAL, CYCCNT, N, NPLUS1, OUTPUT
    L = 1
    H = 1
    S = 1
C SEARCH FOR HIGHEST AND LOWEST OBJECTIVE VALUES
    DO 30 I = 2, NPLUS1
       IF (OBJVAL(I) .GT. OBJVAL(H)) GO TO 10
       IF (OBJVAL(I) .LT. OBJVAL(L)) GO TO 20
       GO TO 30
 10    H = I
       GO TO 30
 20    L = I
 30 CONTINUE
C SEARCH FOR SECOND HIGHEST OBJECTIVE VALUE
    R = OBJVAL(H)
    OBJVAL(H) = -1E-70
    DO 40 I = 2, NPLUS1
       IF (OBJVAL(I) .LE. OBJVAL(S)) GO TO 40
       S = I
 40 CONTINUE
    OBJVAL(H) = R
    RETURN
    END
```

```
      SUBROUTINE OBJECT
      DIMENSION GENMAT(51,50), OBJVAL(51)
      INTEGER CYCLES, H, STEPNO, CYCCNT, S, OUTPUT
      COMMON GENMAT, S, L, H, Y, OBJVAL, CYCCNT, N, NPLUS1, OUTPUT
C
C************************************************************************
C
C     CONVENTION: THE SEARCH VARIABLES ARE LOCATED IN ROW
C                 H OF THE SIMPLEX MATRIX 'GENMAT'. EG.
C                 GENMAT(H,3) WOULD CONTAIN THE VALUE FOR
C                 THE THIRD UNKNOWN. YOU MAY REQUIRE TO
C                 CONSTRAIN THESE VALUES PRIOR TO YOUR
C                 CALCULATIONAL BLOCK (EG. ABSOLUTE VALUES).
C
C        RULES: THE OBJECTIVE FUNCTION VALUE MUST ALWAYS
C               BE CALCULATED IN THE VARIABLE 'Y'.
C
C               ONCE THE SEARCH IS FINISHED IT WILL OUTPUT
C               SOME INFORMATION THEN SET THE 'OUTPUT' FLAG
C               TO 1 FROM 0, AND CALL THIS SUBROUTINE WITH
C               THE BEST POINT IN THE CURRENT SIMPLEX. THIS
C               ALLOWS THE USER TO PROVIDE ADDITIONAL
C               PERTINENT OUTPUT.
C
C               DO NOT REMOVE THE LINE,
C                     'CYCCNT=CYCCNT+1'
C               FROM THE SUBPROGRAM AS IT IS USED IN JOB
C               CONTROL.
C
C************************************************************************
C
C----------------------------------------------------------------
      DIMENSION T(6), R(6), RP(6)
C
C************************************************************************
C        DATA T REFERS TO THE INTERVAL TIMES (SECONDS) FOR THE FLOTATI(
C TEST
C************************************************************************
C ****
C
      DATA T /15, 30, 60, 120, 240/
C
C************************************************************************
C     DATA R REFERS TO THE FRACTION OF COAL REMAINING IN THE PULP A
C THE
C               INTERVAL TIME CORRESPONDING TO DATA T
C************************************************************************
C **
C
      DATA R /.796, .686, .490, .291, .189/
C
C     DEFINE PHI=PHI,RKF=KF AND RKS=KS
C
      PHI = ABS(GENMAT(H,1))
      RKF = ABS(GENMAT(H,2))
      RKS = ABS(GENMAT(H,3))
C
C     COMPUTE OBJECTIVE FOR THIS POINT
C
      Y = 0.
```

```
      DO 10 I = 1, 6
         RP(I) = 100. - (100. - PHI) * EXP(-RKF*T(I)) - PHI * EXP(-RKS*T(
     1   I))
         Y = Y + (R(I) - RP(I)) * (R(I) - RP(I))
   10 CONTINUE
      CYCCNT = CYCCNT + 1
      IF (OUTPUT .EQ. 0) RETURN
C
C     OUTPUT THE RESULTS CORRESPONDING TO THE BEST ESTIMATES
C
      WRITE (6,20) PHI, RKF, RKS
   20 FORMAT ('-', 'ESTIMATED VALUES OF THE PARAMETERS ARE..'/' ', 5X, '
     1PHI=', F6.2, 10X, 'KF=', F6.4, ' MIN**-1 AND KS=', F6.4, ' MIN**-1
     2')
      WRITE (6,30)
   30 FORMAT ('-', 'TIME', 6X, 'OBS. REC.', 1X, 'PRE. REC.', 1X, 'RESIDU
     1AL')
      DO 50 I = 1, 6
         RES = R(I) - RP(I)
         WRITE (6,40) T(I), R(I), RP(I), RES
   40    FORMAT (' ', F5.2, 5X, F5.2, 5X, F6.2, 4X, F5.2)
   50 CONTINUE
      RETURN
      END
```

Appendix IV

Computer Program for Three Parameter Flotation Model

```
/COMPILE                                                          179
C
C
C  **********************************************************************
C  **
C
C
C               FORTRAN PROGRAM OF THE 3 PARAMETER FLOTATION MODEL
C               *******************************************************
C
C                          by A. McINTYRE       MAY 1980
C
C                     FILES/DEVICE NOS. FOR DATA INPUT:
C
C           FILE NAME              DESCRIPTION              DEVICE NO.
C           **********************************************************
C           *SOURCE*    FORTRAN SOURCE PROGRAM                  5
C           DATA        MODEL PARAMETERS FOR ALL PARTICLES      7
C           ASHDAT      MODEL PARAMETERS FOR INCOMBUSTIBLES     8
C
C   THIS PROGRAM IS INTENDED TO BE EXECUTED FROM A DECWRITER TERMINAL
C
C
C  **********************************************************************
C  **
C
C
      INTEGER TNO, SIZE(8,2)
      REAL IMASH(8,4), INCY(8,4), INCA(8,4)
      DIMENSION DATA(8,3), CUMY(8,4), FY(8,7)
      DIMENSION ASHR(8,4), ASHP(8,6), ASHPR(8,4), FASH(8,1), CUMA(8,1)
      DIMENSION ASHDAT(8,3), ES(8,1)
      WRITE (6,10)
   10 FORMAT ('-', T10, 'START ALL INPUTS FROM THE 2ND PRINT POSITION'/
     1T10, 42('*'))
C
C  **********************************************************************
C     SOME COMPUTER TERMINALS IGNORE CHARACTERS IN 1ST PRINT POSITION
C  **********************************************************************
C
   20 FORMAT (1X, I2)
   30 FORMAT (1X, F4.1)
   40 FORMAT (1X, 2A4)
   50 FORMAT (F5.3, 2(1X,E8.2))
   60 FORMAT (8(1X,F5.2))
      WRITE (6,70)
   70 FORMAT ('-', 'FLOTATION TEST NO?.....(IE 06)')
      READ (5,20) TNO
      WRITE (6,80)
   80 FORMAT ('0', 'ENTER NO. OF SIZE INTERVALS (INCLUDE COMPOSITE FEED)
     1. ....(IE 05)')
      READ (5,20) M
      WRITE (6,90)
   90 FORMAT ('0', 'ENTER THE MESH INTERVALS.....(IE 20x48M)')
      DO 110 I = 1, M
        READ (5,40) SIZE(I,1), SIZE(I,2)
        IF (I .EQ. M) GO TO 110
        WRITE (6,100)
  100   FORMAT (' ', 'ENTER NEXT SIZE INTERVAL:')
  110 CONTINUE
```

```
      WRITE (6,120)
  120 FORMAT ('0', 'ENTER NO. OF CELLS IN BANK TO MAXIMUM OF 4..(IE 03)'
     1)
      READ (5,20) N
      WRITE (6,130)
  130 FORMAT ('0', 'ENTER CELL RESIDENCE TME IN SECONDS...(IE 90.1)')
      READ (5,30) TAU
C
C***********************************************************************
C     THE PROGRAM NOW READS MODEL PARAMETERS FROM FILES DATA AND ASHDAT
C***********************************************************************
C
      DO 140 I = 1, M
         READ (7,60) DATA(I,1), DATA(I,2), DATA(I,3)
         READ (8,60) ASHDAT(I,1), ASHDAT(I,2), ASHDAT(I,3)
  140 CONTINUE
C
C***********************************************************************
C     ORGANIZATION OF OUTPUT:
C        TEST IDENTIFICATION PLUS LISTING OF MODEL PARAMETERS
C***********************************************************************
C
      WRITE (6,150) TNO
  150 FORMAT (2('-'), T20, 'PREDICTED CONCENTRATE YIELD AND QUALITY FOR
     1FLOTATION TEST ', I2/62('*'))
      WRITE (6,160)
  160 FORMAT ('-', T20, 'TABLE 1 - MODEL PARAMETERS FOR ALL PARTICLES'/
     1T20, 44('*')/'0', T10, 'MESH INTERVAL', T35, 'PHI', T47, 'K
     2SLOW', T59, 'KFAST '/T46, '(1/SEC)', T58, '(1/SEC)'/T10, 59('*'))
      DO 180 I = 1, M
         WRITE (6,170) (SIZE(I,J),J=1,2), (DATA(I,J),J=1,3)
  170    FORMAT (' ', T11, 2(A4), T34, F5.3, 6X, 2(E9.3,4X))
  180 CONTINUE
      WRITE (6,190)
  190 FORMAT ('-', T20, 'TABLE 2 - MODEL PARAMETERS FOR INCOMBUSTIBLES'/
     1T20, 44('*')/'0', T10, 'MESH INTERVAL', T35, 'PHI', T47, 'K
     2SLOW', T59, 'KFAS T'/T46, '(1/SEC)', T58, '(1/SEC)'/T10, 59('*'))
      DO 200 I = 1, M
         WRITE (6,170) (SIZE(I,J),J=1,2), (ASHDAT(I,J),J=1,3)
  200 CONTINUE
C
C***********************************************************************
C     ORGANIZATION OF OUTPUT:
C        ESTABLISH TABLE FOR CONCENTRATE YIELD ESTIMATION ON AN
C        INCREMENTAL (CELLXCELL) AND CUMULATIVE BASIS
C***********************************************************************
C
      WRITE (6,210)
  210 FORMAT (2('-'), T5, 'MESH', T26, 'CUMULATIVE YIELD', T76, 'INCREME
     1NTAL Y IELD', /, T2, 'INTERVAL', T14, 'CELL NO.1', 2X,
     2 'CELL NO.2', 2X, 'CELL NO. 3', 2X, 'CELL NO.4', 5X, 'CELL N
     30.1', 2X, 'CELL NO.2', 2X, 'CELL NO.3', 2X, 'CELL NO.4', /, 104('*
     4'))
C
C***********************************************************************
C     EXECUTION OF MODEL TO ESTIMATE CONCENTRATE YIELD
C***********************************************************************
C
      DO 230 I = 1, M
         DO 220 J = 1, N
```

```
            SS = (DATA(I,2)*TAU + 1) ** (-J) * DATA(I,1)
            SF = (DATA(I,3)*TAU + 1) ** (-J) * (1 - DATA(I,1))
            CUMY(I,J) = (1 - SS - SF) * 100
            FY(I,1) = 0
            FY(I,J + 1) = CUMY(I,J)
            INCY(I,J) = CUMY(I,J) - FY(I,J)
220     CONTINUE
230 CONTINUE
C
C*************************************************
C    OUTPUT MODEL ESTIMATED CONCENTRATE YIELD
C*************************************************
C
      DO 250 I = 1, M
        WRITE (6,240) SIZE(I,1), SIZE(I,2), (CUMY(I,J),J=1,4),
     1  (INCY(I,J),J=1,4)
240     FORMAT ('0', T2, 2(A4), 4(7X,F4.1), 2X, 4(7X,F4.1))
250 CONTINUE
C
C*************************************************
C    ENTER FEED ASH ON SIZE DISCRETIZED BASIS
C*************************************************
C
      WRITE (6,260)
260 FORMAT (2('-'), 'ENTER FEED ASH FOR EACH SIZE INTERVAL PLUS COMPOS
   1ITE FEED'/T5, 'COARSEST TO FINEST, THEN COMPOSITE. FORMAT CODE: 7
   2(F 5.2)')
      READ (5,60) (FASH(I,1),I=1,M)
C
C***********************************************************************
C    ORGANIZATION OF OUTPUT:
C        ESTABLISH TABLE FOR CONCENTRATE QUALITY MODEL PREDICTION ON AN
C        INCREMENTAL PLUS OVERALL BASIS
C***********************************************************************
C
      WRITE (6,270)
270 FORMAT (2('-'), T32, 'PREDICTED % INCOMBUSTIBLES', 2('0'), T5, 'ME
   1SH IN TERVAL', T21, 'CELL NO.1', 2X, 'CELL NO.2', 2X, 'CELL NO.3',
   22X, 'CELL NO .4', 4X, 'FLOTATION CONC.'/T5, 77('*'))
C
C***********************************************************************
C    EXECUTION OF MODEL TO ESTIMATE PERCENTAGE INCOMBUSTIBLES IN
C            CONCENTRATE
C***********************************************************************
C
      DO 290 I = 1, M
        CUMA(I,1) = 0
        ASHP(I,1) = 0
        DO 280 J = 1, N
          ASS = (ASHDAT(I,2)*TAU + 1) ** (-J) * ASHDAT(I,1)
          ASF = (ASHDAT(I,3)*TAU + 1) ** (-J) * (1 - ASHDAT(I,1))
          ASHR(I,J) = 1 - ASS - ASF
          ASHP(I,J + 1) = ASHR(I,J)
          ASHPR(I,J) = ASHR(I,J) - ASHP(I,J)
          INCA(I,J) = ASHPR(I,J) * FASH(I,1) / INCY(I,J) * 100
          CUMA(I,1) = INCA(I,J) * INCY(I,J) / CUMY(I,N) + CUMA(I,1)
280     CONTINUE
290 CONTINUE
C
C*************************************************
```

```
C     OUTPUT MODEL ESTIMATION OF CONCENTRATE QUALITY
C***************************************************************
C
      DO 310 I = 1, M
        WRITE (6,300) SIZE(I,1), SIZE(I,2), (INCA(I,J),J=1,N), CUMA(I,1)
 300    FORMAT ('0', T7, 2(A4), 2X, 4(7X,F4.1), 8X, F4.1)
 310  CONTINUE
C
C***************************************************************
C     CALCULATE SCHULZ SEPARATION EFFICIENCY INDEX (ES)
C***************************************************************
C
      DO 320 I = 1, M
        SEF = 100 - (FASH(I,1)*1.1)
        SNUM = 100 - (CUMA(I,1)*1.1)
        ES(I,1) = CUMY(M,4) * 100 * (SNUM - SEF) / (SEF*FASH(I,1)*1.1)
 320  CONTINUE
      WRITE (6,330)
 330  FORMAT (2('-'), T38, 'SCHULZ EFFICIENCY INDEX'/T37, 25('*')/T28, '
     1SIZE INTERVAL', T42, 'ES'/T27, 15('*'), T40, 6('*'))
      DO 350 I = 1, M
        WRITE (6,340) (SIZE(I,J),J=1,2), ES(I,1)
 340    FORMAT (' ', T31, 2(A4), T41, F4.1)
 350  CONTINUE
      STOP
      END
```